NUREG/CR-0361
CE 78-08

RANDOM VIBRATION OF A NONLINEAR TWO-DEGREE-OF-FREEDOM OSCILLATOR

S.J. Stott and S.F. Masri

University of Southern California

Prepared for
U.S. Nuclear Regulatory Commission

Available from
National Technical Information Service
Springfield, Virginia 22161
Price: Printed Copy $6.50 ; Microfiche $3.00

The price of this document for requesters outside of the North American Continent can be obtained from the National Technical Information Service.

NUREG/CR-0361
CE 78-08
R5, RA

RANDOM VIBRATION OF A NONLINEAR TWO-DEGREE-OF-FREEDOM OSCILLATOR

S.J. Stott and S.F. Masri

Manuscript Completed: May 1978
Date Published: September 1978

Department of Civil Engineering
University of Southern California
Los Angeles, CA 90007

Division of Reactor Safety Research
Office of Nuclear Regulatory Research
U.S. Nuclear Regulatory Commission
Under Contract No. NRC-04-76-262
FIN No. B-5976

RANDOM VIBRATION OF A NONLINEAR

TWO-DEGREE-OF-FREEDOM OSCILLATOR

ABSTRACT

An analytical and experimental investigation is made of the dynamic response of a nonlinear two-degree-of-freedom oscillator that models some of the basic phenomena involved in the response of complex nuclear power plant systems under dynamic environments.

An approximate analytical solution is obtained for the stationary response of the system when subjected to stationary random excitation. Experimental measurements performed with an electronic analog computer and numerically simulated solutions generated by means of a digital computer verify the findings.

Results are given for the power spectral density and root-mean-squared level of the response. The effects of various system parameters on the response of the nonlinear system are determined.

TABLE OF CONTENTS

LIST OF FIGURES

LIST OF TABLES

Table

RANDOM VIBRATION OF A NONLINEAR

TWO-DEGREE-OF-FREEDOM OSCILLATOR

SUMMARY

One of the more serious design problems associated with the coolant loop of a nuclear power plant is the postulated rupture of the piping and the subsequent blowdown of the steam supply system. The occurrence of this type of accident has received increasing attention in the development of protective systems, such as those for emergency core cooling and redundant instrumentation, that effect a safe shutdown of the nuclear reactor. Concern for the functional integrity of these safety systems during the faulted condition has led to the installation of a variety of rupture supports that are intended to restrict gross movements of the piping system and to preclude a chain of failures. Since these restraints must not interfere with normal operation of the steam supply system, they are constructed with initial gaps that allow the piping to expand and contract in the operating condition. However, when a pipe breaks, it rapidly moves across the gap and is restrained by the support. Under the high blowdown loads that develop, inelastic behavior of the pipe material is also inevitable. Additionally, pumps and valves that are part of the primary coolant loop will experience nonlinearities because of gaps, friction, and nonproportional damping.

In order to analyze these complicated systems, it is necessary to use relatively simple models that are readily amenable to mathematical analysis or numerical solution techniques. A two-degree-of-freedom model

that exhibits "dead space" characteristics would allow assessment of the displacement response of a nonlinear piping system. Such a model would be valuable in determining

(a) Optimum design of pipe restraints.

(b) Structural response characteristics of complicated mechanical equipment with "deadspace" nonlinearities, such as valves and pumps.

(c) Interaction effects between equipment with nonlinear shock isolators, and their supporting structure.

An acceptable approximation for this problem class is a two-degree-of-freedom oscillator with "deadspace" characteristics subjected to stochastic random excitation. This simple analytic model allows for the study of two different problem classes. First, it makes possible the study of how an SDOF system with motion-limiting stops responds to to stochastic base excitation. Secondly, the response of a SDOF system with an auxiliary mass damper (similar to a building/equipment system) can be obtained. A comparison of both these problem classes would allow the determination of not only anticipated response data but also the optimum means by which to limit response.

Therefore, included in this report is a detailed study of a two-degree-of-freedom system with "deadspace" characteristics, along with a data presentation that is used to display the effects of various system parameters and to compare the displacement response of this model with other types of dynamic systems.

ACKNOWLEDGEMENTS

This study was supported in part by a contract with the U.S. Nuclear Regulatory Commission. The assistance of D. Chu in the analog computer studies is appreciated.

LIST OF SYMBOLS

A_1	Displacement amplitude of primary mass (M_1) with damper operating without motion-limiting stops
A_2	Displacement amplitude of auxiliary mass operating without motion-limiting stops
C_1, C_2, C_3	Damping constants
D	Clearance within which auxiliary mass can oscillate
DVN	Dynamic vibration neutralizer
FFT	Fast Fourier transform
F_o	Amplitude of harmonic excitation force
F(t)	Excitation force applied to M_1
$\lvert H_d(\omega) \rvert$	Amplification factor ("transfer function") corresponding to a discrete harmonic frequency (ω), $\left(x_{1_{max}}\right) \Big/ (F_o/K_1)$
K_1, K_2, K_3	Spring constants
M_1	Mass of primary system
M_2	Mass of auxiliary system (damper)
PSD	Power spectral density
RMS	Root mean squared
SDOF	Single degree of freedom
$S_f(\omega)$	Spectral density of excitation force
S_o	Uniform spectral density, $F(t)/M_1$
$S_x(\omega)$	Spectral density of displacement response
T_1	Period of SDOF, $2\pi/\omega_1$
2DOF	Two degrees of freedom
Z_{max}	Maximum relative displacement between M_1 and M_2 for the DVN under harmonic excitation

e	Coefficient of restitution ($0 \leq e \leq 1$)
i	$\sqrt{-1}$
t	Time
$x_j(t)$	Displacement of j-th mass
$\dot{x}_j(t)$	Velocity of j-th mass
$\ddot{x}_j(t)$	Acceleration of j-th mass
$y(t)$	Relative displacement between M_1 and M_2, $[x_2(t) - x_1(t)]$
α_o	Phase angle (initially unknown)
ζ_1	Fraction of critical damping, $C_1/2\sqrt{K_1M_1}$
ζ_2	Fraction of critical damping, $C_2/2\sqrt{K_2M_2}$
ζ_3	Fraction of critical damping, $C_3/2\sqrt{K_3M_3}$
μ	Mass ratio (M_2/M_1)
σ_{x_1}	RMS displacement of M_1 when provided with damper
σ_{x_o}	RMS displacement of M_1 in absence of damper (SDOF), $\sqrt{\pi S_o/(2\zeta_1\omega_1^3)}$
ω	Excitation frequency (harmonic)
ω_1	Frequency, $\sqrt{K_1/M_1}$
ω_2	Frequency, $\sqrt{K_2/M_2}$
ω_3	Frequency, $\sqrt{K_3/M_3}$

RANDOM VIBRATION OF A NONLINEAR TWO-DEGREE-OF-FREEDOM OSCILLATOR

BACKGROUND INFORMATION

In technical literature the most frequently analyzed group of energy transfer devices has been the family of auxiliary mass dampers (sometimes referred to as "dynamic absorbers"), which can be categorized into one of the following three basic groups:

a. Dynamic vibration neutralizer (DVN)*

b. Impact damper

c. Lanchester damper

The DVN has been rigorously studied for many years because of its simplicity and obviously practical engineering applications. Its fundamental research dates back to as early as 1928 for harmonic excitation [1,2]** and 1961 for random excitation.[3,4] The displacement response attenuation of this device is excellent. However, one of the basic problems encountered in its practical use is the excessive relative motion that the auxiliary mass undergoes at certain excitation frequencies, espcially if the auxiliary mass is small in comparison to the mass of the primary system. Ormondroyed and Den Hartog[1] proposed the use of elastic stops to limit the excessive motion of the auxiliary mass. The advantage of using elastic stops is that their separation can

---

* See List of Symbols for definition of notations.

** Numbers in parentheses designate references listed at the end of this report.

be adjusted so as not to disturb the motion of the damper within most of its operational frequency range; but at critical frequency values they would limit the relative motion of the damper auxiliary mass to the displacement clearance allowed. Timoshenko[2] expressed a great deal of interest in this modified version of the DVN, but it has not been until recently that others [5-11] have researched in detail the response of this system under the influence of harmonic excitation.

The impact damper is a simple yet quite efficient auxiliary mass device that uses momentum transfer between the impacting masses and also dissipation of mechanical energy during impacts to attenuate the response of the primary mass. The original investigative research of impact dampers was performed by Paget,[12] Leiber and Jensen,[13] Grubin,[14] and Egle.[15] Warburton[16] and, later, Masri and Caughey[17] derived an exact solution for the symmetric motion of this problem class. In recent years several authors [18-25] have rigorously studied all aspects of this system. Impact dampers have been used in commercial industry and, as described by Masri and Rocke,[26] have even been analyzed and installed on satellite antenna systems designed by the Hughes Aircraft Company (e.g., MARISAT, 1975-1976). Unfortunately, there are several practical difficulties associated with the use of impact dampers:

a. Excessive acoustic emissions are generated by impact dampers, especially at their tuned frequencies. Present government safety requirements for acceptable acoustic environmental levels for industrial workers and the susceptibility of spacecraft or industrial components to internally generated

acoustics have severely restricted the use of these devices. However, several authors[27,28] have recently proposed methods that may possibly be used to eliminate the problem.

b. Impact dampers are highly tuned devices and thus, the efficiency of the damper becomes negligible if too many or too few impacts occur per cycle of the primary system.

The Lanchester damper is probably the least practical of the entire family of energy transfer devices, since it relies solely on energy dissipated by a damping mechanism during the relative motion of the auxiliary mass to attenuate the response of the primary mass. As would be expected, the efficiency of the damper increases dramatically with an increase in the auxiliary mass weight; and excessive amounts of heat are generated in the damping mechanism during the optimum performance of the system. Unfortunately, for industrial applications it is advantageous to minimize the weight of the auxiliary mass and it is difficult to dissipate internally generated heat.

INTRODUCTION

The system model shown in Figure 1 is a nonlinear two-degree-of-freedom (2DOF) oscillator, which is subjected to a random excitation forcing function (i.e., F[t]). This system model simulates a single-degree-of-freedom (SDOF) oscillator attached to a DVN with motion-limiting stops (often referred to as a modified, or nonlinear, DVN) and can for various extreme parameter arrangements represent any of the members of the auxiliary mass damper family. For example, if $K_3 = C_3 = 0.0$, the model represents an impact damper; if $D/2 = \infty$, the model

represents a DVN; and if $D/2 = \infty$, $K_3 = 0.0$, and $C_3 >> 1.0$, the model represents a Lanchester damper.

Masri[10] has shown that the performance of the modified DVN under deterministic (i.e., harmonic) excitation alleviates many of the deficiencies inherent in the conventional DVN, and possesses response characteristics superior to it. For harmonic excitation the improved performance of the modified DVN can be attributed to a new damping mechanism, similar to that of an impact damper, that is used when the stops are engaged during the motion of the auxiliary mass. Instead of relying solely on the force exerted by M_2 to counteract the excitation force, which is the case in the DVN, the addition of stops introduces the mechanism of momentum transfer and energy dissipation during contact, which enhances the performance of the system. Unfortunately, no analytical solutions are available in published literature regarding the dynamic response of the modified DVN to stochastic (i.e., random) excitation.

The lack of analytical studies concerning the random excitation of a modified DVN is probably due to the fact that this problem does not lend itself to treatment by standard analytical techniques. The nonlinearity in this system involves the relative displacement as well as the relative velocity of the two masses. This difficulty makes perturbation methods[29] for random vibration of nonlinear systems, as well as equivalent linearization techniques,[30-31] inapplicable to this problem class.

SCOPE OF RESEARCH

Two separate analytic solutions are derived for the stationary displacement response of a highly nonlinear auxiliary mass damper (a DVN with motion-limiting stops) attached to an SDOF oscillator that is subjected to random excitation. One of these solution methods is an approximate analytical (i.e., "theoretical") solution and the other generates "experimental" data by numerical integration of the system model equations of motion. To determine the accuracy as well as inherent limitations of these analytic solutions, two computer methodologies, obtained from the algorithms derived for both solution methods, are evaluated by comparing their numerically generated data with each other, with data generated by electronic analog computer, and (where applicable) with published special-case solutions (e.g., random excitation of impact dampers[19]). The effects of various damper parameters on the response of the primary system are determined, and future applications for the solutions and their associated computer methodologies are appraised.

This study was conducted under the following assumptions:

a. The force F(t) is normally distributed random excitation, with statistics as shown in Figure 2 and calibrated as specified in Appendix A.

b. All RMS data results presented are the statistical ensemble average (N = 24) of generated data, per Appendix B.

DESCRIPTION OF PROBLEM

The general equations of motion for the nonlinear system model displayed in Figure 1 are derived as follows.

The equation of motion for M_1 when there is no contact with the nonlinear walls is

$$M_1\ddot{x}_1 + C_1\dot{x}_1 + K_1x_1 + K_3 (x_1 - x_2) + C_3 (\dot{x}_1 - \dot{x}_2) = F(t) \quad (1)$$

Let y be the relative displacement of M_2 with respect to M_1

$$y(t) = x_2(t) - x_1(t) \quad (2)$$

Using Equation 2, Equation 1 can be rewritten in a more convenient form as

$$\ddot{x}_1 + 2\zeta_1\omega_1\dot{x}_1 + \omega_1^2 x_1 - \mu \left(\omega_3^2 y + 2\zeta_3\omega_3\dot{y}\right) = \frac{F(t)}{M_1} \quad (3)$$

The equation of motion for M_1 when there is a contact with the nonlinear walls is

$$\left[M_1\ddot{x}_1 + C_1\dot{x}_1 + K_1x_1 - K_3y - C_3\dot{y} + K_2 \left(x_1 - x_2 - D/2\right) + C_2 \left(\dot{x}_1 - \dot{x}_2\right)\right] = F(t) \quad (4)$$

Rewriting Equation 4, one obtains

$$\left[M_1\ddot{x}_1 + C_1\dot{x}_1 + K_1x_1 - K_3y - C_3\dot{y} - K_2 \left(y + D/2\right) - C_2\left(\dot{y}\right)\right] = F(t) \quad (5)$$

Let the following nonlinear functions represent the dead-space characteristics of the model.

$$g_1(y) = \begin{cases} 0 & \text{when } |y| \leq D/2 \\ y + D/2 & \text{when } |y| > D/2 \end{cases} \quad (6)$$

$$g_2(y) = \begin{cases} 0 & \text{when } |y| \leq D/2 \\ y - D/2 & \text{when } |y| > D/2 \end{cases} \quad (7)$$

$$h(y,\dot{y}) = \begin{cases} 0 & \text{when } |y| \leq D/2 \\ y & \text{when } |y| > D/2 \end{cases} \quad (8)$$

Using Equations 6 and 8, Equations 5 and 3 can be combined into the following general equation

$$\ddot{x}_i + 2\zeta_1\omega_1 x_1 + \omega_1^2 x_1 - \mu \left[\omega_3^2 y + 2\zeta_3\omega_3\dot{y} + \omega_2^2 g_1(y) + 2\zeta_2\omega_2 h(y,\dot{y})\right] = \frac{F(t)}{M_1} \quad (9)$$

The equation of motion for M_2 when there is no contact with the nonlinear walls is

$$M_2\ddot{x}_2 + C_3 (\dot{x}_2 - \dot{x}_1) + K_3 (x_2 - x_1) = 0 \quad (10)$$

Rewriting Equation 10, one obtains

$$\ddot{x}_2 + 2\zeta_3\omega_3\dot{y} + \omega_3^2 y = 0 \quad (11)$$

The equation of motion for M_2 when there is contact with the nonlinear walls is

$$M_2\ddot{x}_2 + K_3 y + C_3\dot{y} + K_2 [y - D/2] + C_2 [\dot{y}] = 0 \quad (12)$$

Using Equations 7 and 8, Equations 11 and 12 can be combined into the following general equation:

$$\ddot{x}_2 + 2\zeta_3\omega_3\dot{y} + \omega_3^2 y + \omega_2^2 g_2(y) + 2\zeta_2\omega_2 h\,(y,\dot{y}) = 0 \tag{13}$$

Thus the general equations of motion for the system model are represented by Equations 9 and 13.

Rewriting Equations 3 and 11, which represent the system equations of motion when there are no impacts, one obtains:

$$a_{11}\ddot{x}_1 + b_{11}\dot{x}_1 + c_{11}x_1 + b_{12}\dot{x}_2 + c_{12}x_2 = F(t) \tag{14}$$

$$b_{12}\dot{x}_1 + c_{12}x_1 + a_{22}\ddot{x}_2 + b_{22}\dot{x}_2 + c_{22}x_2 = 0 \tag{15}$$

where

$$a_{11} = M_1 \tag{16}$$

$$a_{22} = M_2 \tag{17}$$

$$b_{11} = C_1 + C_3 \tag{18}$$

$$b_{12} = -C_3 \tag{19}$$

$$b_{22} = C_3 \tag{20}$$

$$c_{11} = K_1 + K_3 \tag{21}$$

$$c_{12} = -K_3 \tag{22}$$

$$c_{22} = K_3 \tag{23}$$

For a harmonic excitation force

$$F(t) = F_0 \cos \omega t \tag{24}$$

and elastic stops that are very stiff ($\omega_2/\omega_1 >> 1.0$) compared to the stiffness of the primary system, Masri[10] has shown that under the assumption of steady-state motion with two symmetric impacts per cycle on opposite sides of the stops, the solution of Equations 14 and 15 between these impacts (i.e., $0 \leq \omega t \leq \pi$) is defined as

$$x_1(t) = \sum_{j=1}^{4} \lambda_{1j} \exp(S_j t) + \mathrm{Re}\{A_1 \exp[i(\omega t + \alpha_o)]\} \quad (25)$$

$$x_2(t) = \sum_{j=1}^{4} r_j \lambda_{1j} \exp(S_j t) + \mathrm{Re}\{A_2 \exp[i(\omega t + \alpha_o)]\} \quad (26)$$

where the origin of the time axis has been shifted such that $t = 0$ at $|x_2 - x_1| = D/2$. This will modify the excitation force so that

$$F(t) = F_o \cos(\omega t + \alpha_o) = \mathrm{Re}\{F_o \exp[i(\omega t + \alpha_o)]\} \quad (27)$$

where α_o is an initially unknown phase angle. The S_1, S_2, S_3 and S_4 values are the roots of the characteristic equation

$$(a_{11}S^2 + b_{11}S + c_{11})(a_{22}S^2 + b_{22}S + c_{22}) - (b_{12}S + c_{12})^2 = 0 \quad (28)$$

and the λ's are related by

$$\frac{\lambda_{1j}}{\lambda_{2j}} = -\frac{b_{12}S_j + C_{12}}{a_{11}S_j^2 + b_{11}S_j + C_{11}} \equiv r_j \quad (j = 1, 2, 3, 4) \quad (29)$$

The phase angle α_o is given by

$$\alpha_o = \tan^{-1} \frac{\alpha_1 D \pm \alpha_2}{\alpha_3 D \pm \alpha_4} \qquad (30)$$

and the rest of the parameters are defined in Reference 10.

The amount of mechanical energy dissipated during the collision of M_2 with the nonlinear stops (i.e., K_2, ζ_2) is governed by the equivalent coefficient of restitution, e, which may assume values from 0 to 1 (i.e., 0 is equal to a completely plastic impact and 1 is equal to a perfectly elastic impact). Masri[10] has shown that for harmonic excitation, the equivalent value of e for this system model is dependent solely on ζ_2 when the elastic stops are stiff, and the contact duration with this type of impact will represent less than 5% of the fundamental period of the primary system. Included in Tables 1 and 2 are equivalent e data values determined by Masri.[10]

COMPUTER SOLUTION

Included in this section is a brief description of the two digital computer logics (ID117 and ID401) created to obtain numerical data for the analytic solutions of the system model proposed in this report.

The characteristics of the excitation forcing function F(t), which was supplied by a computer "software" Gaussian random number generator (i.e., IBM 360 Scientific Subroutine Package, subroutines GAUSS and RANDU), are exhibited in Figure 2. To obtain the probability density in Figure 2(A), a time history data sample of 3,000 values was used.

To obtain the PSD displayed in Figure 2(B), 20 statistical averages were required. Additional information about the excitation force can be found in Appendix A.

For the parameters presented in this report, the system response was computed for a sufficient number of periods ($\simeq 50\ T_1$) to achieve a stationary condition and acquire a data sample. Because of the random nature of this problem, 24 data samples were statistically averaged, as discussed in Appendix B, to determine the system's RMS response.

Figure 3 shows typical PSD plots of the displacement response $x_1(t)$ of the primary system M_1 for a representative set of parameters. The PSD plots were obtained by using standard time series algorithms that employed FFT techniques (i.e., ID117d). The parameter $\omega_1^2[S_x(\omega)/S_o]^{1/2}$ was used to represent the PSD of the system response in a form that allows easy comparison with an equivalent linear system. For such a linear system the above-mentioned parameter is equal to $\left\{[1 - (\omega/\omega_1)^2]^2 + (2\zeta_{eq}\omega/\omega_1)^2\right\}^{-1/2}$, where ζ_{eq} is the "equivalent" value of viscous damping (i.e., the ζ that an SDOF system without a damper should have in order for its displacement response to be the same as the primary mass M_1 of an SDOF system damped by a nonlinear DVN). Figure 3(A) shows the response of an SDOF system (a special case of the present system when $D/\sigma_{x_o} \simeq \infty$ and $\mu = 0.0$). The PSD of an approximate conventional DVN ($D/\sigma_{x_o} \simeq \infty$) with mass ratio ($\mu = 0.10$) and ratio of critical damping in the coupling dashpot ($\zeta_3 = 0.01$) is given in Figure 3(B). Note that this PSD plot exhibits the two peaks on both sides of resonance ($\omega/\omega_1 = 1.0$) that are usually encountered in the response of a typical linear system damped by the conventional DVN. Unlike the

results shown in Figures 3(A) and 3(B), the plot displayed in Figure 3(C) corresponds to a system acting as an impact damper[16] (where $\omega_3/\omega_1 = \zeta_3 = 0$ and $\omega_2/\omega_1 >> 1$). Note that there is a definite shift in the location of peak of the PSD curve, which is shifted from $\omega/\omega_1 = 1$ for a linear system to $\omega/\omega_1 \approx 1/\sqrt{1+\mu}$.

Figure 4 illustrates a typical PSD for a set of parameters in which the system response relies appreciably on the limiting or bounding action of the elastic stops, thereby permitting momentum transfer between M_1 and M_2 to play a considerable role. The system characteristics are such that the neutralizer exhibits response features that rely on the action of the conventional DVN. They also rely on the elastic stops that come into play because the relative motion between the two masses exceeds the "deadspace" between the stops. As a result of this dual action, the performance of this nonlinear neutralizer is enhanced (compared to that of Figure 3[B]) in that the two sharp peaks in the PSD plot are considerably attenuated, whereas the response level around the resonance region (where the conventional DVN shows its best performance) does not materially deteriorate. It should be noted that in Figure 4 a comparison is also made between experimental data and equivalent harmonic data presented by Masri.[6] It is important to note the agreement between these values, which demonstrates the strong correlation in their respective transfer functions.

Computer Logic ID117

The experimental response of the system shown in Figure 1 to stochastic excitation was determined through the use of a digital

computer using standard techniques[32] for the numerical solution of the governing equations of motion (i.e., Equations 9 and 13). This program is written in the following three formats:

a. ID117B is the standard program version.

b. ID117C is a modified version of ID117B which has fewer output options and requires less computer core space. It is an economical program for the generation of large amounts of data.

c. ID117D is a modified version of ID117C which is used for obtaining the PSD of the displacement response using FFT techniques.

Computer Logic ID401

The main idea behind this proposed analytical (i.e., "theoretical") solution is that, based on experimental observations and digital computer simulation studies (e.g., Figure 4), it is reasonable to assume to first-order approximation that the displacement spectral density $S_{x_1}(\omega)$ of the primary system, when provided with a nonlinear DVN with a small mass ratio and a slight amount of viscous damping, can be approximated by

$$S_{x_1}(\omega) = \left|H_d(\omega)\right|^2 S_f(\omega) \qquad (32)$$

where $S_f(\omega)$ is the excitation PSD, and $|H_d(\omega)|$ is the amplitude of the frequency response function of the primary system when provided with a nonlinear DVN and subjected to harmonic excitation of frequency ω. This assumption is similar to that successfully used by Masri and

Ibrahim[19] to obtain the displacement response solution for the random excitation of an impact damper.

The magnification factor $|H_d(\omega)|$ is given by

$$|H_d(\omega)| = \frac{x_{1_{max}}}{F_o/K_1} \tag{33}$$

in the range $0 \leq \omega t \leq \pi$. However,

$$x_{1_{max}} = (1/2)[Sol(1) + Sol(2)] \tag{34}$$

where Sol(1) and Sol(2) are the peak values of $x_1(t)$ in Equation 25, obtained for the upper and lower set of signs, respectively, in Equation 30. With $|H_d(\omega)|$ determined from Equation 33, the RMS displacement response, σ_{x_1}, of the primary system is given by

$$\sigma_{x_1}^2 \equiv E[x_1^2] = S_o \int_{\omega=-\infty}^{+\infty} |H_d(\omega)|^2 \, d\omega \tag{35}$$

where S_o is the uniform spectral density of $F(t)/M_1$. The final theoretical response value is obtained by the numerical integration of Equation 35 by Simpson's rule.

On the basis of experimental observations, the following approximation was incorporated in the evaluation of σ_{x_1} as given by Equation 35; for clearance ratios $D/2 > \sqrt{2}\, Z_{max}$, where Z_{max} is the maximum relative displacement between M_1 and M_2 for a conventional DVN (i.e., when $D = \infty$), the system is treated as a DVN. In other words, if at a given frequency ω, the ratio $(D/2)/Z_{max}$ is too large (note

that Z_{max} is a function of ω), the damper mass M_2 will have very few collisions with the elastic stops. Thus $|H_d(\omega)|$ will be approximately the same as when it is provided with a conventional DVN.

Figures 5 through 11 compare the theoretical values of $|H_d(\omega)|$ derived using ID401 with normalized PSD values (10 statistical averages) obtained by the digital simulation techniques (i.e., ID117E) for typical system parameters. Figures 12 through 21 compare normalized RMS displacement values obtained by both methods (24 statistical averages were used for the experimental results).

EFFECTS OF SYSTEM PARAMETERS

Figures 22 through 56 contain a summary of experimental results (24 statistical averages) obtained by digital simulation (i.e., ID117C) and are presented because such data are nonexistent in present literature. It should be noted that where applicable, these experimental data were verified by the approximate theory (i.e., ID401); but for clarity of presentation only experimental results are displayed. Since the values shown are experimental results, some of the fluctuations observed would most likely be eliminated with more ensemble averages, as discussed in Appendix B. Response data were also experimentally determined for the case of "soft" elastic stops ($\omega_2/\omega_1 \leq 1$), a case for which the present approximate solution (ID401) does not apply.

The effects of system parameters can be summarized as follows:

a. In general, as μ is increased, the RMS displacement (σ_{x_1}) of the primary system M_1 is decreased (i.e., "effectiveness" or "performance" of the damper is increased).

b. The damper performance is enhanced as the system viscous damping (ζ_1, ζ_3) is decreased.

c. A modified DVN with "hard" elastic stops is superior to the conventional DVN in attenuating the response, and it is less sensitive to tuning effects (ω_3/ω_1).

d. A conventional impact damper ($\omega_3/\omega_1 = 0$, $\omega_2/\omega_1 >> 1$) is more effective than the conventional DVN in controlling the response of randomly excited systems.

e. A modified DVN with "soft" stops is considerably better than the conventional DVN or the modified DVN with "hard" stops in reducing normalized RMS displacement and is less sensitive than the impact damper to clearance effects.

CONCLUSIONS

An approximate analytic solution (i.e., ID401) has been presented for determining the response of a viscously damped, single-degree-of-freedom primary system that is provided with a dynamic vibration neutralizer with motion-limiting stops, and is subjected to stationary random excitation. The solution of this highly nonlinear, dissipative two-degree-of-freedom system is derived by making use of the system's steady-state response to harmonic excitation (for which an exact solution is obtained) and by assuming that, for the range of parameters discussed in this paper, the approximate response to random excitation can be obtained by superposition of the response to discrete harmonic excitation. In Figures 5 through 21 the approximate analytic solution, in spite of its relative simplicity, is shown to be in good agreement

both qualitatively and quantitatively with solutions that were obtained with a digital computer (i.e., ID117B, ID117C, ID117D) and experimental measurements from an electronic analog computer (i.e., Figure 12[A]).

In Figures 22 through 56 a detailed parameter study of "experimental" data (i.e., ID117C) is presented, since such data are nonexistent in published literature. This parameter study shows that the nonlinear damper under discussion is significantly more effective than the conventional dynamic vibration neutralizer in attenuating the response of systems subjected to stationary random vibration. Additionally, from Figure 57, which displays analog data, it is observed that for the nonlinear DVN, the displacement (x_1) is less than that of the conventional DVN; whereas at the same time, the relative displacement (Y) of the nonlinear DVN is limited to the clearance distance (D). Additionally, it should be noted that the SDOF response (σ_{x_1}), which is shown in Figure 57(A) for times greater than 400 T_1, displays a considerable amount of variance for what must be considered an extremely large ensemble length. For this reason, statistical averaging of response data was required.

The only limitations observed for the computer programs presented in this report are for the program logic ID401 and they are as follows:

a. The elastic stops must be very stiff ($\omega_2/\omega_1 >> 1.0$) compared to stiffness of the primary system.

b. The nonlinear DVN should have only a small amount of viscous damping (ζ_3) and small auxiliary mass ratio (μ).

However, Figures 12 through 21 demonstrate clearly that good agreement still exists between experimental and theoretically predicted

response data for a sizeable mass ratio (μ = 20%), a significant amount of viscous damping ($\zeta_3 \approx 5\%$), and a coupling spring ratio (ω_3/ω_1) spanning the range from 0.8 to 1.2.

There are several obvious areas of additional study available to the interested investigator using these computer methods:

a. Determine the response of the modified DVN system to harmonic and random excitation when the elastic stop (K_2), the coupling spring (K_3), or both of these springs are hysteretic.

b. Derive an approximate analytical method for the modified DVN with soft stops ($\omega_2/\omega_1 \leq 1$).

ILLUSTRATIONS

Included in this section are all the figures and tables associated with this report. They are numbered and displayed in the sequential order in which they are referenced in the text. The following parameters are used only for the included figures and tables; all other parameters are defined in the List of Symbols preceding the report.

SF(W/W1)	$S_F(\omega/\omega_1)$
SIGMAO	σ_{x_0}
SO	S_o
SQRT	$\sqrt{}$
SX(W)	$S_x(\omega)$
W1	ω_1
W/W1	ω/ω_1
W3/W1	ω_3/ω_1

$\bar{x}$	The mean average value of x
XRMS	σ_{x_1}

The following special notes apply to the included figures and tables:

a. For all plots presented, data referred to as "experimental" were generated by computer programs ID117B, ID117C, or ID117D, and data referred to as "theory" or "theoretical" were generated using the approximate analytic method of computer program ID401.

b. The "analog" data presented in Figure 12(A) and Figure 57 were obtained using the analog computer system of the University of Southern California Structural Dynamics Laboratory (Civil Engineering Department).

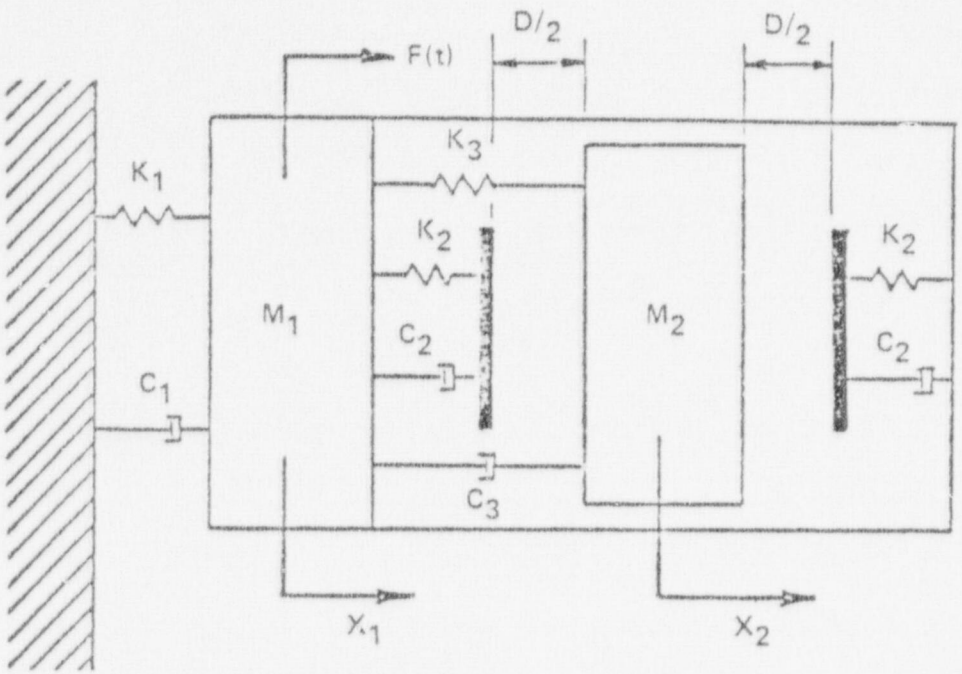

FIGURE 1 MODEL OF SYSTEM

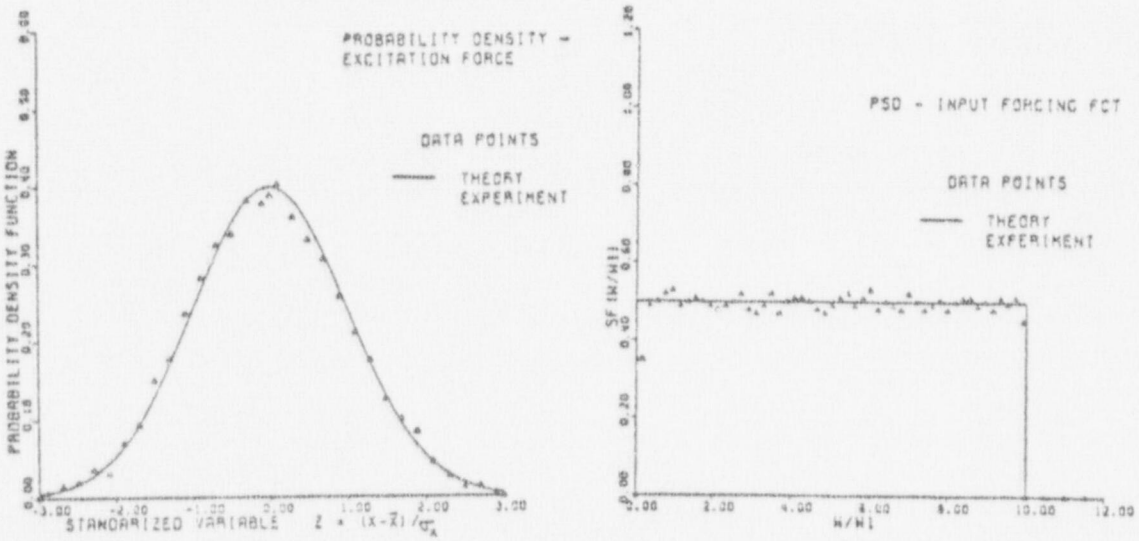

(A) (B)

FIGURE 2 CHARACTERISTICS OF COMPUTER GENERATED RANDOM FORCING FUNCTION

$D/(F_0/K_1)$	15	20	25
ζ_2	e	e	e
0	1.0	1.0	1.0
0.1	0.75	0.75	0.78
0.2	0.51	0.53	0.55
0.3	0.35	0.38	0.40
0.4	0.23	0.28	0.30
0.5	0.15	0.20	0.22
0.6	0.11	0.15	0.18
0.7	0.07	0.10	0.11

TABLE 1 DEPENDENCE OF EQUIVALENT COEFFICIENT OF RESTITUTION (e) ON ζ_2 AND $D/(F_0/K_1)$. SYSTEM PARAMETERS:

$\Omega/\omega_1 = 1.0$, $\zeta_1 = 0.01$, $\omega_{3/\omega 1} = 0.01$, $\zeta_3 = 0.0$, $\mu = 0.10$, $\omega_{2/\omega 1} = 5.0$

$D/(F_0/K_1)$	15	20	25
ζ_2	e	e	e
0	1.0	1.0	1.0
0.1	0.70	0.72	0.74
0.2	0.49	0.50	0.51
0.3	0.33	0.34	0.36
0.4	0.22	0.23	0.25
0.5	0.13	0.15	0.17
0.6	0.07	0.09	0.11
0.7	0.02	0.04	0.06

TABLE 2. DEPENDENCE OF EQUIVALENT COEFFICIENT OF RESTITUTION (e) ON ζ_2 AND $D/(F_{0/K_1})$. SYSTEM PARAMETERS: $\Omega/\omega_1 = 1.0$, $\zeta_1 = 0.01$, $\omega_{3/\omega_1} = 0.01$, $\zeta_3 = 0.0$, $\mu = 0.10$, $\omega_{2/\omega_1} = 10.0$

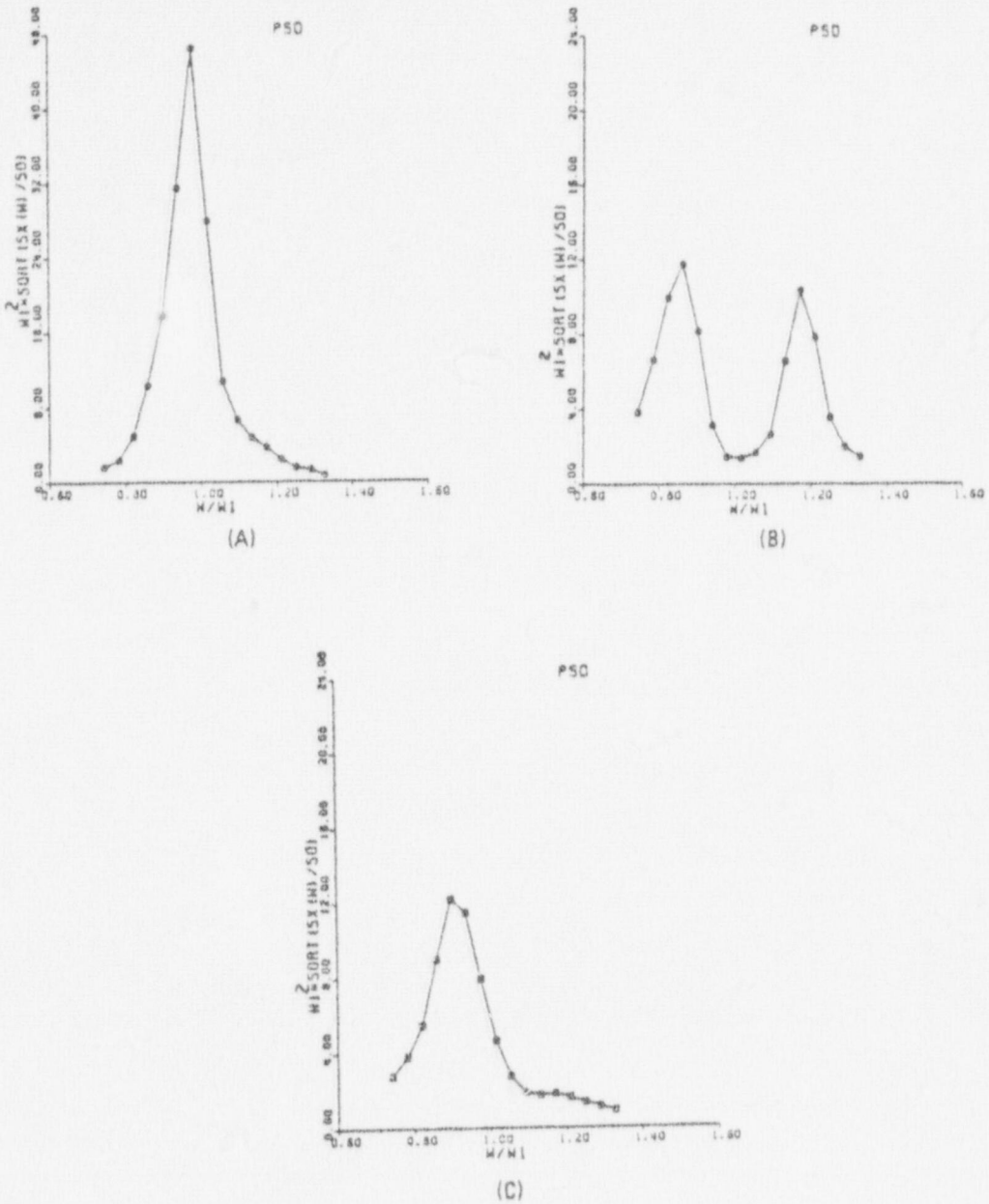

FIGURE 3 TYPICAL SYSTEM RESPONSE

$\omega_3/\omega_1 = 1.0$, $\zeta_1 = \zeta_3 = 0.01$, $\zeta_2 = 0.4$, $\omega_2/\omega_1 = 10.0$.

(A) SDOF, $\mu = 0$, $D/\sigma_{x_o} = 50$; (B) DVN, $\mu = 0.10$, $D/\sigma_{x_o} = 50$;

(C) Impact damper, $\mu = 0.10$, $D/\sigma_{x_o} = 2$.

——— Experimental

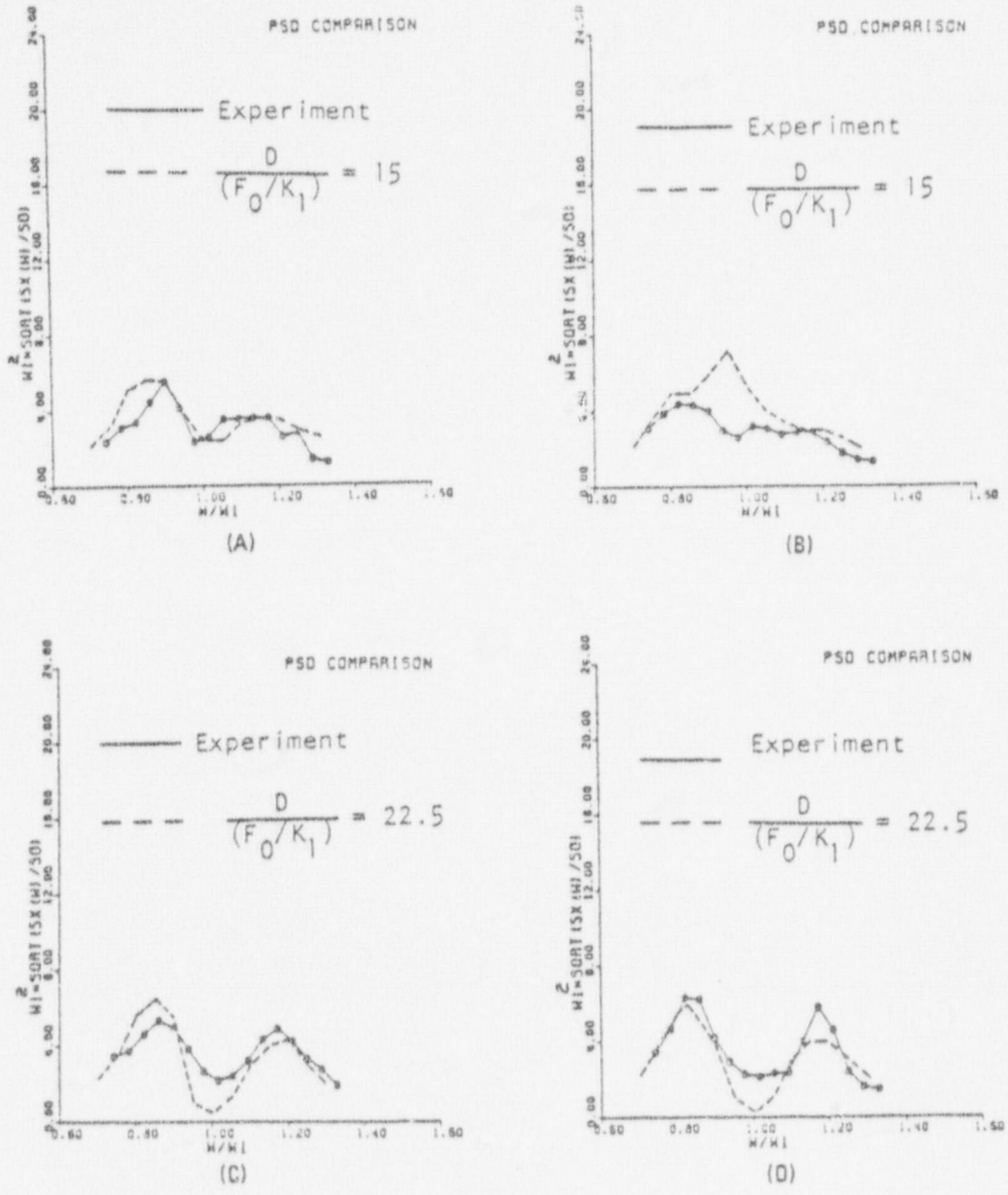

FIGURE 4 TYPICAL SYSTEM RESPONSE

$\omega_3/\omega_1 = 1.0$, $\mu = 0.10$, $\zeta_2 = 10.0$, $\zeta_1 = \zeta_3 = 0.01$.

(A) $D/\sigma_{x_o} = 2$, $\omega_2/\omega_1 = 0.1$; (B) $D/\sigma_{x_o} = 2$, $\omega_2/\omega_1 = 1.0$;

(C) $D/\sigma_{x_o} = 4$, $\omega_2/\omega_1 = 0.1$; (D) $D/\sigma_{x_o} = 4$, $\omega_2/\omega_1 = 1.0$.

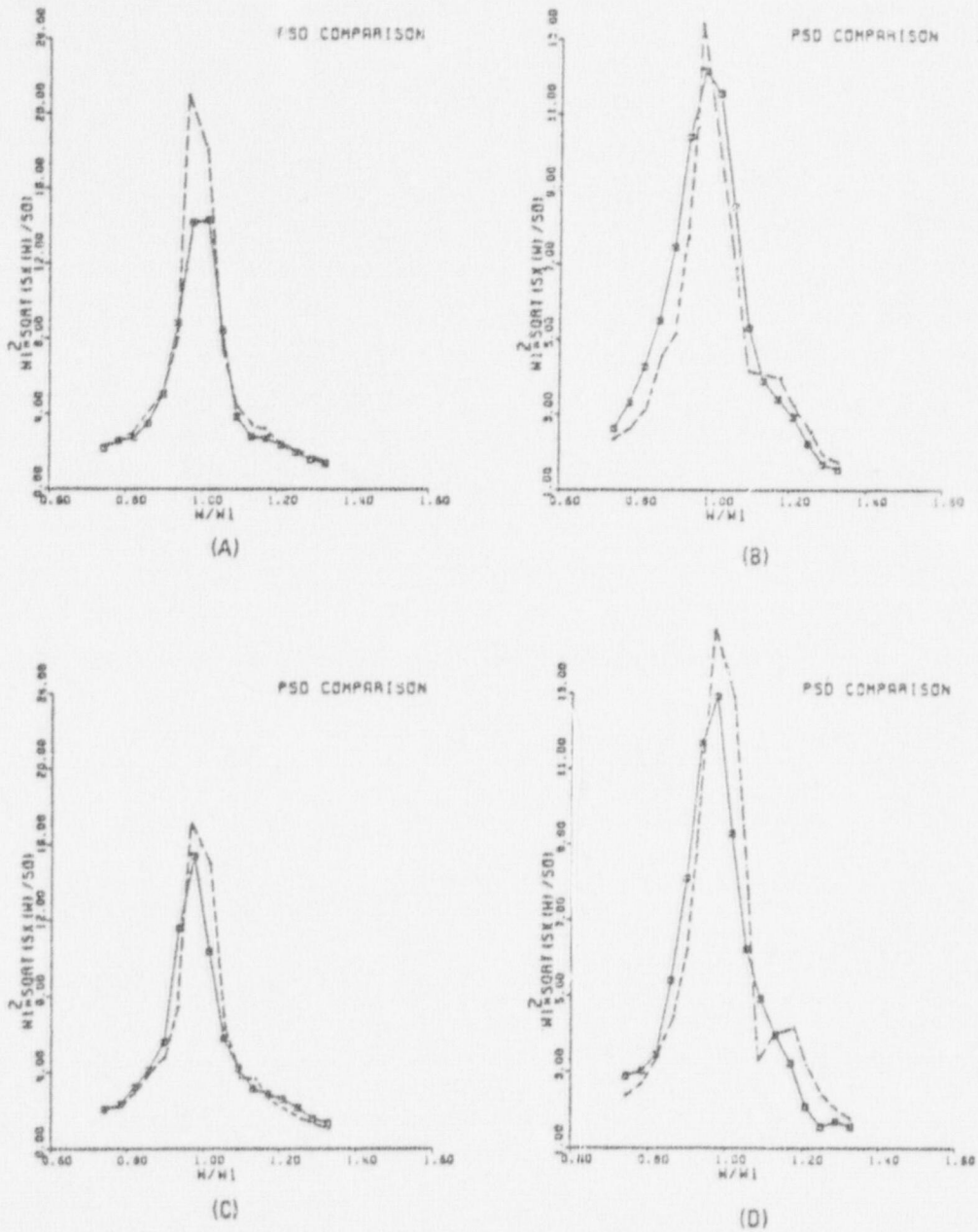

FIGURE 5 COMPARISON OF EXPERIMENTAL AND THEORETICAL PSD

$\omega_3/\omega_1 = 1.0$, $\zeta_1 = \zeta_3 = 0.01$, $\mu = 0.01$, $\omega_2/\omega_1 = 10.0$, $\zeta_2 = 0.4$.

(A) $D/\sigma_{x_o} = 2$; (B) $D/\sigma_{x_o} = 4$; (C) $D/\sigma_{x_o} = 6$; (D) $D/\sigma_{x_o} = 8$.

– – – – Theory ——— Experimental

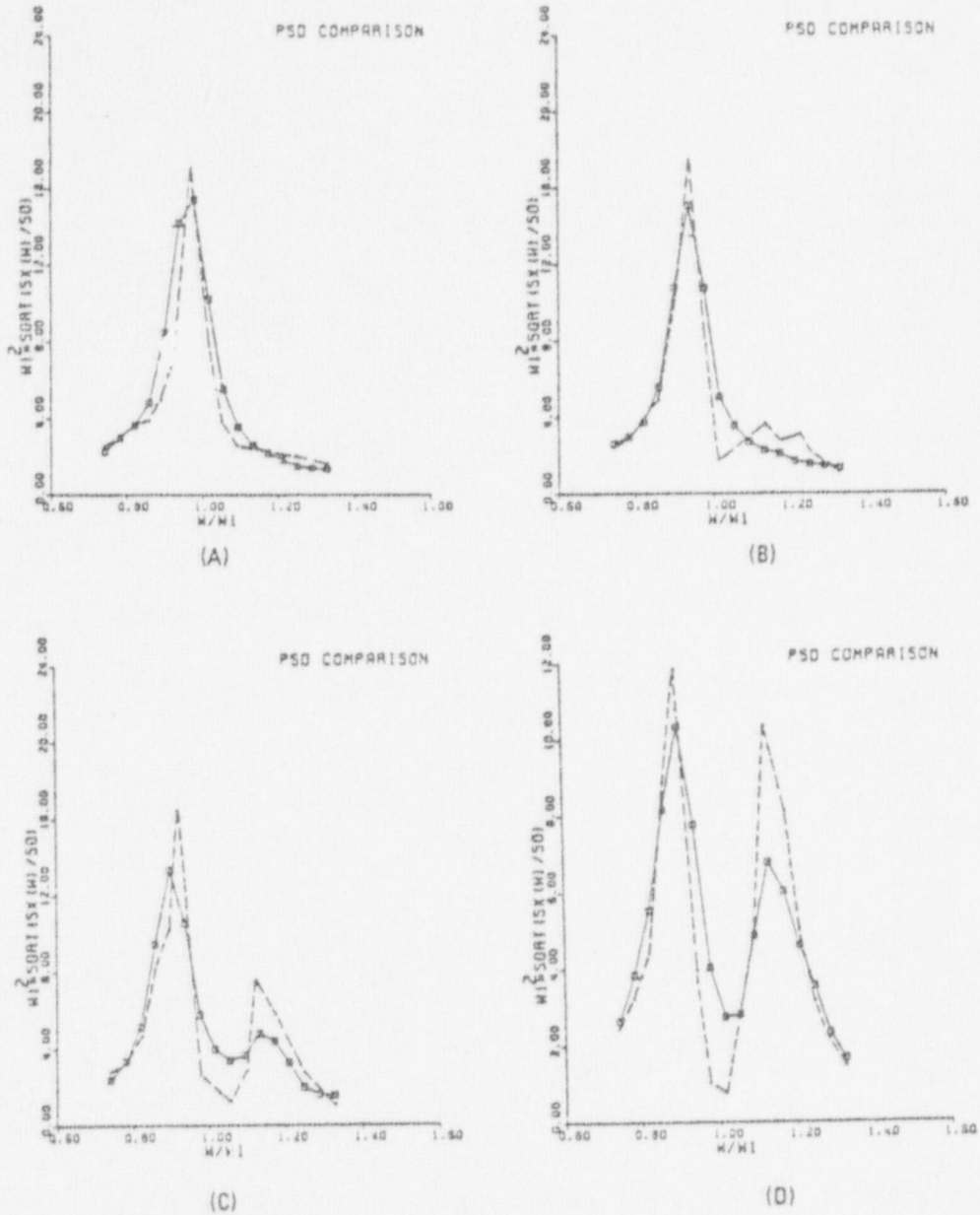

FIGURE 6 COMPARISON OF EXPERIMENTAL AND THEORETICAL PSD

$\omega_3/\omega_1 = 1.0$, $\zeta_1 = \zeta_3 = 0.01$, $\mu = 0.05$, $\omega_2/\omega_1 = 10.0$, $\zeta_2 = 0.4$.

(A) $D/\sigma_{x_o} = 2$; (B) $D/\sigma_{x_o} = 4$; (C) $D/\sigma_{x_o} = 8$; (D) $D/\sigma_{x_o} = 10$.

— — — Theory ——— Experimental

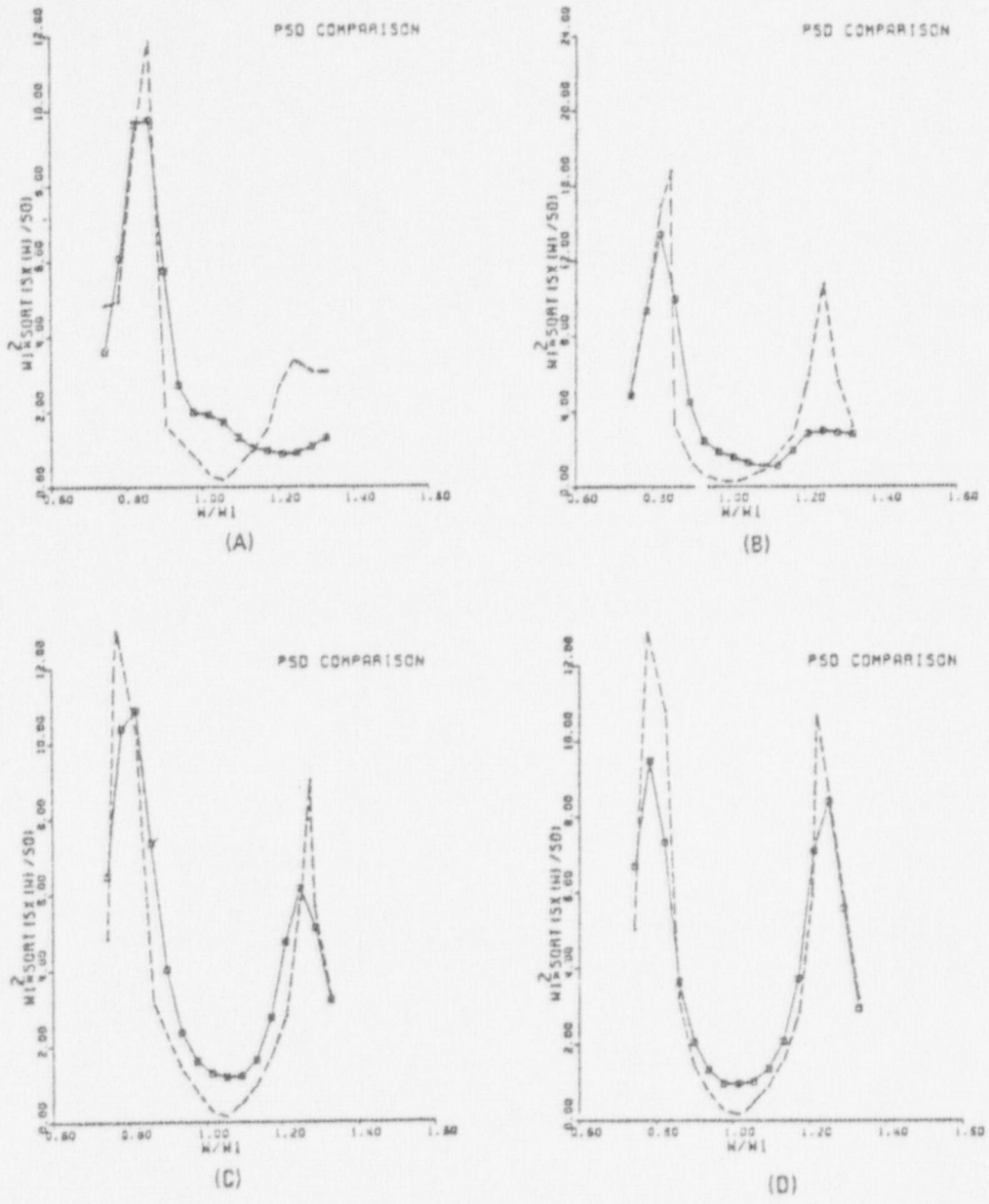

FIGURE 7 COMPARISON OF EXPERIMENTAL AND THEORETICAL PSD

$\omega_3/\omega_1 = 1.0$, $\zeta_1 = \zeta_3 = 0.01$, $\mu = 0.20$, $\omega_2/\omega_1 = 10.0$, $\zeta_2 = 0.4$.

(A) $D/\sigma_{x_o} = 2$; (B) $D/\sigma_{x_o} = 4$; (C) $D/\sigma_{x_o} = 6$; (D) $D/\sigma_{x_o} = 8$.

— — — Theory ——— Experimental

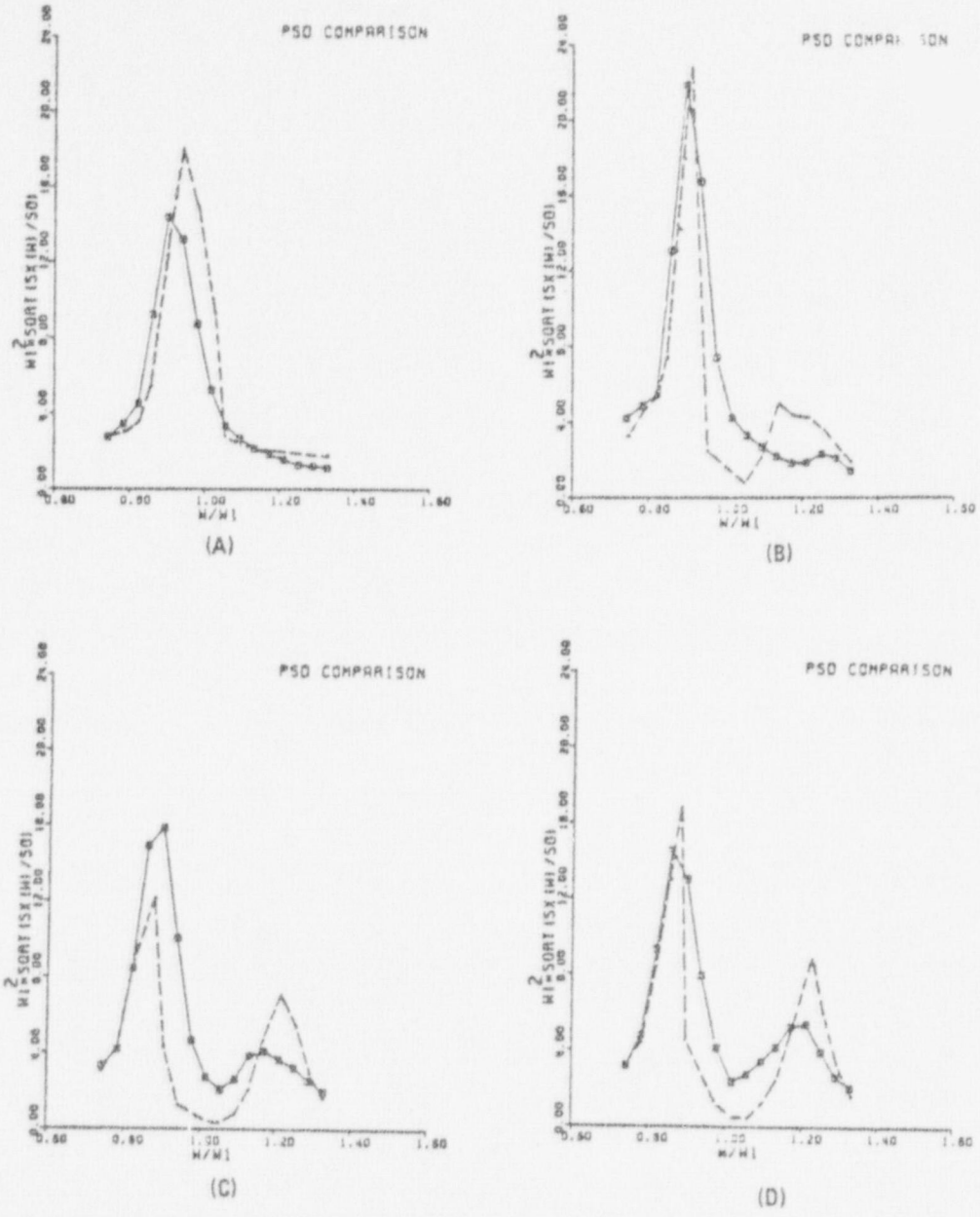

FIGURE 8 COMPARISON OF EXPERIMENTAL AND THEORETICAL PSD

$\omega_3/\omega_1 = 1.0$, $\zeta_1 = \zeta_3 = 0.01$, $\mu = 0.10$, $\omega_2/\omega_1 = 10.0$, $\zeta_2 = 0.1$.

(A) $D/\sigma_{x_o} = 2$; (B) $D/\sigma_{x_o} = 4$; (C) $D/\sigma_{x_o} = 6$; (D) $D/\sigma_{x_o} = 8$.

— — — Theory ——— Experimental

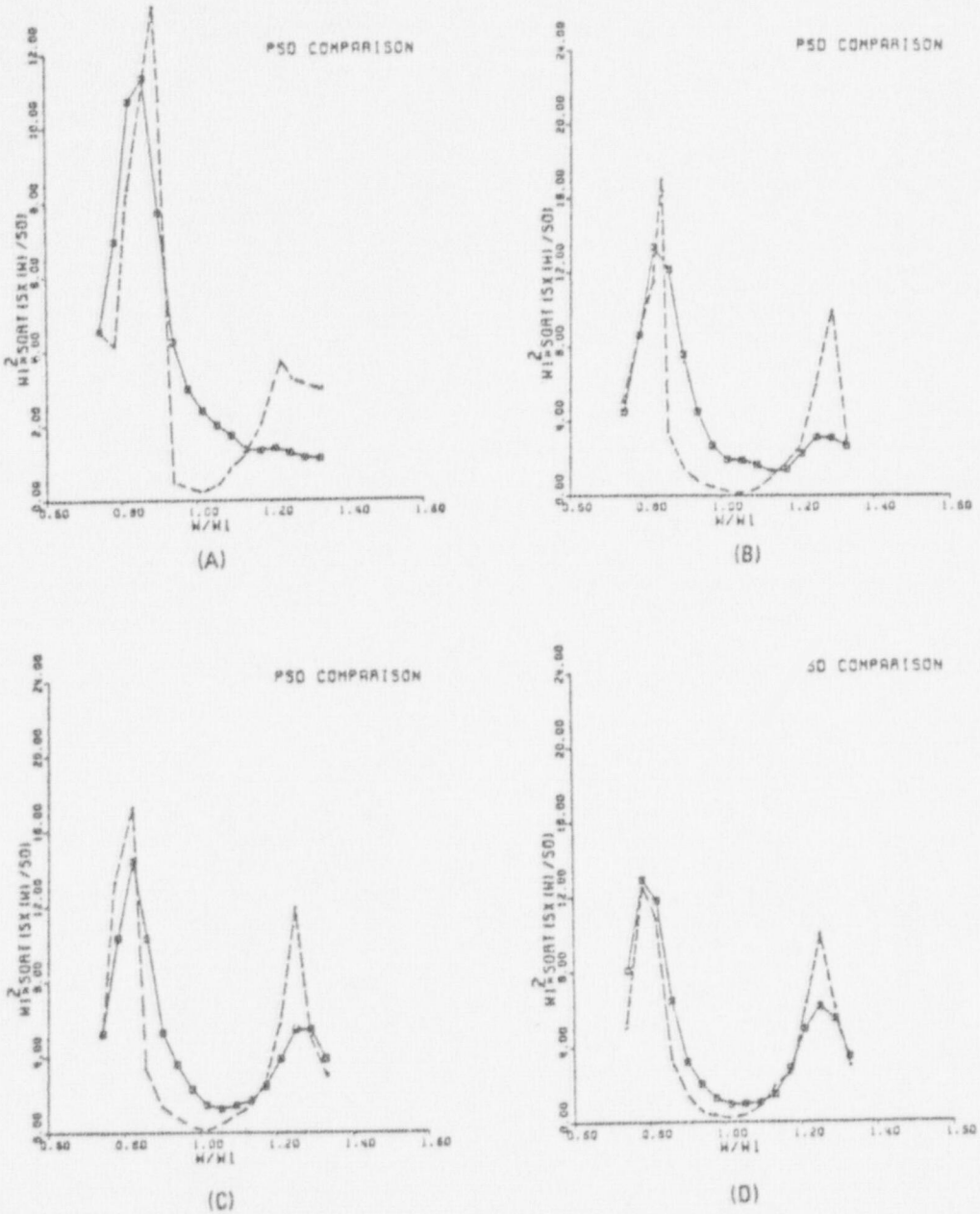

FIGURE 9 COMPARISON OF EXPERIMENTAL AND THEORETICAL PSD

$\omega_3/\omega_1 = 1.0$, $\zeta_1 = \zeta_3 = 0.01$, $\mu = 0.20$, $\omega_2/\omega_1 = 10.0$, $\zeta_2 = 0.1$.

(A) $D/\sigma_{x_o} = 2$; (B) $D/\sigma_{x_o} = 4$; (C) $D/\sigma_{x_o} = 6$; (D) $D/\sigma_{x_o} = 8$.

— — — Theory ——— Experimental

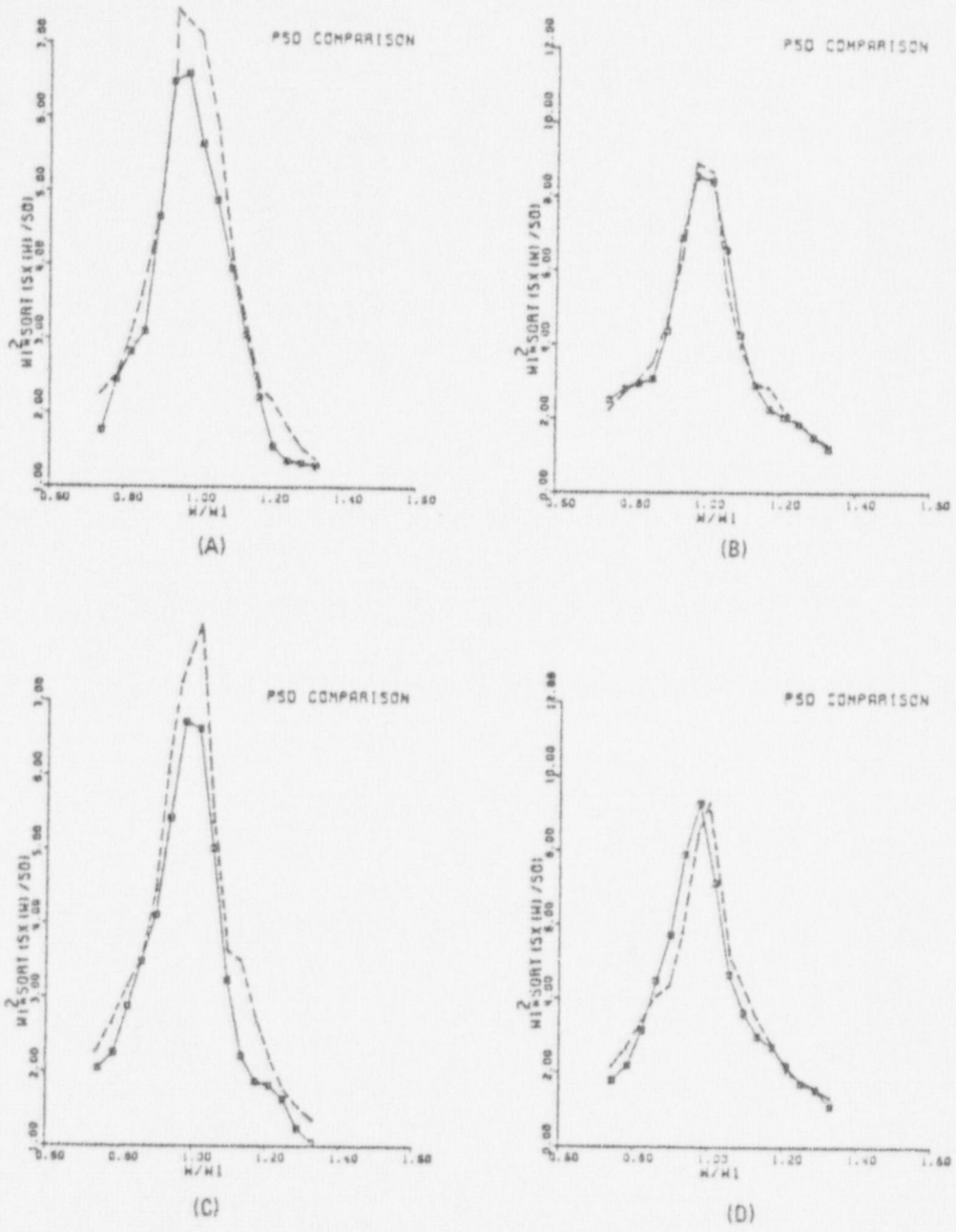

FIGURE 10 COMPARISON OF EXPERIMENTAL AND THEORETICAL PSD

$\omega_3/\omega_1 = 1.0$, $\zeta_1 = \zeta_3 = 0.05$, $\mu = 0.01$, $\omega_2/\omega_1 = 10.0$, $\zeta_2 = 0.4$.

(A) $D/\sigma_{x_o} = 2$; (B) $D/\sigma_{x_o} = 4$; (C) $D/\sigma_{x_o} = 6$; (D) $D/\sigma_{x_o} = 8$.

– – – Theory ——— Experimental

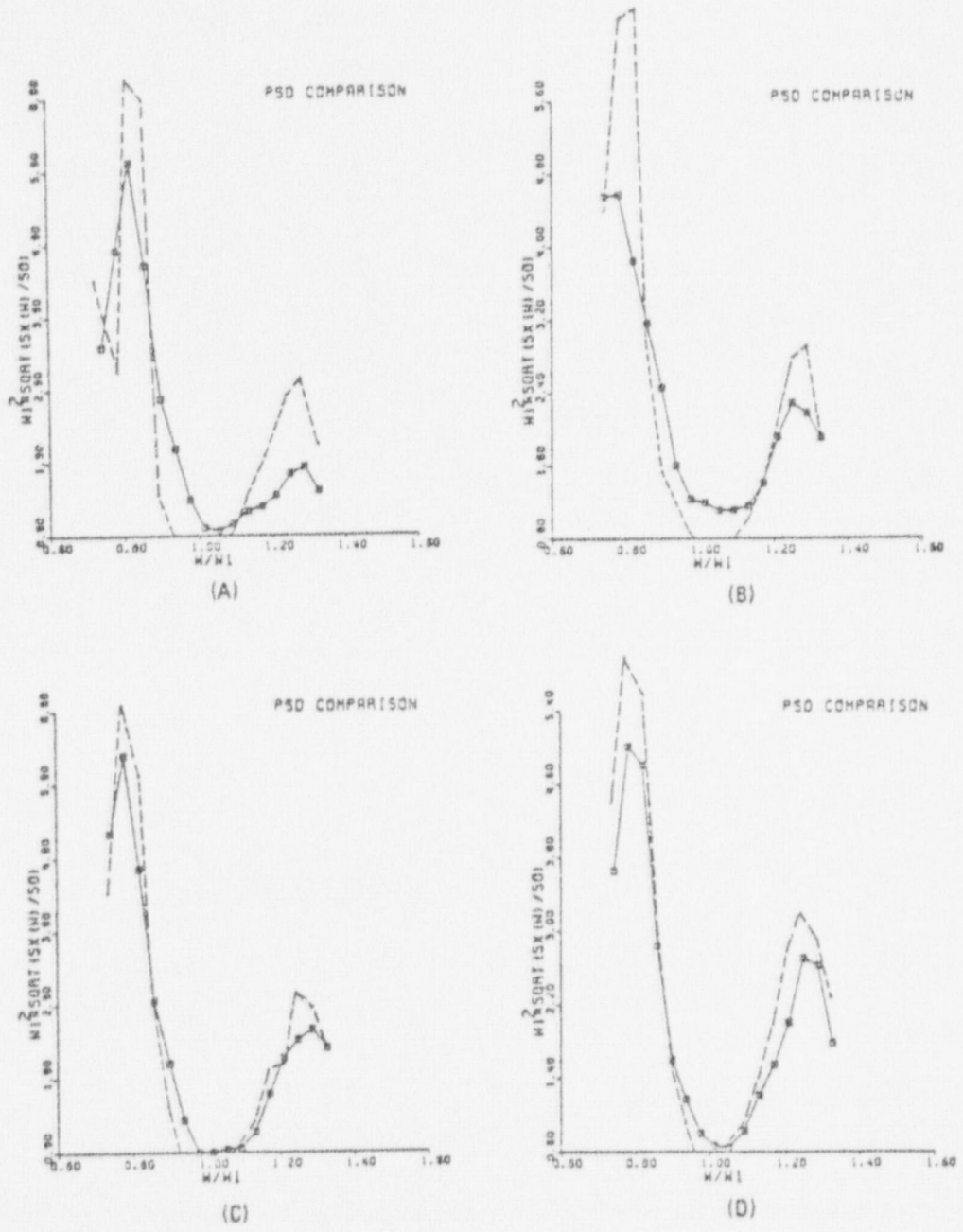

FIGURE 11 COMPARISON OF EXPERIMENTAL AND THEORETICAL PSD

$\omega_3/\omega_1 = 1.0$, $\zeta_1 = \zeta_3 = 0.05$, $\mu = 0.20$, $\omega_2/\omega_1 = 10.0$, $\zeta_2 = 0.4$.

(A) $D/\sigma_{x_o} = 4$; (B) $D/\sigma_{x_o} = 6$; (C) $D/\sigma_{x_o} = 8$; (D) $D/\sigma_{x_o} = 10$.

— — — Theory ——— Experimental

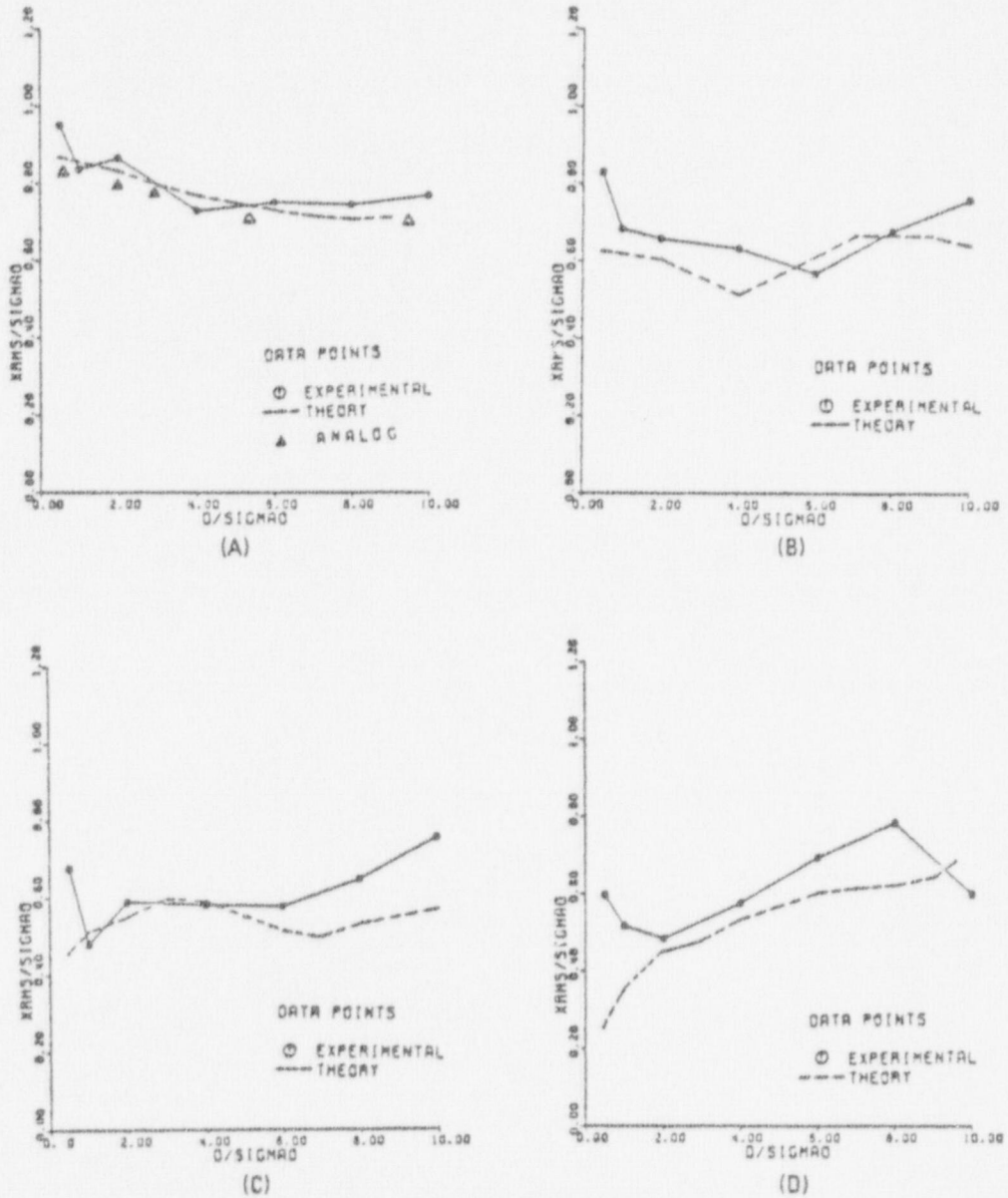

FIGURE 12 COMPARISON OF THEORETICAL AND EXPERIMENTAL RMS DISPLACEMENTS

$\omega_3/\omega_1 = 1.0$, $\zeta_1 = \zeta_3 = 0.01$, $\zeta_2 = 0.4$, $\omega_2/\omega_1 = 10.0$.

(A) $\mu = 0.01$; (B) $\mu = 0.05$; (C) $\mu = 0.10$; (D) $\mu = 0.20$.

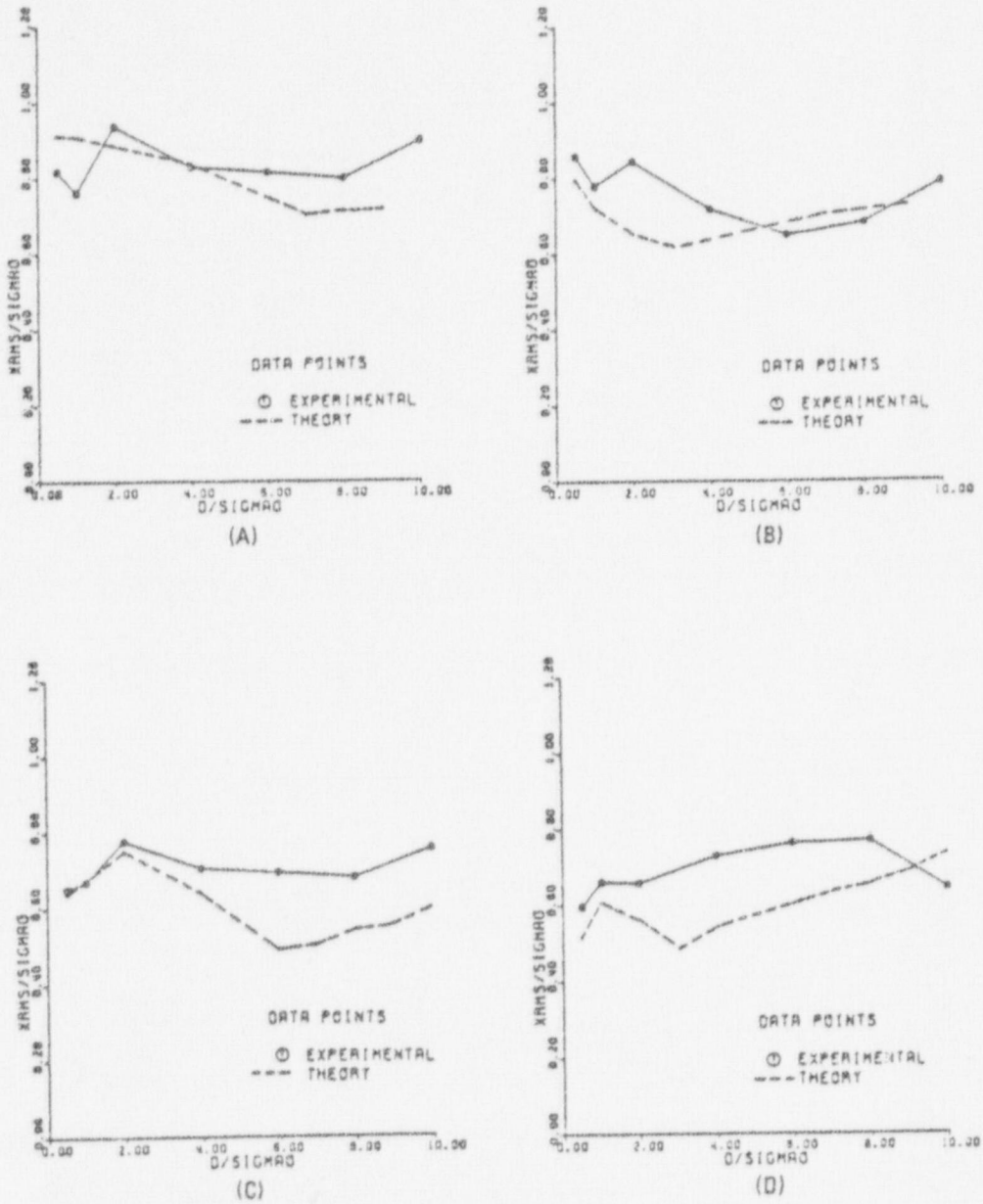

FIGURE 13 COMPARISON OF THEORETICAL AND EXPERIMENTAL RMS DISPLACEMENTS

$\omega_3/\omega_1 = 1.0$, $\zeta_1 = \zeta_3 = 0.01$, $\zeta_2 = 0.1$, $\omega_2/\omega_1 = 10.0$.

(A) $\mu = 0.01$; (B) $\mu = 0.05$; (C) $\mu = 0.10$; (D) $\mu = 0.20$.

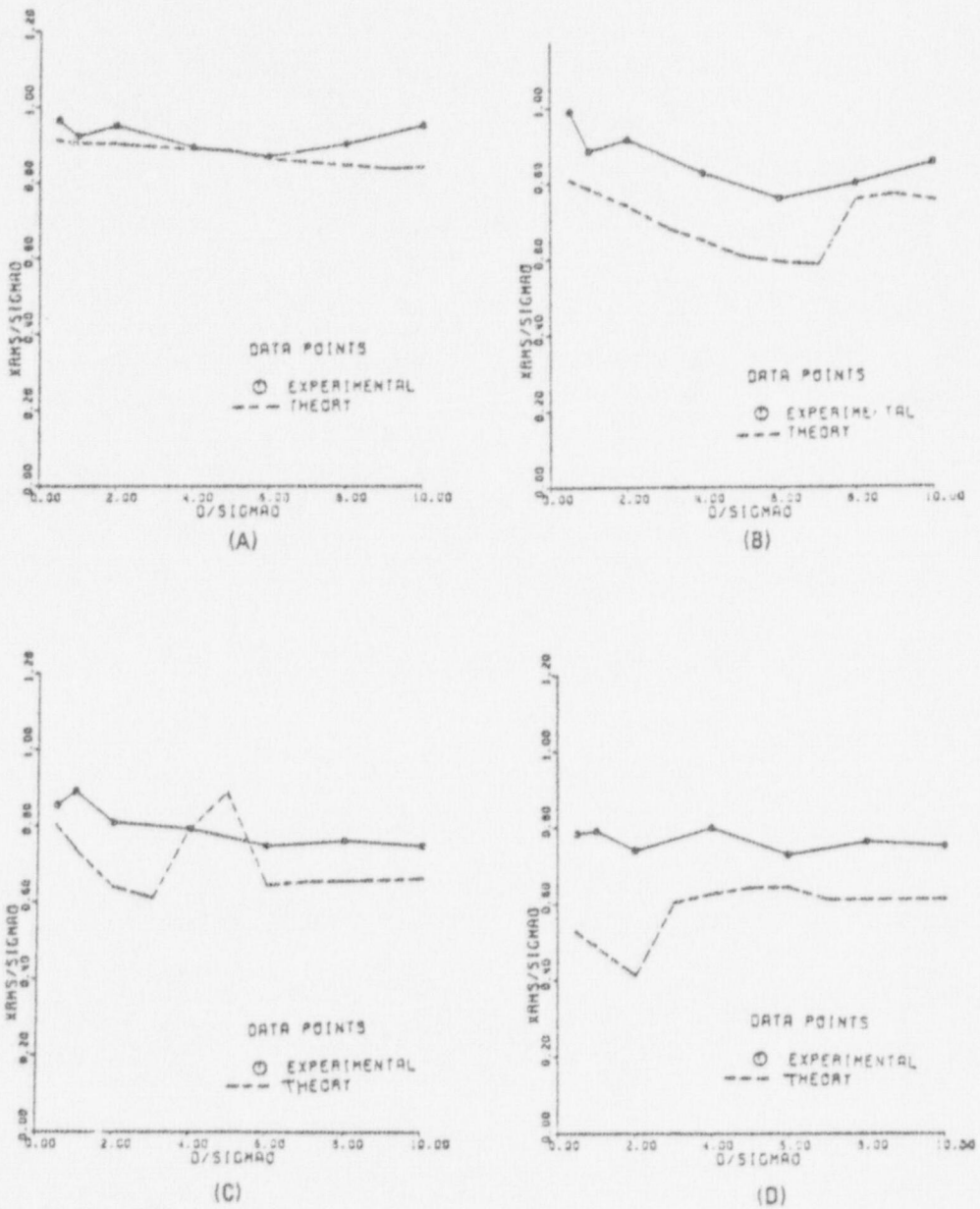

FIGURE 14 COMPARISON OF THEORETICAL AND EXPERIMENTAL RMS DISPLACEMENTS

$\omega_3/\omega_1 = 1.0$, $\zeta_1 = \zeta_3 = 0.05$, $\zeta_2 = 0.4$, $\omega_2/\omega_1 = 10.0$.

(A) $\mu = 0.01$; (B) $\mu = 0.05$; (C) $\mu = 0.10$; (D) $\mu = 0.20$.

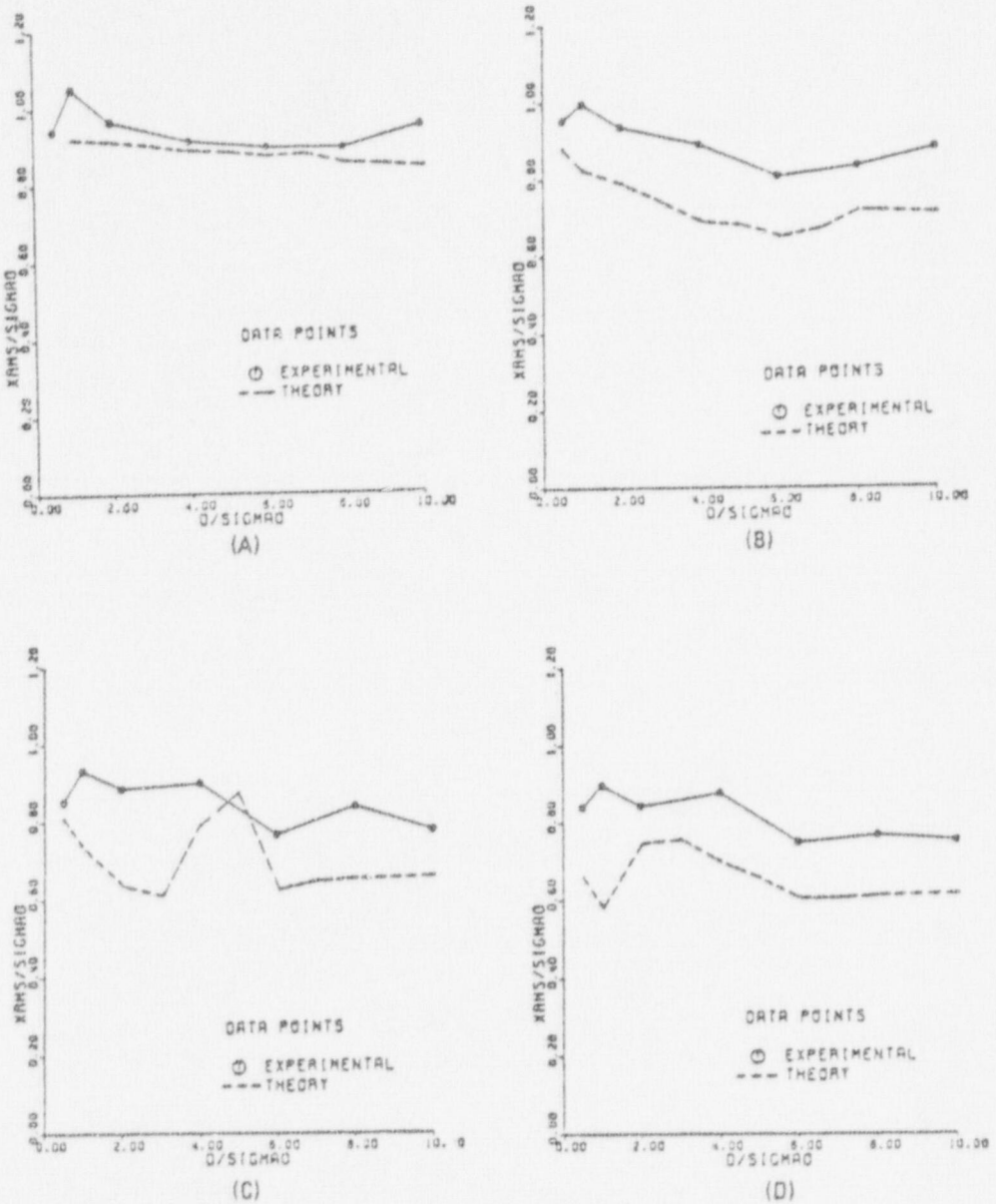

FIGURE 15 COMPARISON OF THEORETICAL AND EXPERIMENTAL RMS DISPLACEMENTS

$\omega_3/\omega_1 = 1.0$, $\zeta_1 = \zeta_3 = 0.05$, $\zeta_2 = 0.1$, $\omega_2/\omega_1 = 10.0$.

(A) $\mu = 0.01$; (B) $\mu = 0.05$; (C) $\mu = 0.10$; (D) $\mu = 0.20$.

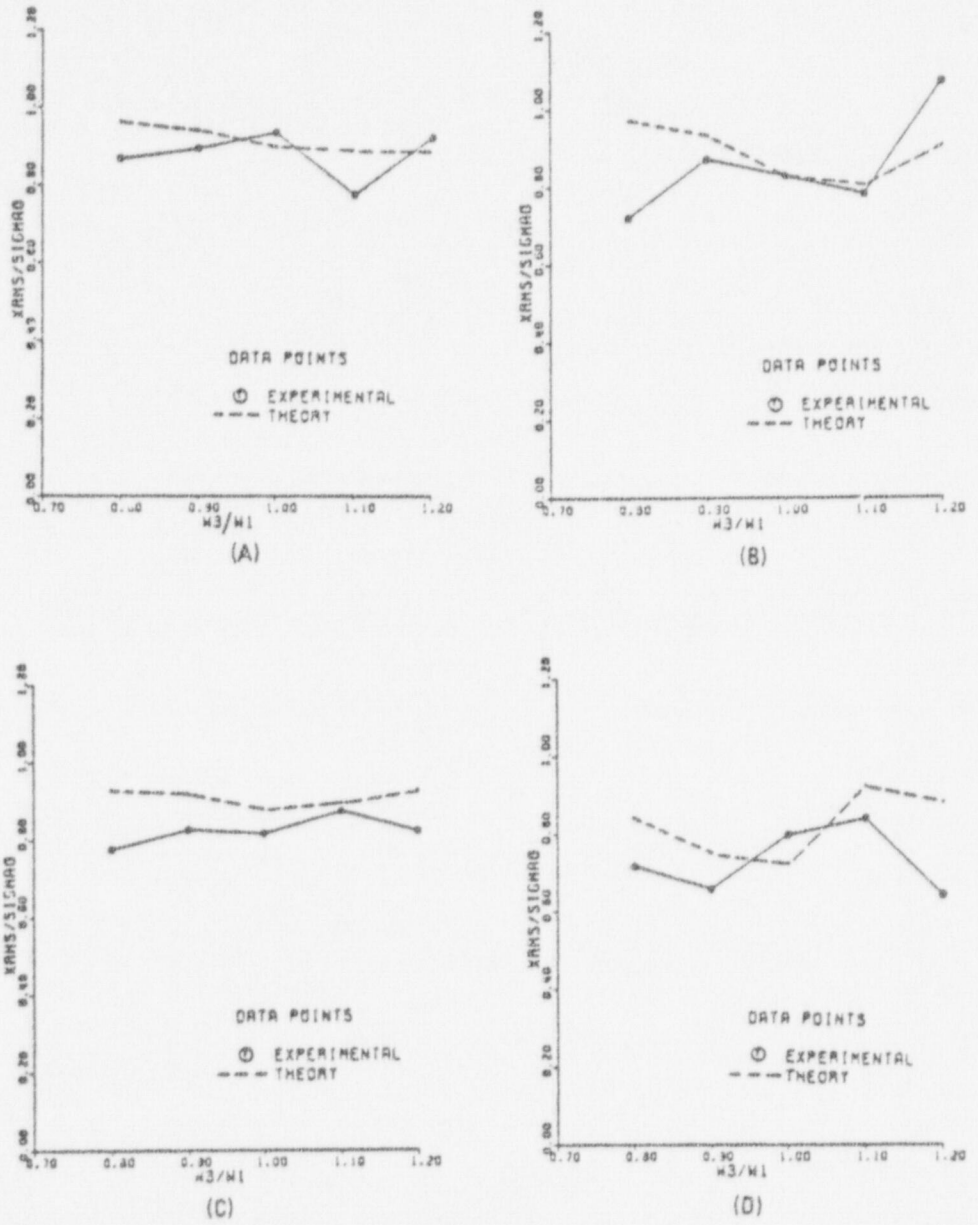

FIGURE 16 COMPARISON OF THEORETICAL AND EXPERIMENTAL RMS DISPLACEMENTS

$\zeta_1 = \zeta_3 = 0.01$, $\mu = 0.01$, $\omega_2/\omega_1 = 10.0$, $\zeta_2 = 0.1$.

(A) $D/\sigma_{x_o} = 2$; (B) $D/\sigma_{x_o} = 4$; (C) $D/\sigma_{x_o} = 6$; (D) $D/\sigma_{x_o} = 8$.

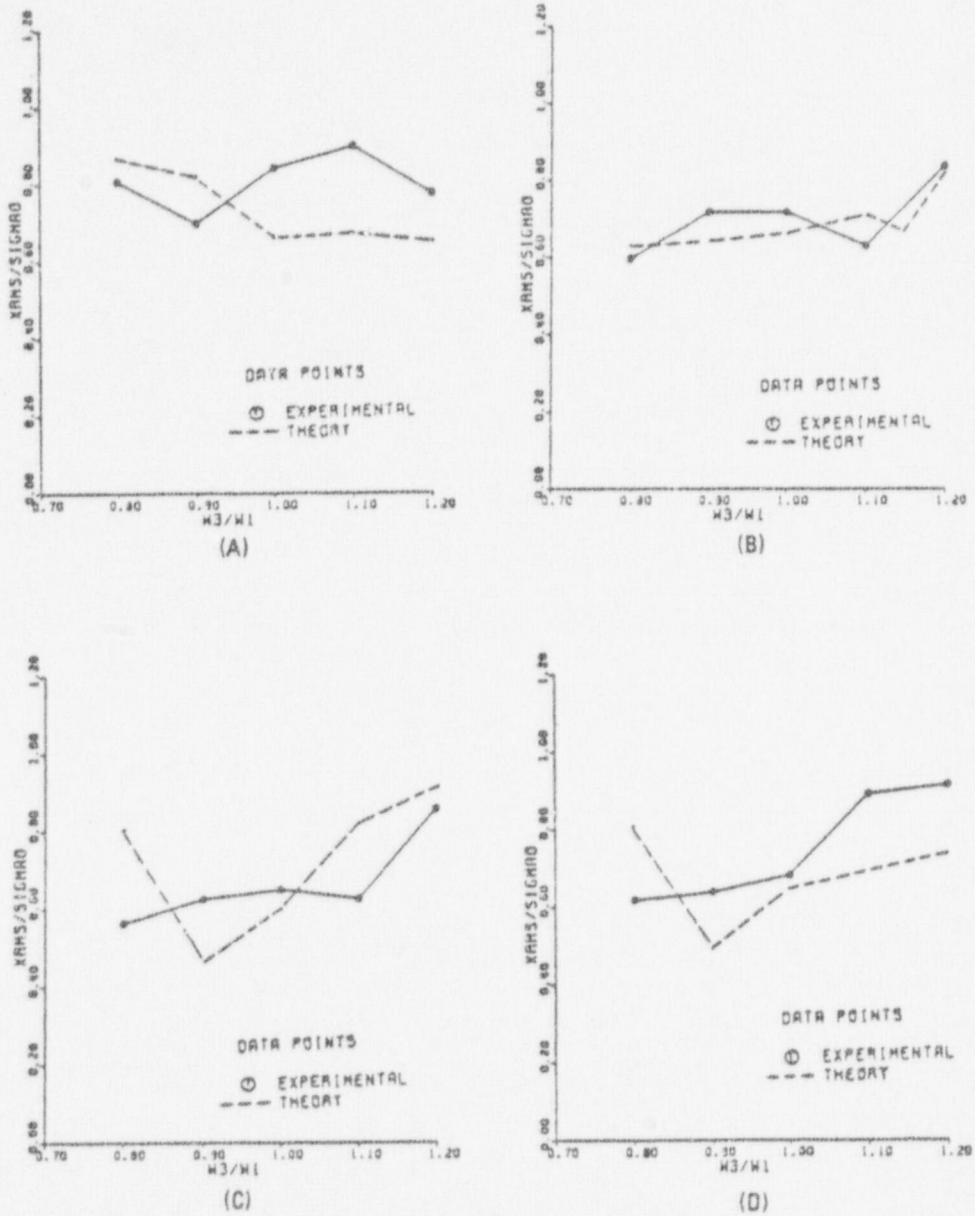

FIGURE 17 COMPARISON OF THEORETICAL AND EXPERIMENTAL RMS DISPLACEMENTS

$\zeta_1 = \zeta_3 = 0.01$, $\mu = 0.05$, $\omega_2/\omega_1 = 10.0$, $\zeta_2 = 0.1$.

(A) $D/\sigma_{x_o} = 2$; (B) $D/\sigma_{x_o} = 4$; (C) $D/\sigma_{x_o} = 6$; (D) $D/\sigma_{x_o} = 8$.

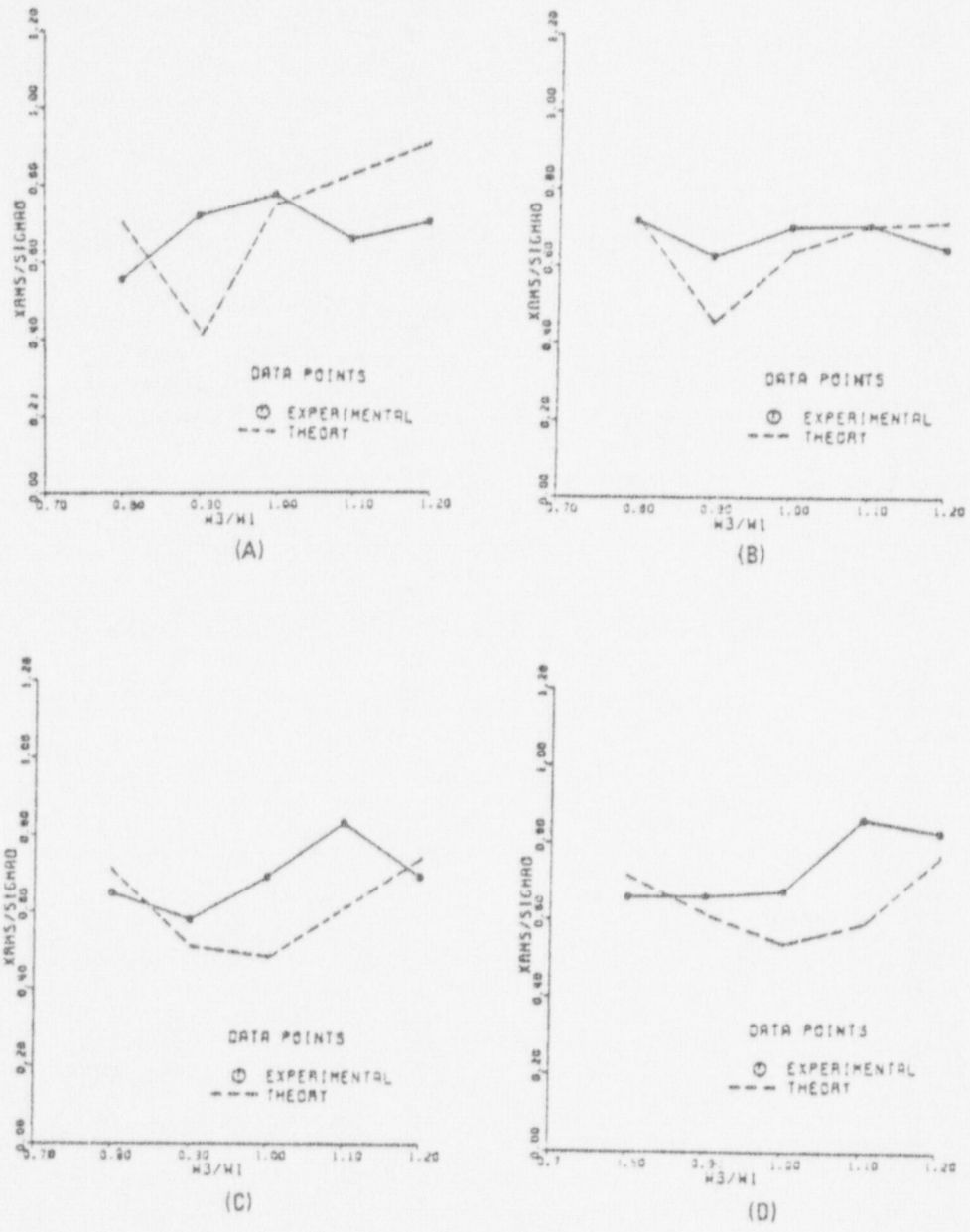

FIGURE 18 COMPARISON OF THEORETICAL AND EXPERIMENTAL RMS DISPLACEMENTS

$\zeta_1 = \zeta_3 = 0.01$, $\mu = 0.10$, $\omega_2/\omega_1 = 10.0$, $\zeta_2 = 0.1$.

(A) $D/\sigma_{x_o} = 2$; (B) $D/\sigma_{x_o} = 4$; (C) $D/\sigma_{x_o} = 6$; (D) $D/\sigma_{x_o} = 8$.

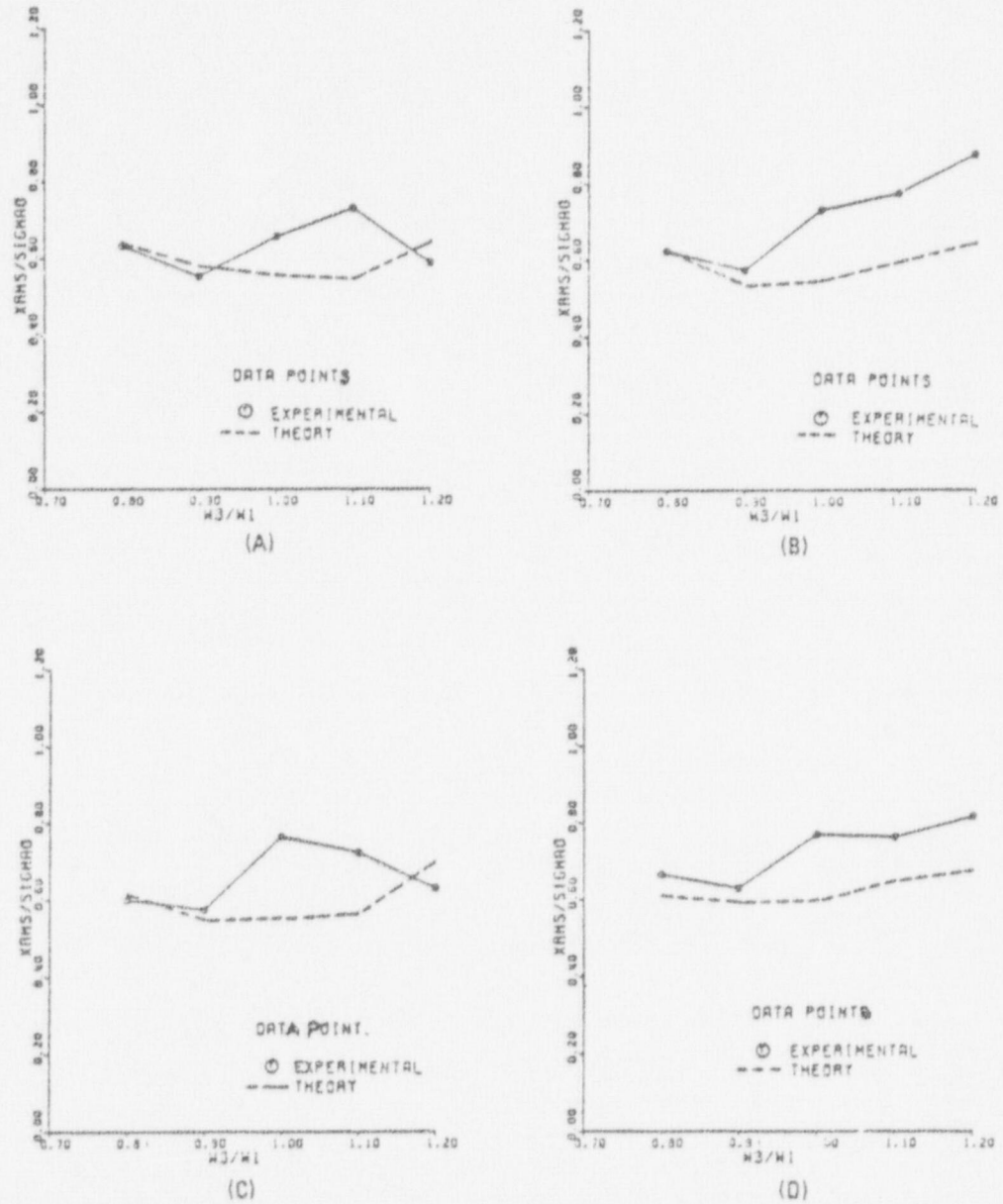

FIGURE 19 COMPARISON OF THEORETICAL AND EXPERIMENTAL RMS DISPLACEMENTS

$\zeta_1 = \zeta_3 = 0.01$, $\mu = 0.20$, $\omega_2/\omega_1 = 10.0$, $\zeta_2 = 0.1$.

(A) $D/\sigma_{x_o} = 2$; (B) $D/\sigma_{x_o} = 4$; (C) $D/\sigma_{x_o} = 6$; (D) $D/\sigma_{x_o} = 8$.

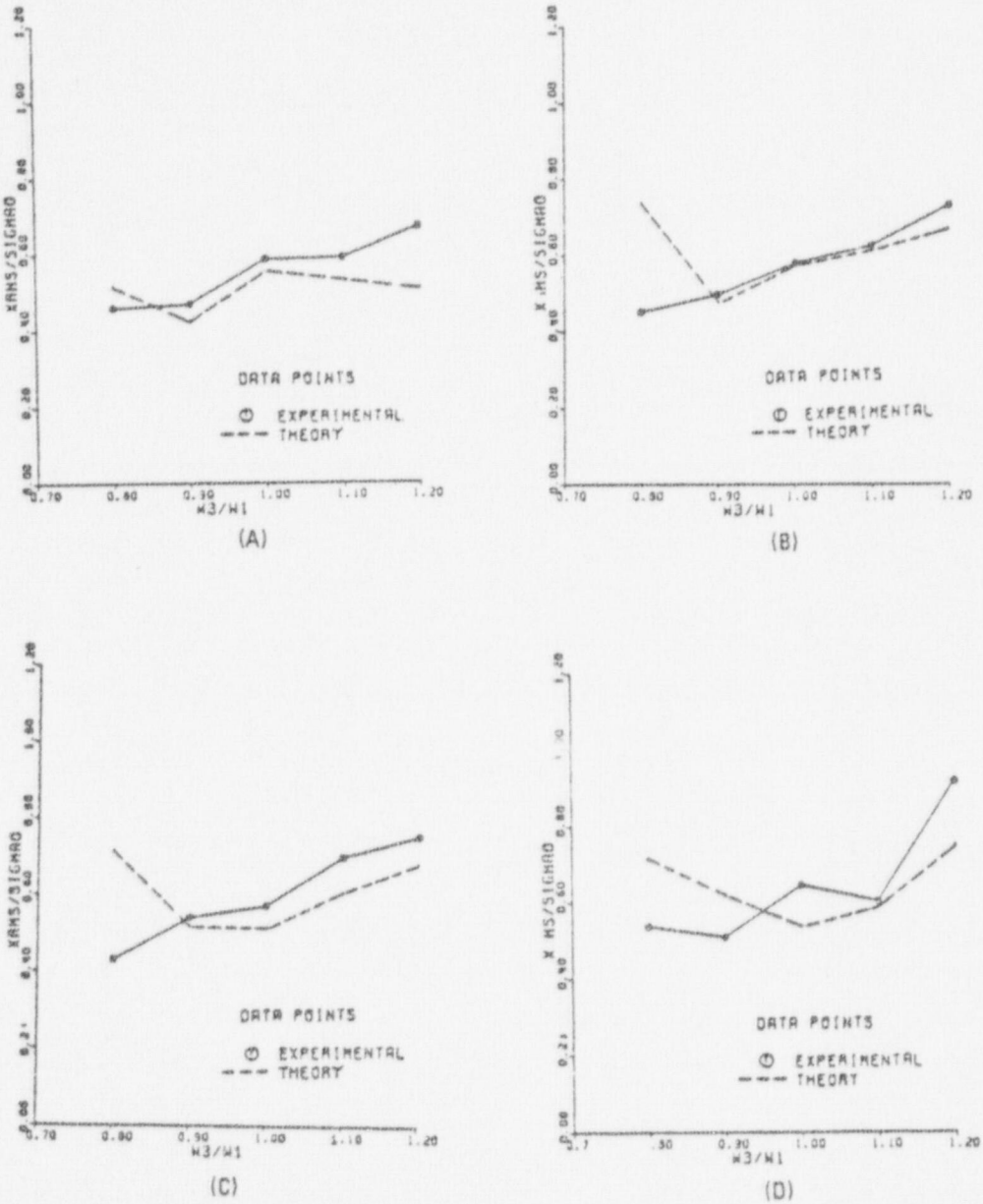

FIGURE 20 COMPARISON OF THEORETICAL AND EXPERIMENTAL RMS DISPLACEMENTS

$\zeta_1 = \zeta_3 = 0.01$, $\mu = 0.10$, $\omega_2/\omega_1 = 10.0$, $\zeta_2 = 0.4$.

(A) $D/\sigma_{x_o} = 2$; (B) $D/\sigma_{x_o} = 4$; (D) $D/\sigma_{x_o} = 6$; (D) $D/\sigma_{x_o} = 8$.

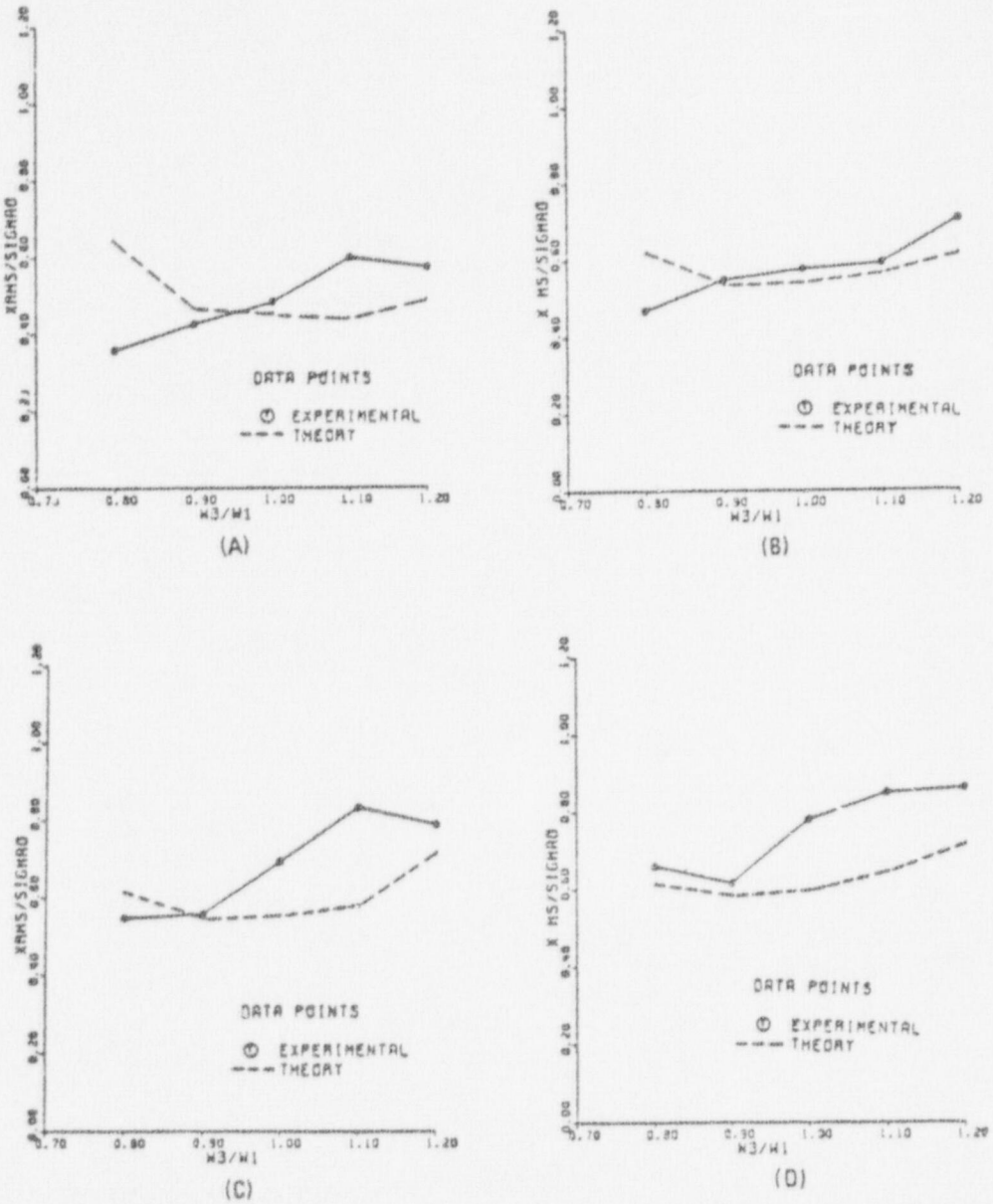

FIGURE 21 COMPARISON OF THEORETICAL AND EXPERIMENTAL RMS DISPLACEMENTS

$\zeta_1 = \zeta_3 = 0.01$, $\mu = 0.20$, $\omega_2/\omega_1 = 10.0$, $\zeta_2 = 0.4$.

(A) $D/\sigma_{x_o} = 2$; (B) $D/\sigma_{x_o} = 4$; (C) $D/\sigma_{x_o} = 6$; (D) $D/\sigma_{x_o} = 8$.

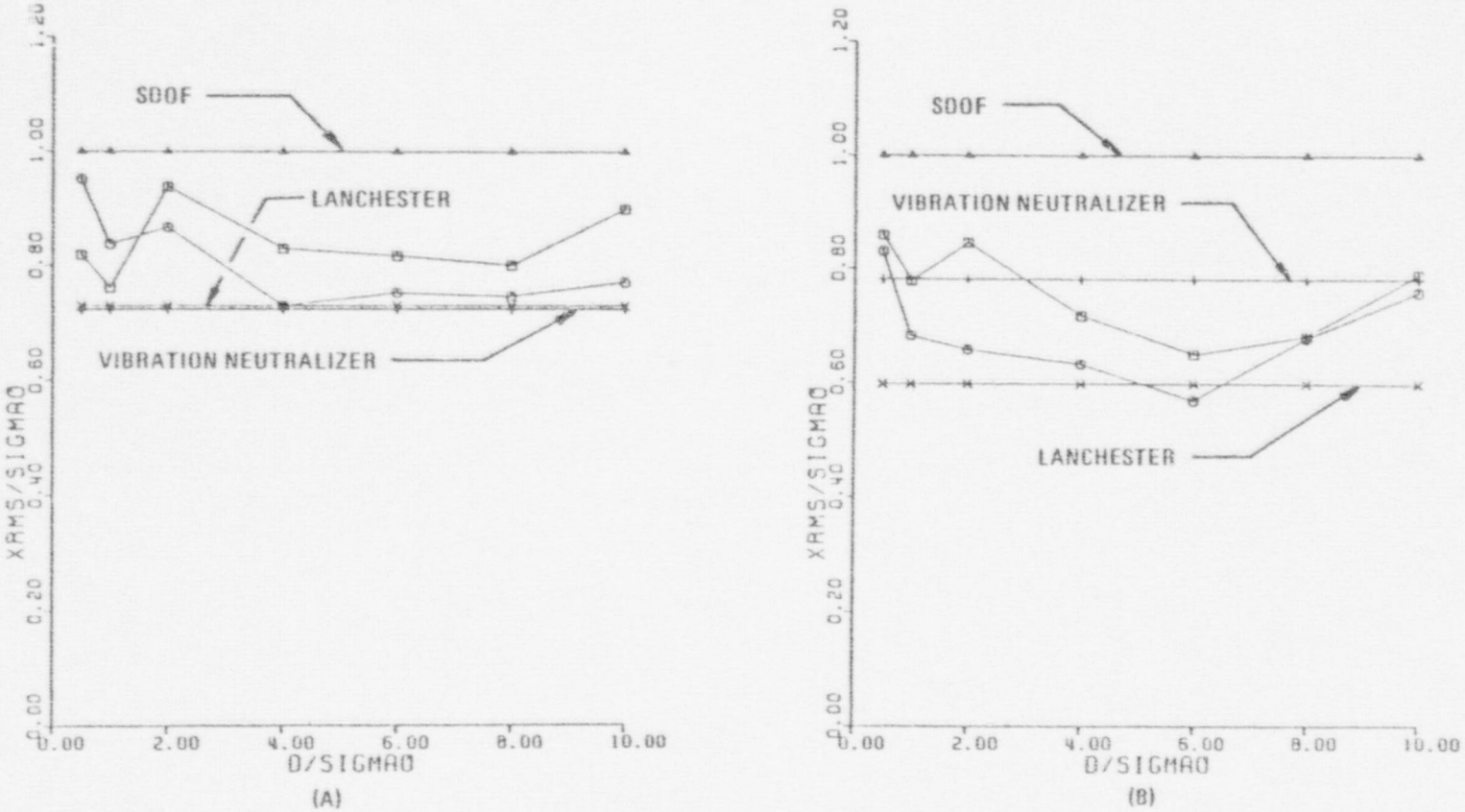

FIGURE 22 EXPERIMENTAL PARAMETER STUDY

$\omega_3/\omega_1 = 1.0$, $\zeta_1 = \zeta_3 = 0.01$.

(A) $\mu = 0.01$, (B) $\mu = 0.05$

Symbol	ζ_2	ω_2/ω_1
□	0.1	10.0
○	0.4	10.0

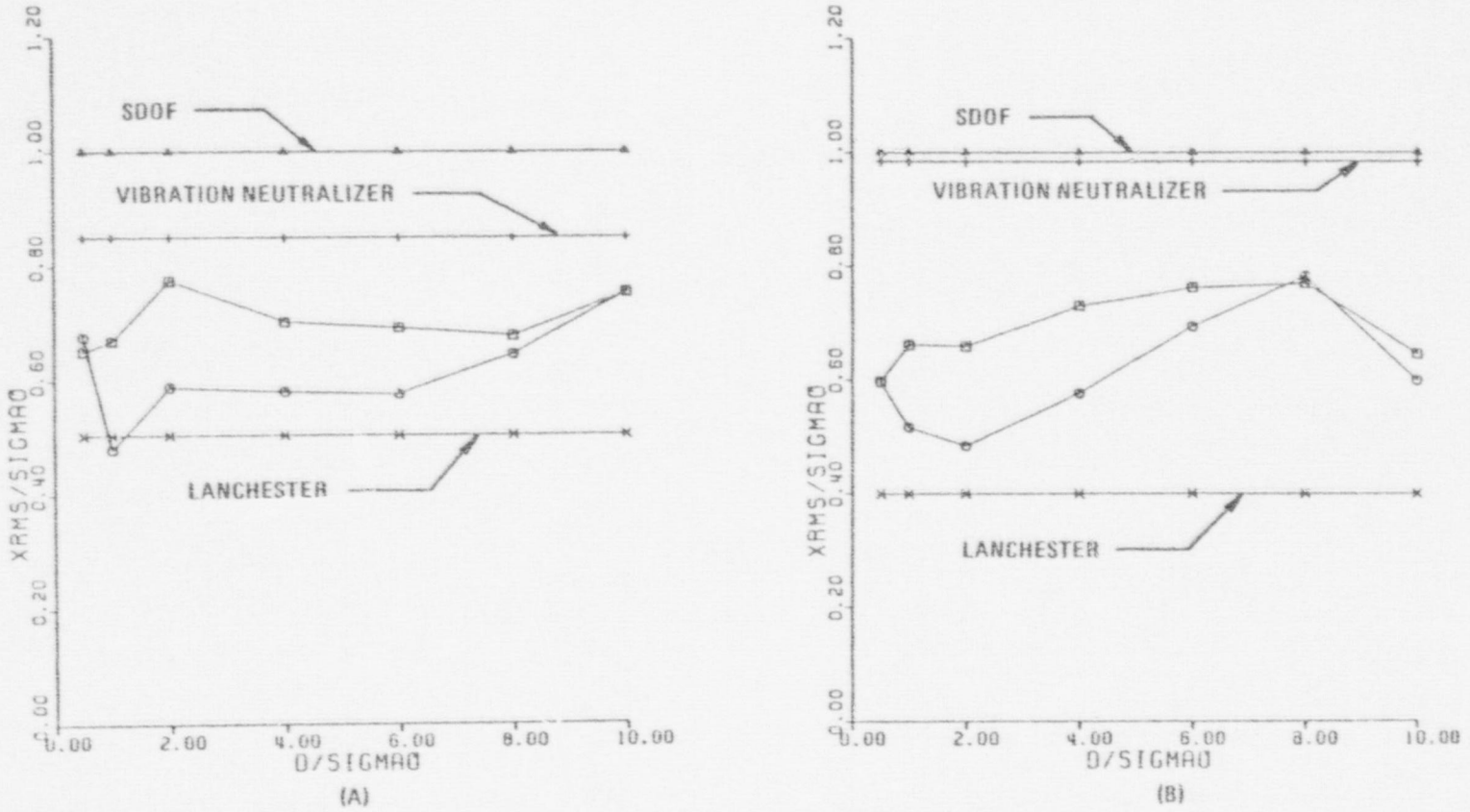

FIGURE 23 EXPERIMENTAL PARAMETER STUDY

$\omega_3/\omega_1 = 1.0$, $\zeta_1 = \zeta_3 = 0.01$.

(A) $\mu = 0.10$, (B) $\mu = 0.20$

Symbol	ζ_2	ω_2/ω_1
□	0.1	10.0
○	0.4	10.0

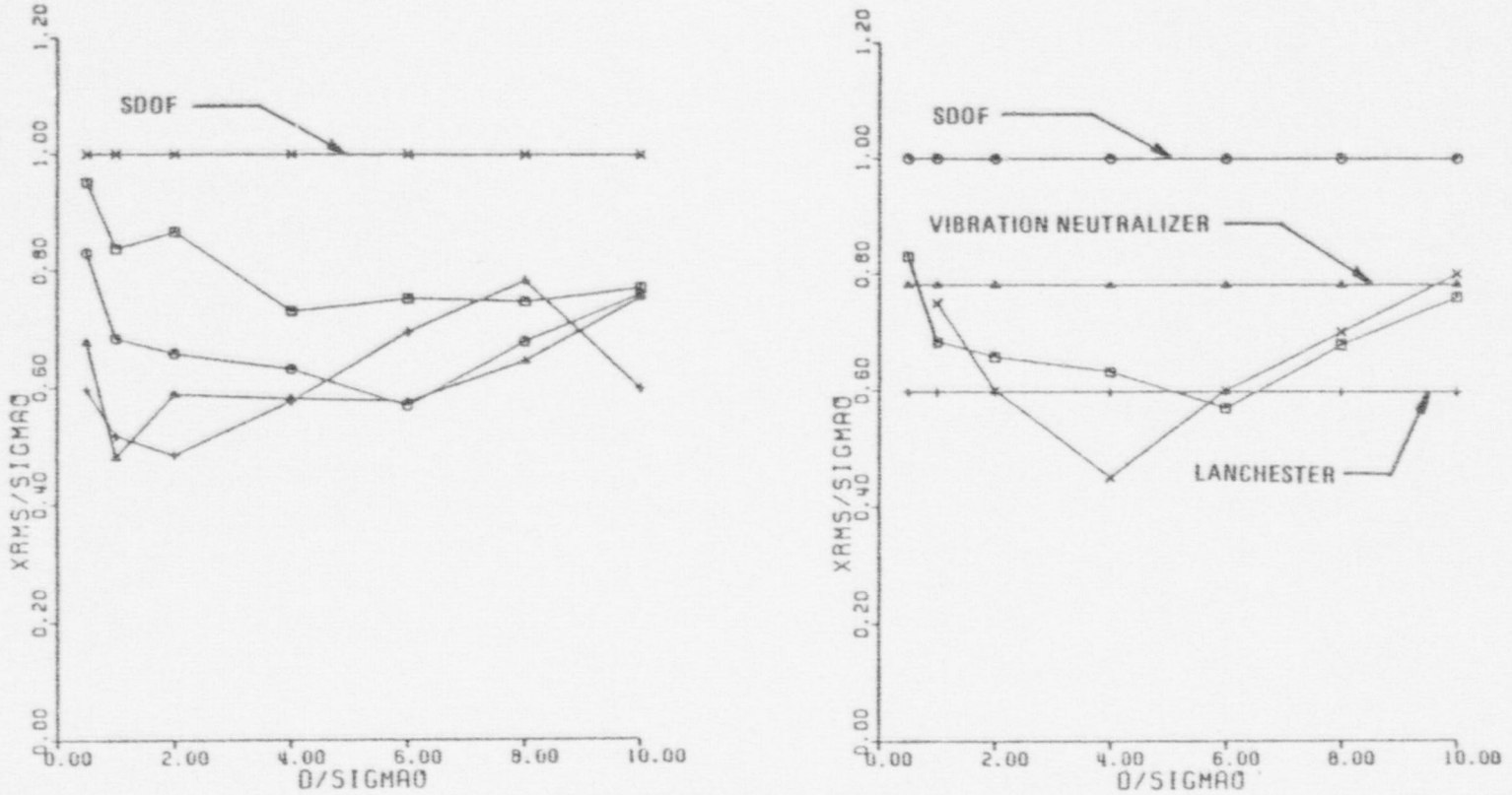

FIGURE 24 EXPERIMENTAL PARAMETER STUDY

(A) $\omega_3/\omega_1 = 1.0$, $\zeta_1 = \zeta_3 = 0.01$, $\omega_2/\omega_1 = 10.0$, $\zeta_2 = 0.4$

Symbol	μ
□	0.01
○	0.05
Δ	0.10
+	0.20

(B) $\zeta_1 = \zeta_3 = 0.01$, $\mu = 0.05$

Symbol	ω_3/ω_1	ω_2/ω_1	ζ_2
□	1.0	10.0	0.4
X	0	10.0	0.4

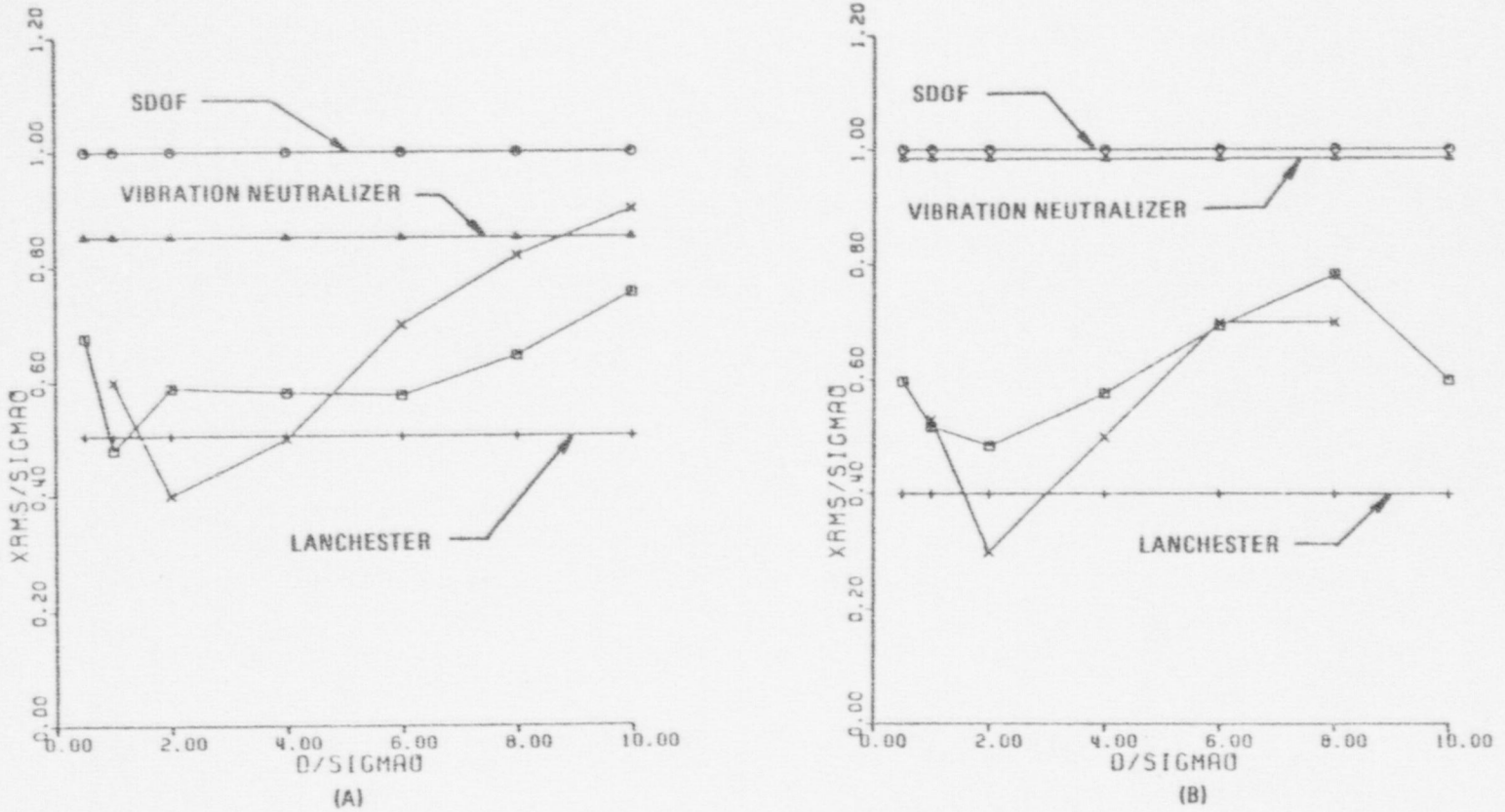

FIGURE 25 EXPERIMENTAL PARAMETER STUDY

$\zeta_1 = \zeta_3 = 0.01$

(A) $\mu = 0.10$, (B) $\mu = 0.20$

Symbol	ω_3/ω_1	ω_2/ω_1	ζ_2
□	1.0	10.0	0.4
X	0	10.0	0.4

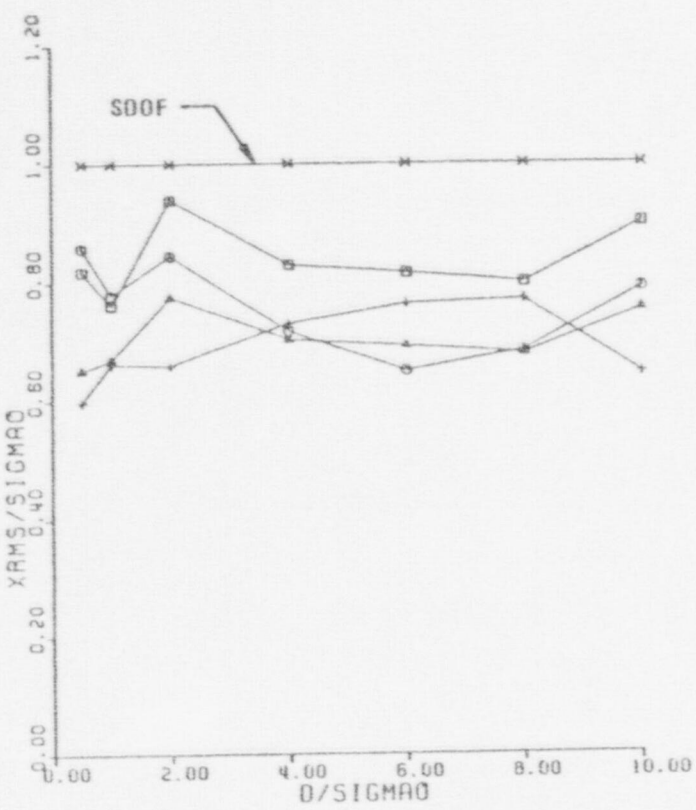

(A)

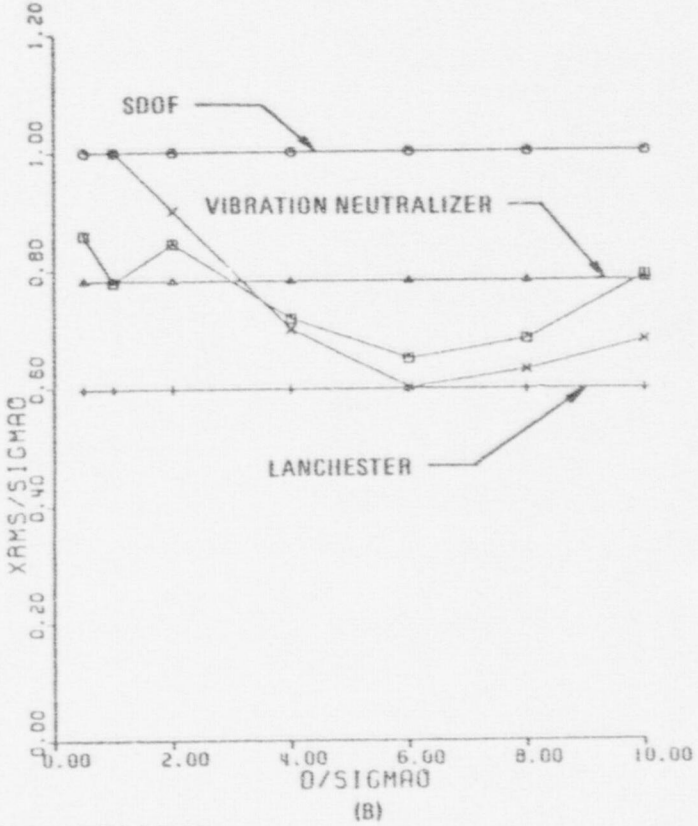

(B)

FIGURE 26 EXPERIMENTAL PARAMETER STUDY

(A) $\omega_3/\omega_1 = 1.0$, $\zeta_1 = \zeta_3 = 0.01$, $\omega_2/\omega_1 = 10.0$, $\zeta_2 = 0.10$; (B) $\zeta_1 = \zeta_3 = 0.01$, $\mu = 0.05$.

Symbol	μ
□	0.01
○	0.05
Δ	0.10
+	0.20

Symbol	ω_3/ω_1	ω_2/ω_1	ζ_2
□	1.0	10.0	0.1
X	0	10.0	0.1

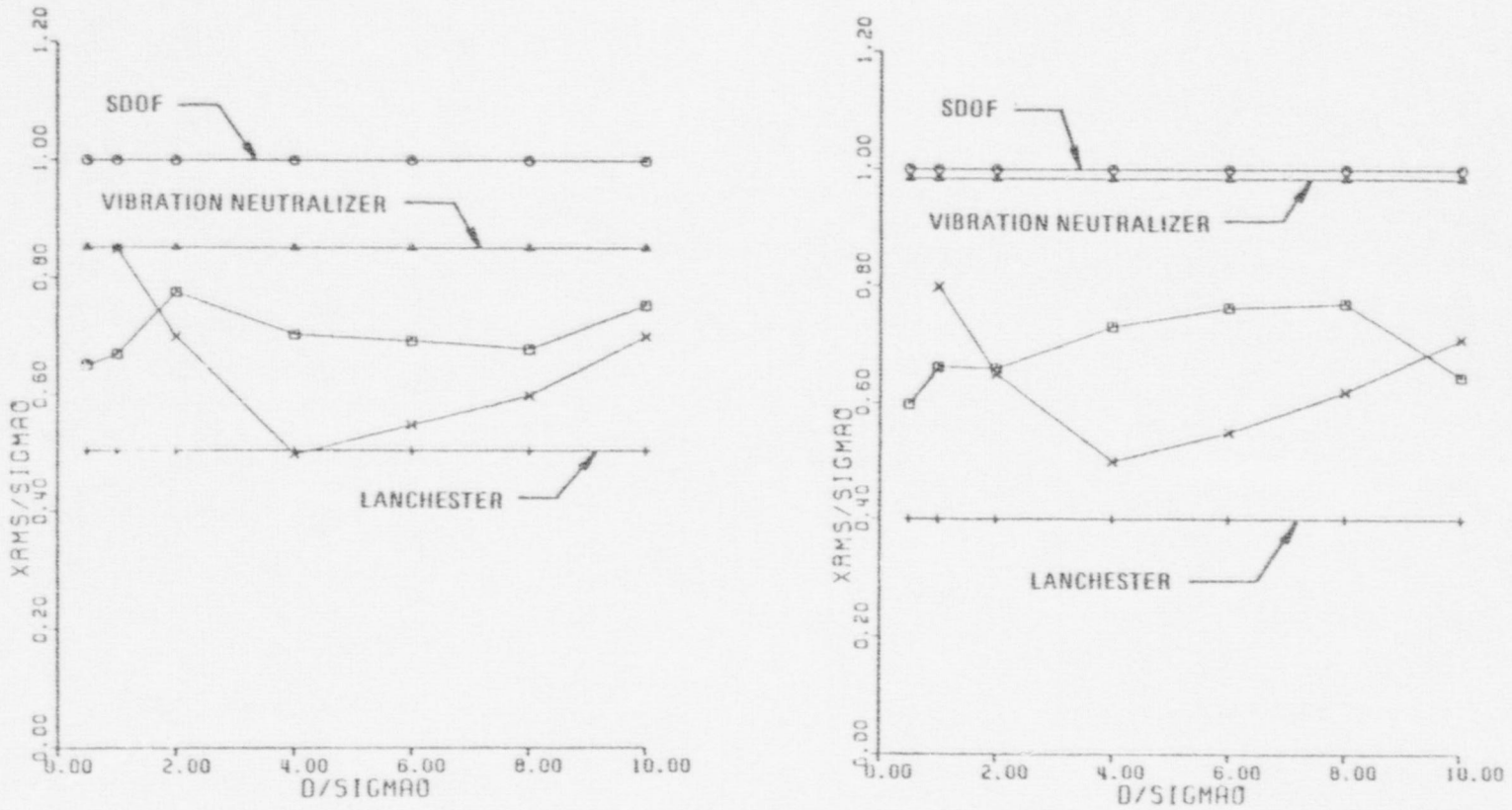

FIGURE 27 EXPERIMENTAL PARAMETER STUDY

$\zeta_1 = \zeta_3 = 0.01$, $\omega_2/\omega_1 = 10.0$, $\zeta_2 = 0.1$.

(A) $\mu = .10$; (B) $\mu = .20$

Symbol	ω_3/ω_1
□	1.0
X	0

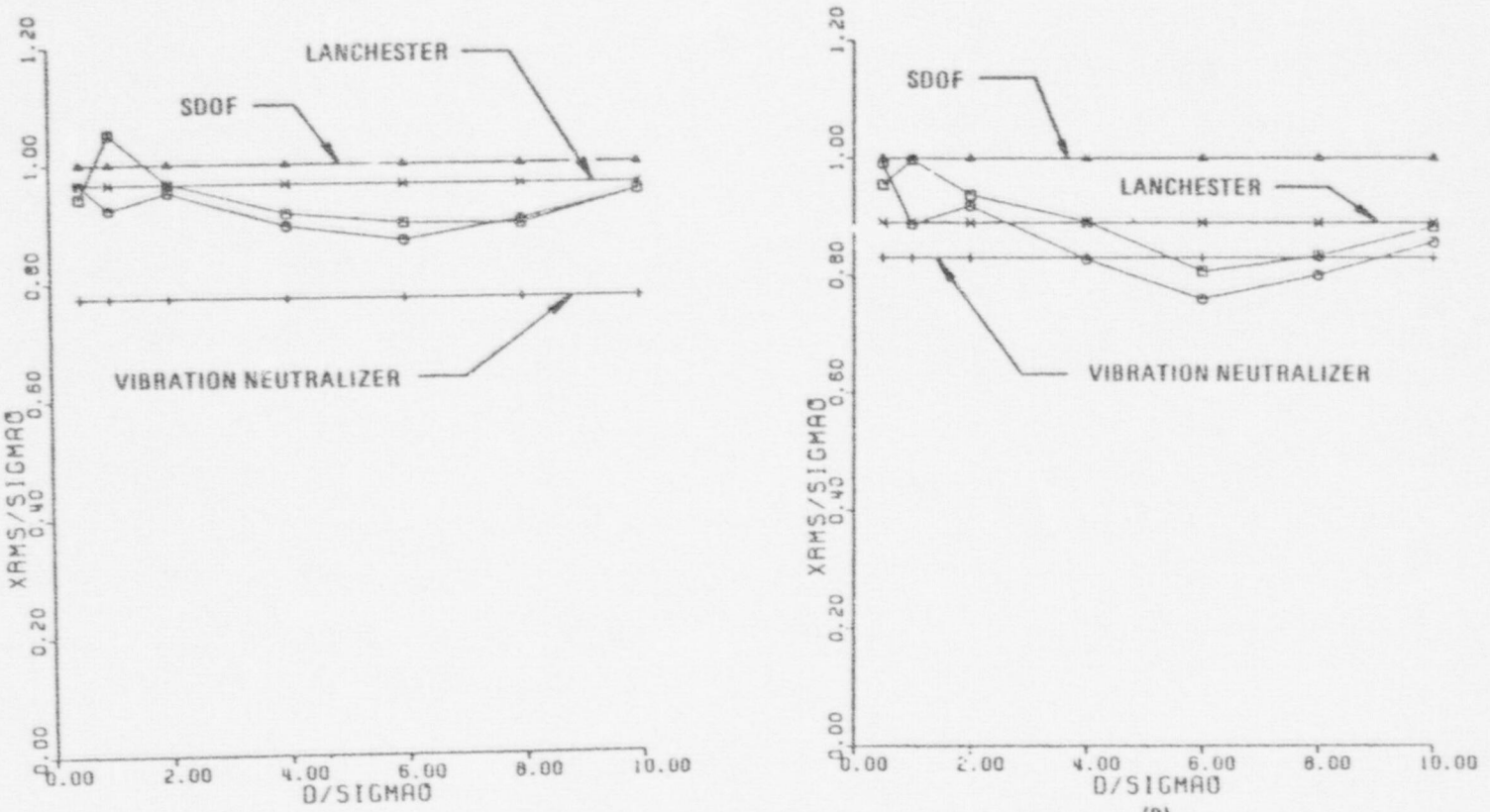

FIGURE 28 EXPERIMENTAL PARAMETER STUDY

$\omega_3/\omega_1 = 1.0$, $\zeta_1 = \zeta_3 = 0.05$, $\omega_2/\omega_1 = 10.0$

(A) $\mu = 0.01$; (B) $\mu = 0.05$

Symbol	ζ_2
□	0.1
○	0.4

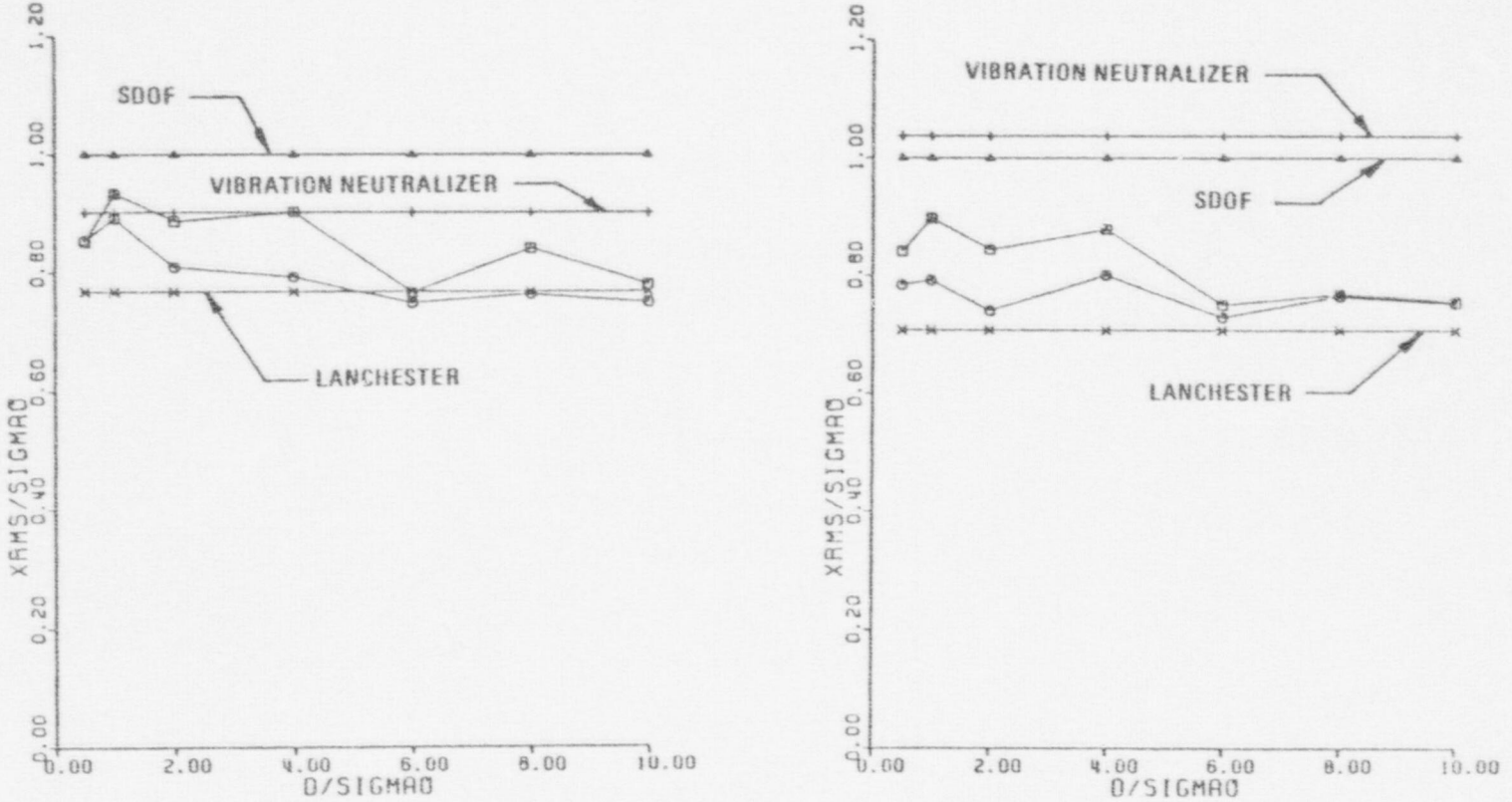

FIGURE 29 EXPERIMENTAL PARAMETER STUDY

$\omega_3/\omega_1 = 1.0$, $\zeta_1 = \zeta_3 = 0.05$, $\omega_2/\omega_1 = 10.0$.

(A) $\mu = 0.10$, (B) $\mu = 0.20$

Symbol	ζ_2
□	0.1
○	0.4

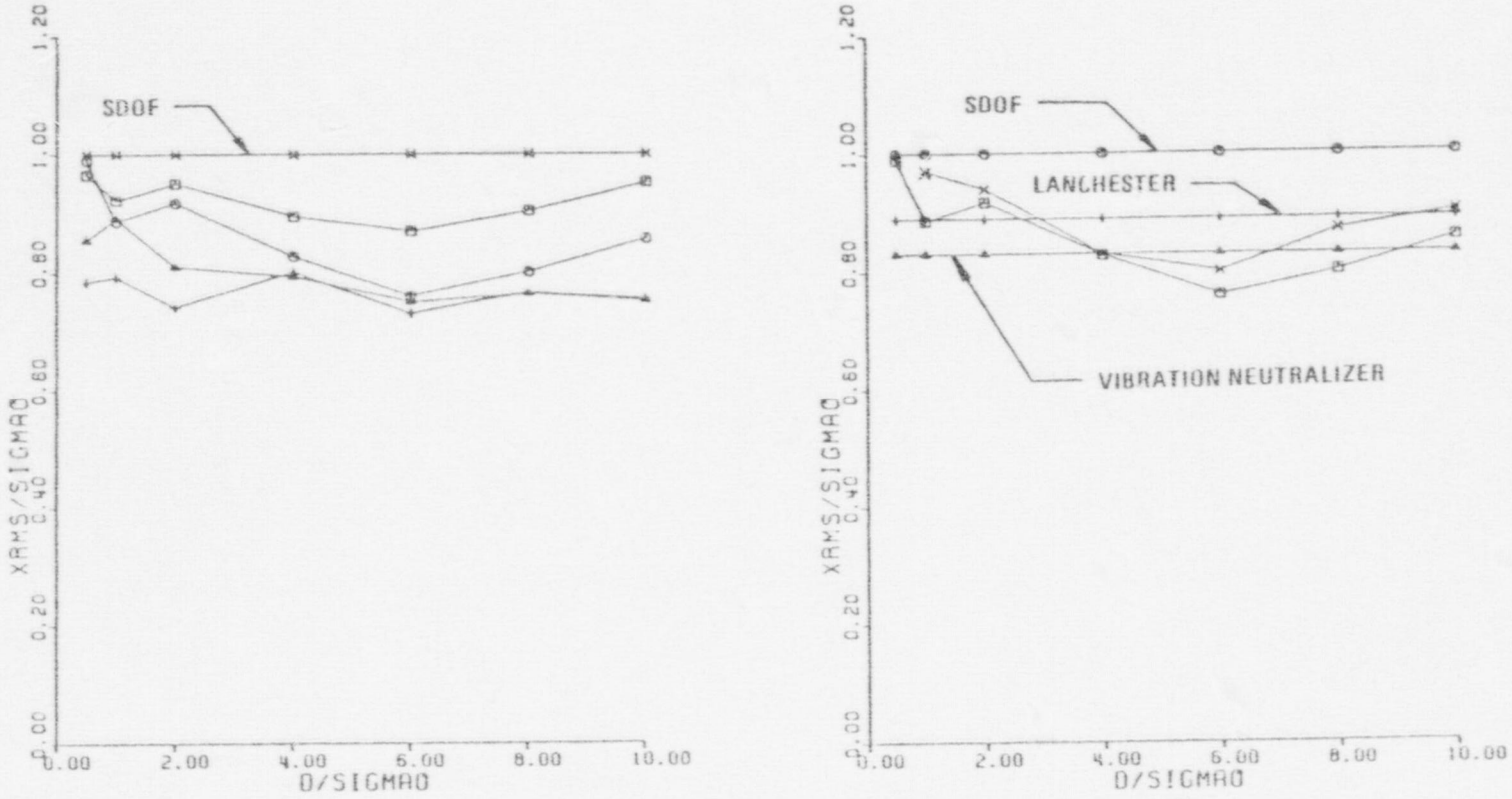

FIGURE 30 EXPERIMENTAL PARAMETER STUDY

(A) $\omega_3/\omega_1 = 1.0$, $\zeta_1 = \zeta_3 = 0.05$, $\omega_2/\omega_1 = 10.0$, $\zeta_2 = 0.4$; (B) $\zeta_1 = \zeta_3 = 0.05$, $\mu = 0.05$

Symbol	μ
□	0.01
○	0.05
Δ	0.10
+	0.20

Symbol	ω_3/ω_1	ω_2/ω_1	ζ_2
□	1.0	10.0	0.4
X	0	10.0	0.4

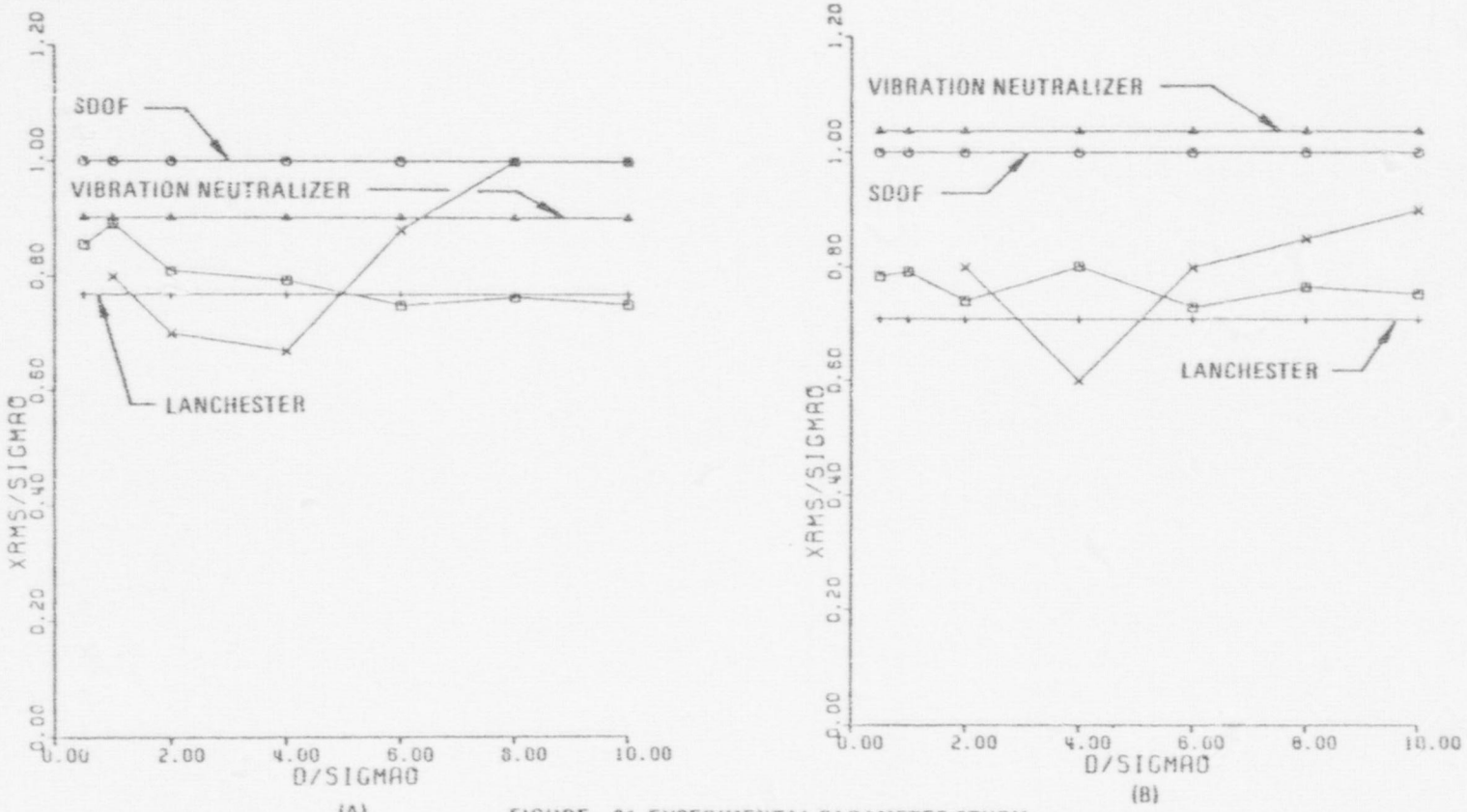

FIGURE 31 EXPERIMENTAL PARAMETER STUDY

$\zeta_1 = \zeta_3 = 0.05$, $\omega_2/\omega_1 = 10.0$, $\zeta_2 = 0.4$.

(A) $\mu = 0.10$; (B) $\mu = 0.20$

Symbol	ω_3/ω_1
□	1.0
X	0

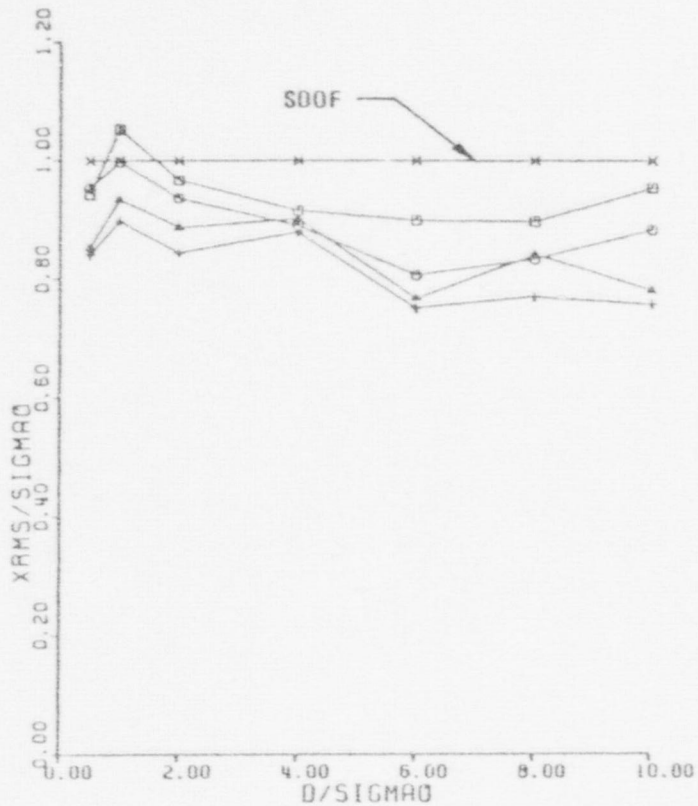

(A)

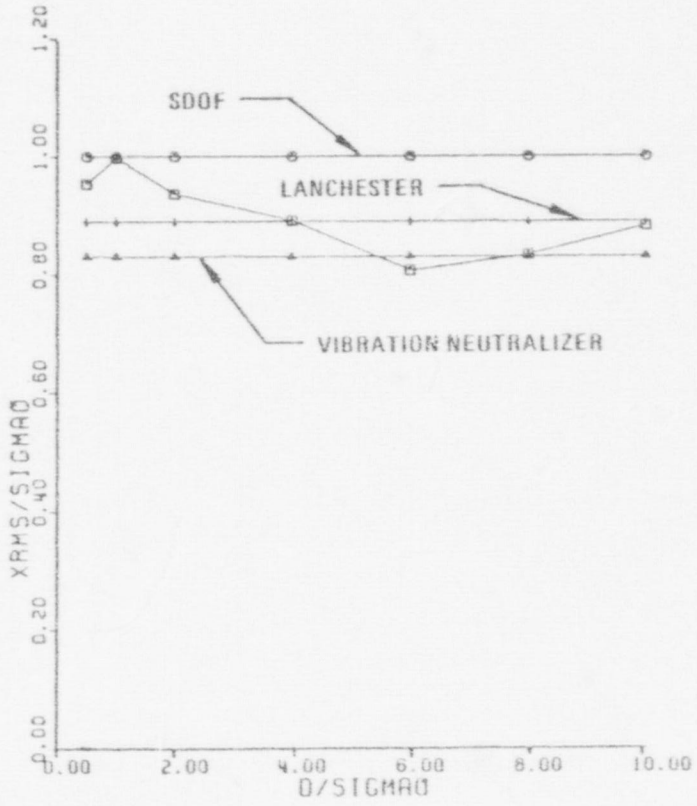

(B)

FIGURE 32 EXPERIMENTAL PARAMETER STUDY

(A) $\omega_3/\omega_1 = 1.0$, $\zeta_1 = \zeta_3 = 0.05$, $\omega_2/\omega_1 = 10.0$, $\zeta_2 = 0.1$; (B) $\zeta_1 = \zeta_3 = 0.05$, $\mu = 0.05$.

Symbol	μ
□	0.01
○	0.05
Δ	0.10
+	0.20

Symbol	ω_3/ω_1	ω_2/ω_1	ζ_2
□	1.0	10.0	0.1

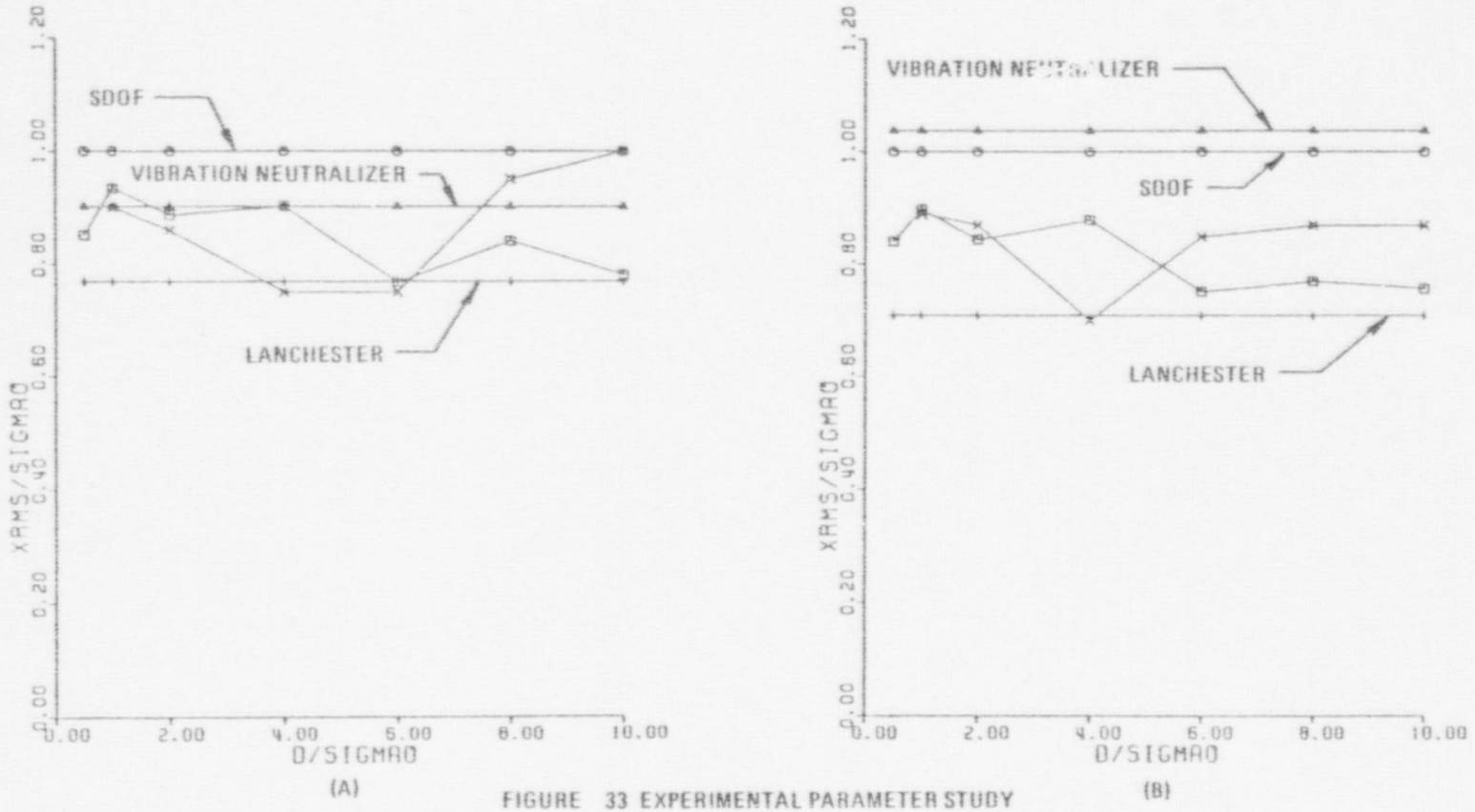

FIGURE 33 EXPERIMENTAL PARAMETER STUDY

$\zeta_1 = \zeta_3 = 0.05$, $\omega_2/\omega_1 = 10.0$, $\zeta_2 = 0.1$

(A) $\mu = 0.10$; (B) $\mu = 0.20$

Symbol	ω_3/ω_1
□	1.0
X	0

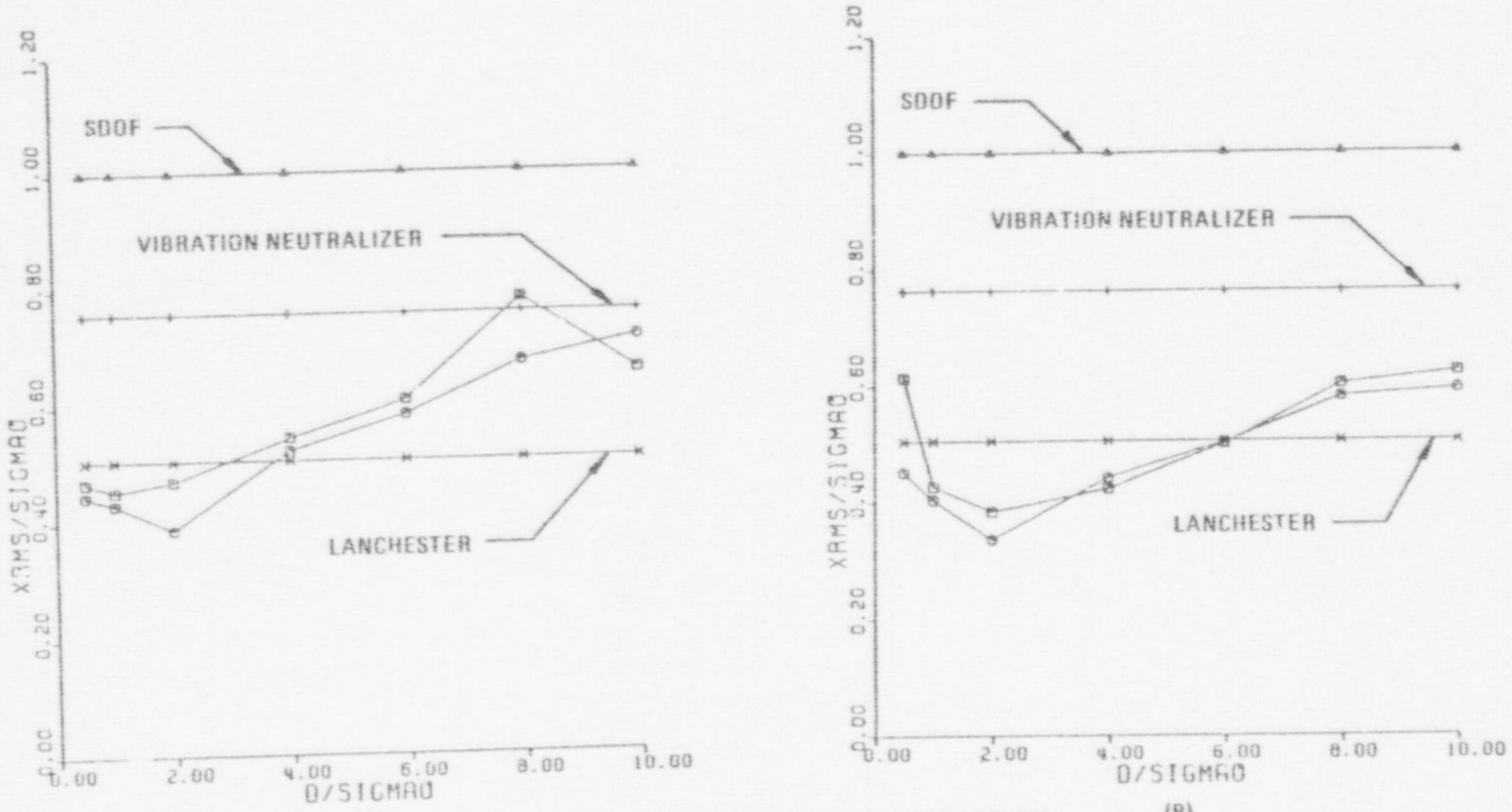

FIGURE 34 EXPERIMENTAL PARAMETER STUDY

$\zeta_1 = \zeta_3 = 0.01$, $\mu = 0.10$

(A) $\omega_3/\omega_1 = 0.8$; (B) $\omega_3/\omega_1 = 0.9$

Symbol	ω_2/ω_1	ζ_2
□	1.0	10.0
○	0.1	10.0

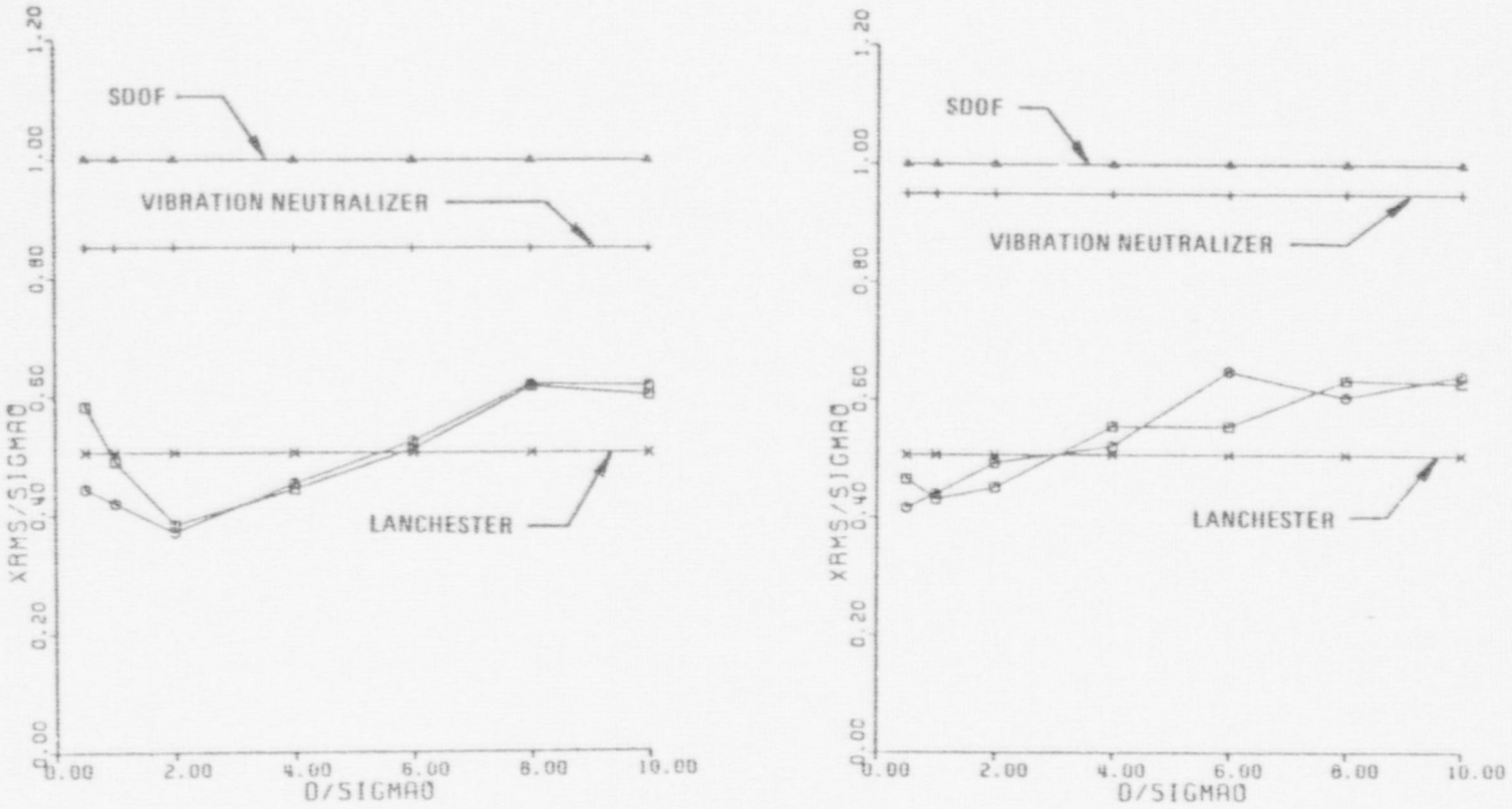

FIGURE 35 EXPERIMENTAL PARAMETER STUDY

$\zeta_1 = \zeta_3 = 0.01$, $\mu = 0.10$

(A) $\omega_3/\omega_1 = 1.0$; (B) $\omega_3/\omega_1 = 1.1$

Symbol	ω_2/ω_1	ζ_2
□	1.0	10.0
○	0.1	10.0

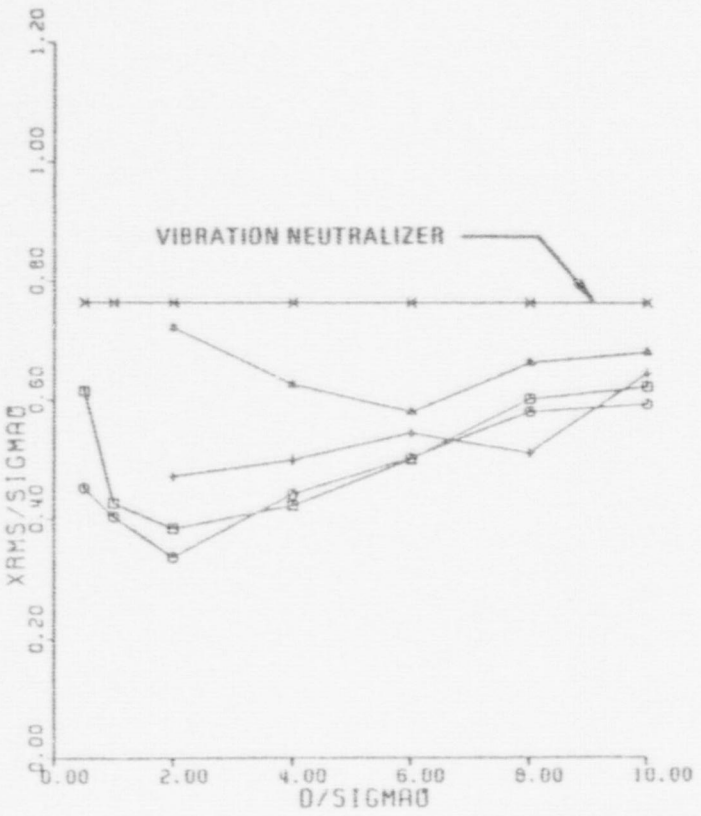

(A)

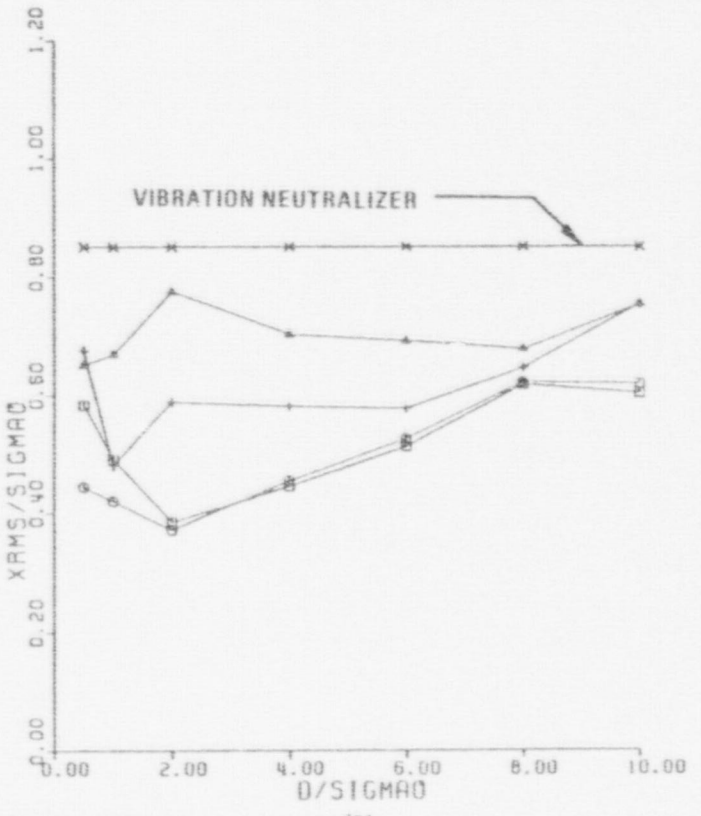

(B)

FIGURE 36 EXPERIMENTAL PARAMETER STUDY

$\zeta_1 = \zeta_3 = 0.01$, $\mu = 0.10$

(A) $\omega_3/\omega_1 = 0.9$; (B) $\omega_3/\omega_1 = 1.0$

Symbol	ω_2/ω_1	ζ_2
□	1.0	10.0
○	0.1	10.0
△	10.0	0.1
+	10.0	0.4

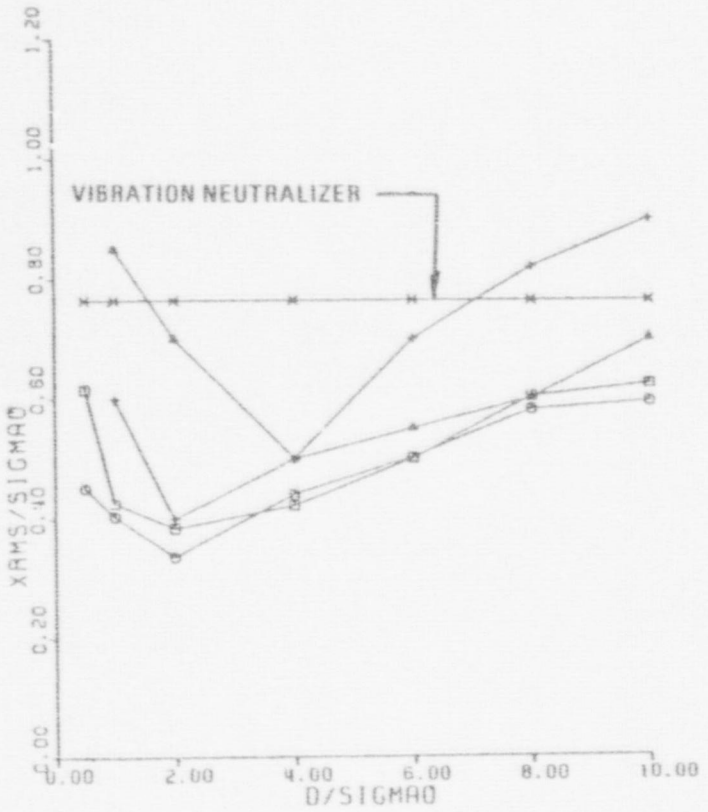

(A)

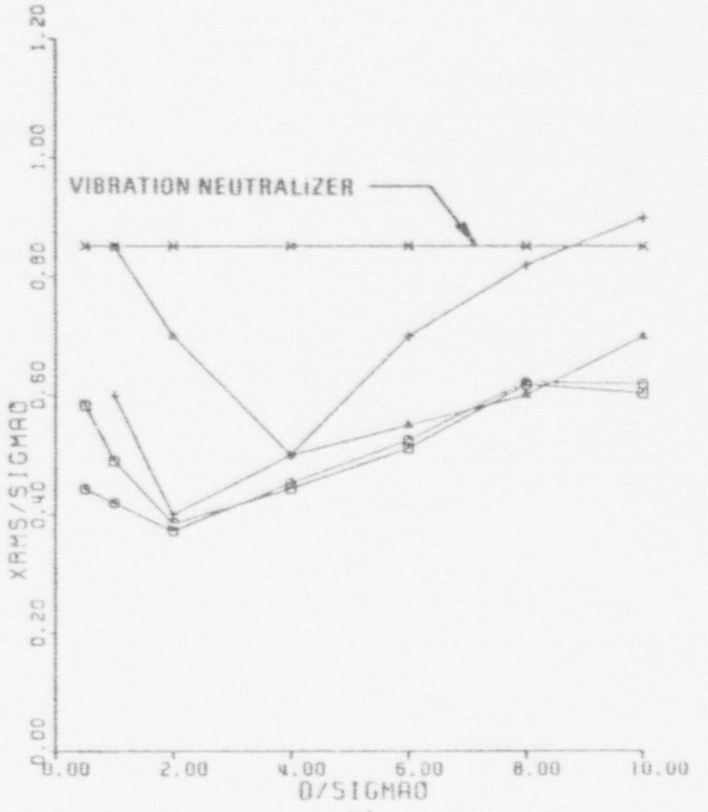

(B)

FIGURE 37 EXPERIMENTAL PARAMETER STUDY

$\zeta_1 = \zeta_3 = 0.01$, $\mu = 0.10$

(A) Symbol	ω_3/ω_1	ω_2/ω_1	ζ_2
□	0.9	1.0	10.0
○	0.9	0.10	10.0
△	0	10.0	0.1
+	0	10.0	0.4

(B) Symbol	ω_3/ω_1	ω_2/ω_1	ζ_2
□	1.0	1.0	10.0
○	1.0	0.10	10.0
△	0	10.0	0.1
+	0	10.0	0.4

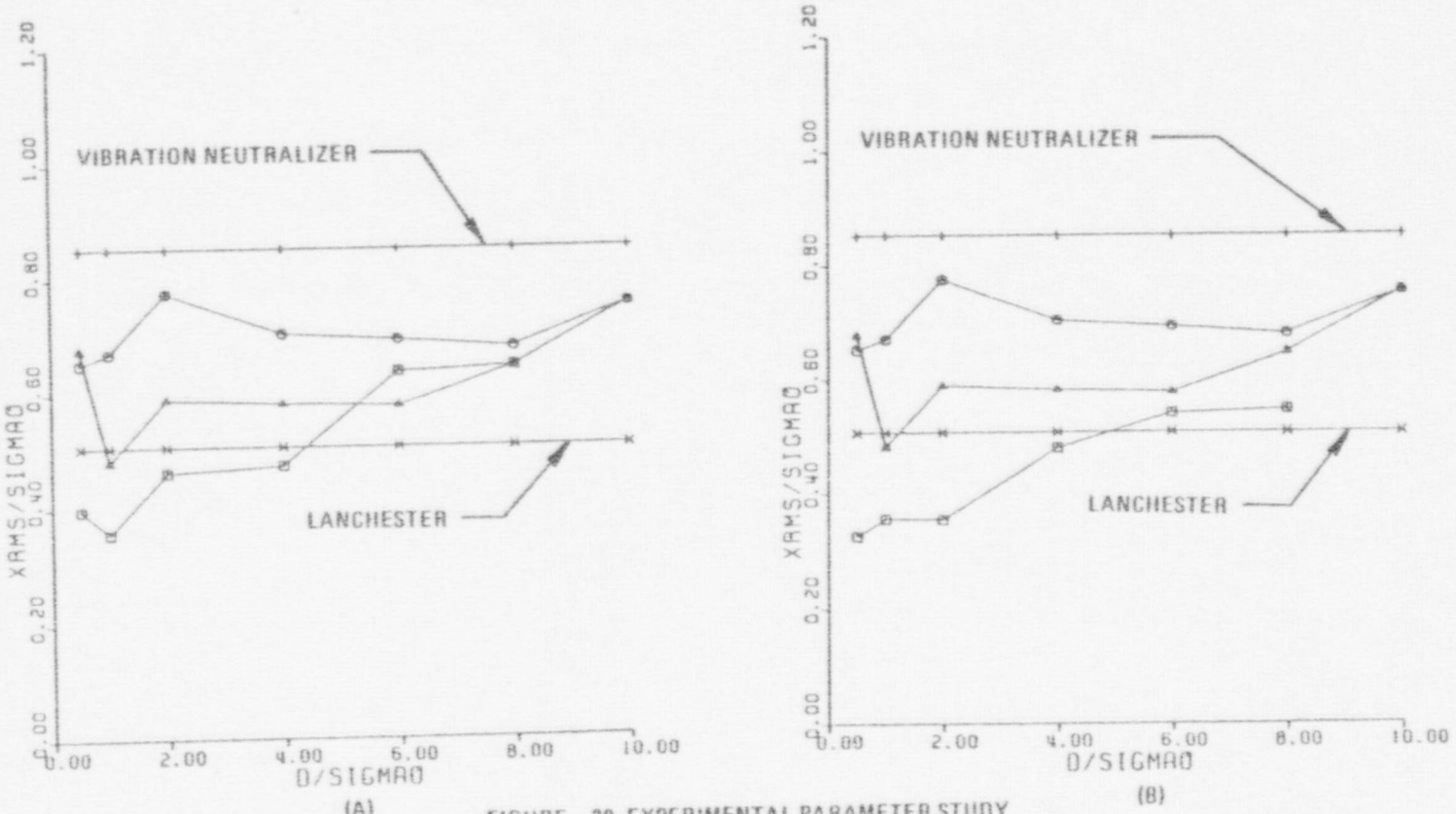

FIGURE 38 EXPERIMENTAL PARAMETER STUDY

$\omega_3/\omega_1 = 1.0,\ \mu = 0.10,\ \zeta_1 = \zeta_3 = 0.01$

(A) Symbol	ω_2/ω_1	ζ_2	(B) Symbol	ω_2/ω_1	ζ_2
□	0.10	1.0	□	0.10	5.0
○	10.0	0.1	○	10.0	0.1
△	10.0	0.4	△	10.0	0.4

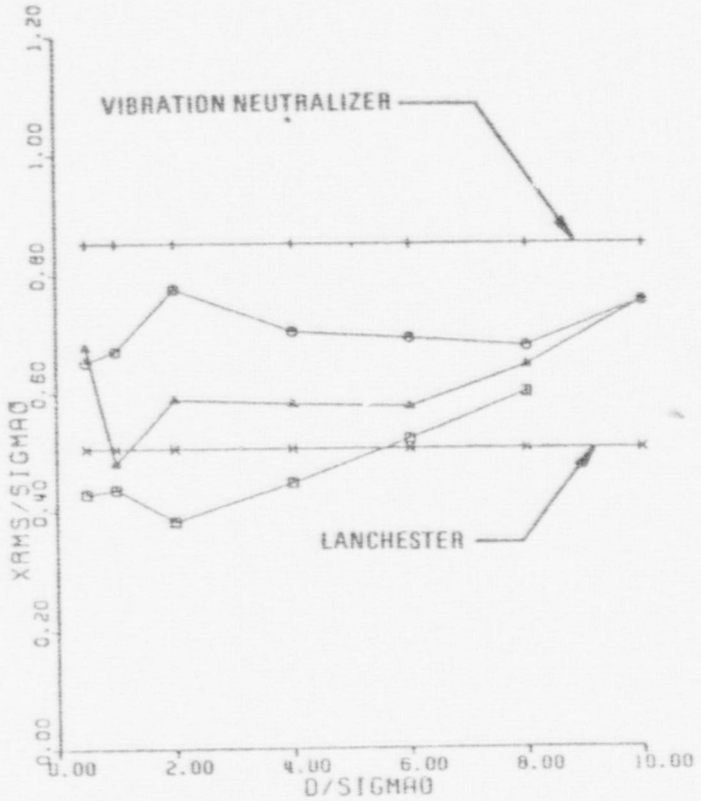

FIGURE 39 EXPERIMENTAL PARAMETER STUDY

$\omega_3/\omega_1 = 1.0,\ \mu = 0.10,\ \zeta_1 = \zeta_3 = 0.01$

Symbol	ω_2/ω_1	ζ_2
□	0.10	20.0
○	10.0	0.1
W	10.0	0.4

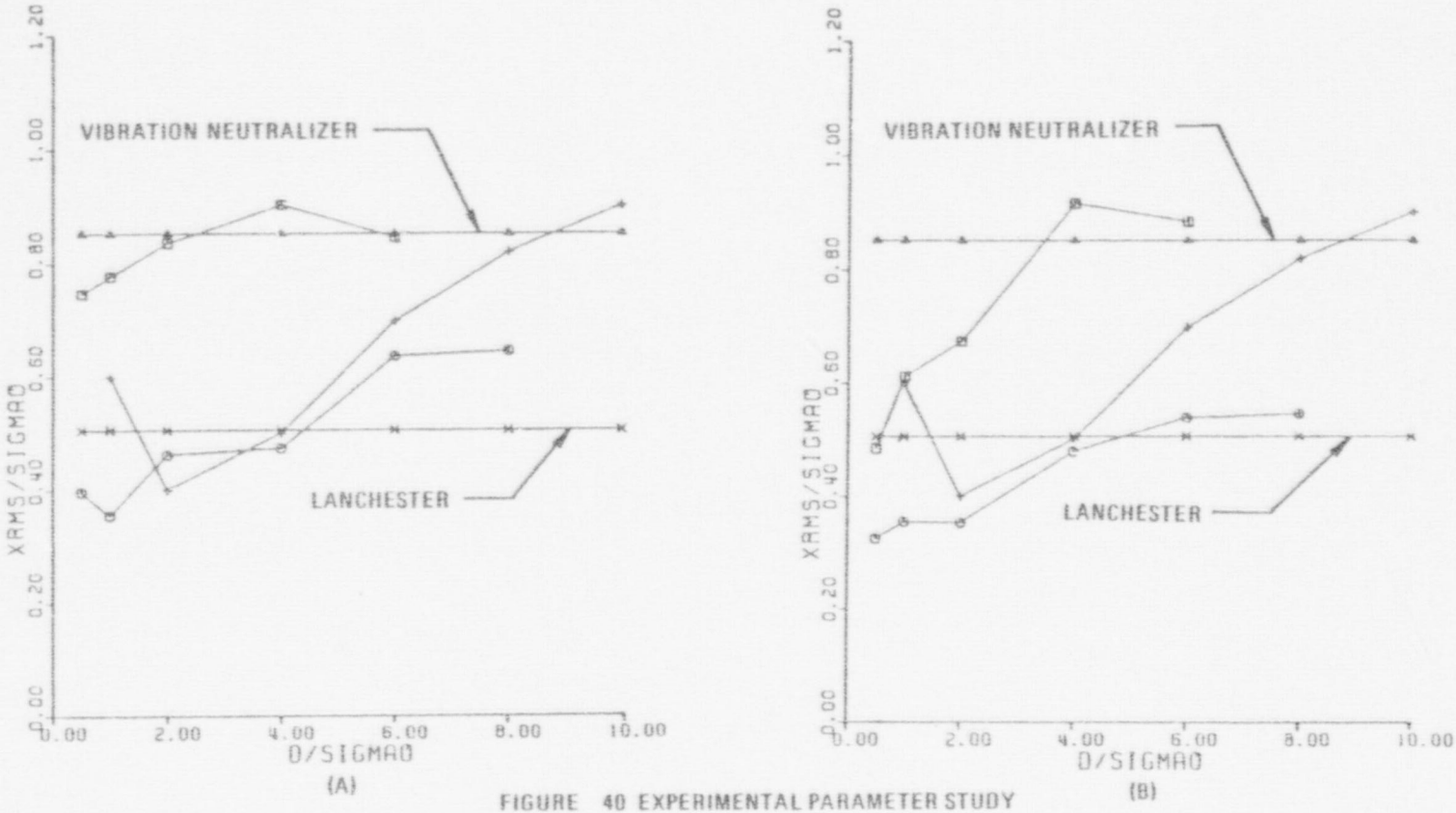

FIGURE 40 EXPERIMENTAL PARAMETER STUDY

$\zeta_1 = \zeta_3 = 0.01$, $\mu = 0.10$

(A)

Symbol	ω_3/ω_1	ω_2/ω_1	ζ_2
□	0.01	0.10	1.0
○	1.0	0.10	1.0
+	0	10.0	0.1

(B)

Symbol	ω_3/ω_1	ω_2/ω_1	ζ_2
□	0.01	0.10	5.0
○	1.0	0.10	5.0
+	0	10.0	0.1

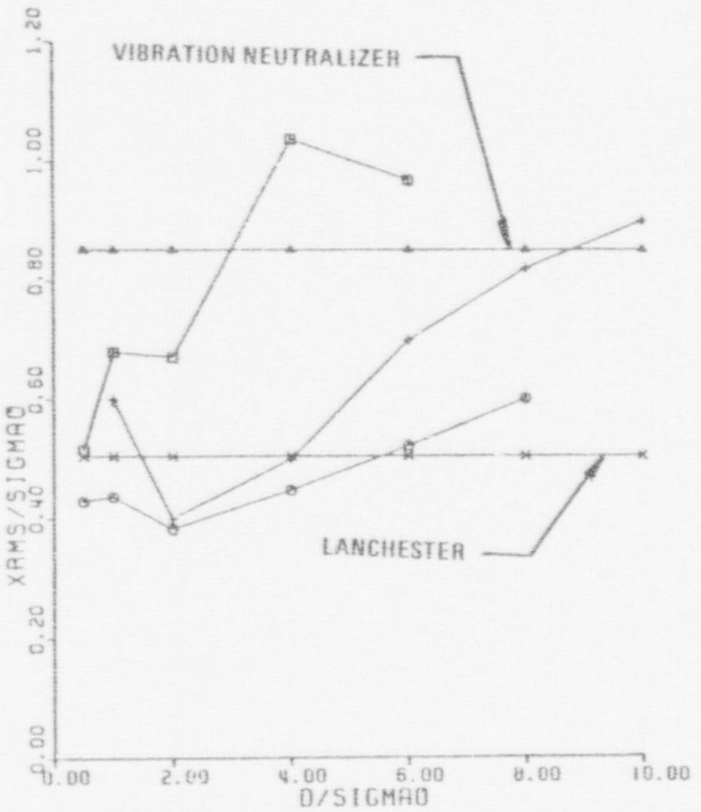

FIGURE 41 EXPERIMENTAL PARAMETER STUDY

$\zeta_1 = \zeta_3 = 0.01$, $\mu = 0.10$

Symbol	ω_3/ω_1	ω_2/ω_1	ζ_2
□	0.01	0.10	20.0
○	1.0	0.10	20.0
+	0	10.0	0.1

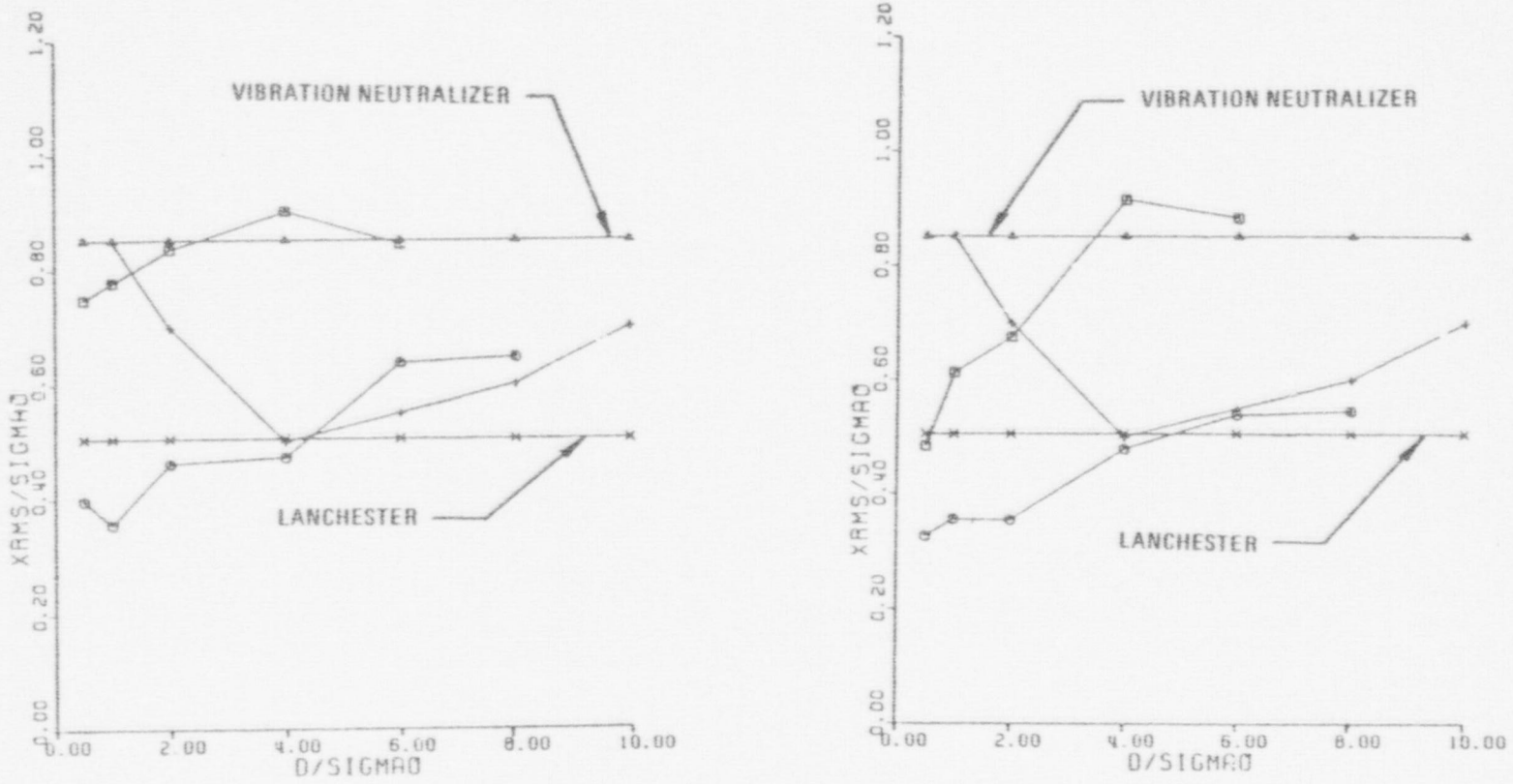

FIGURE 42 EXPERIMENTAL PARAMETER STUDY

$\zeta_1/\zeta_3 = 0.01$, $\mu = 0.10$

(A)

Symbol	ω_3/ω_1	ω_2/ω_1	ζ_2
□	0.01	0.10	1.0
○	1.0	0.10	1.0
+	0	10.0	0.4

(B)

Symbol	ω_3/ω_1	ω_2/ω_1	ζ_2
□	0.01	0.10	5.0
○	1.0	0.10	5.0
+	0	10.0	0.4

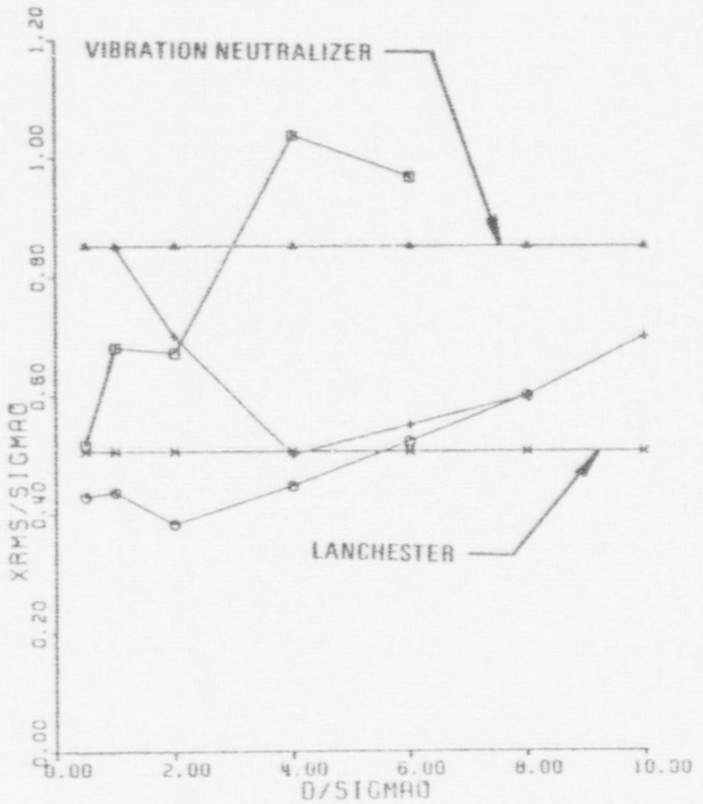

FIGURE 43 EXPERIMENTAL PARAMETER STUDY

$\zeta_1 = \zeta_3 = 0.01$, $\mu = 0.10$

Symbol	ω_3/ω_1	ω_2/ω_1	ζ_2
□	0.01	0.10	20.0
O	1.0	0.10	20.0
+	0	10.0	0.4

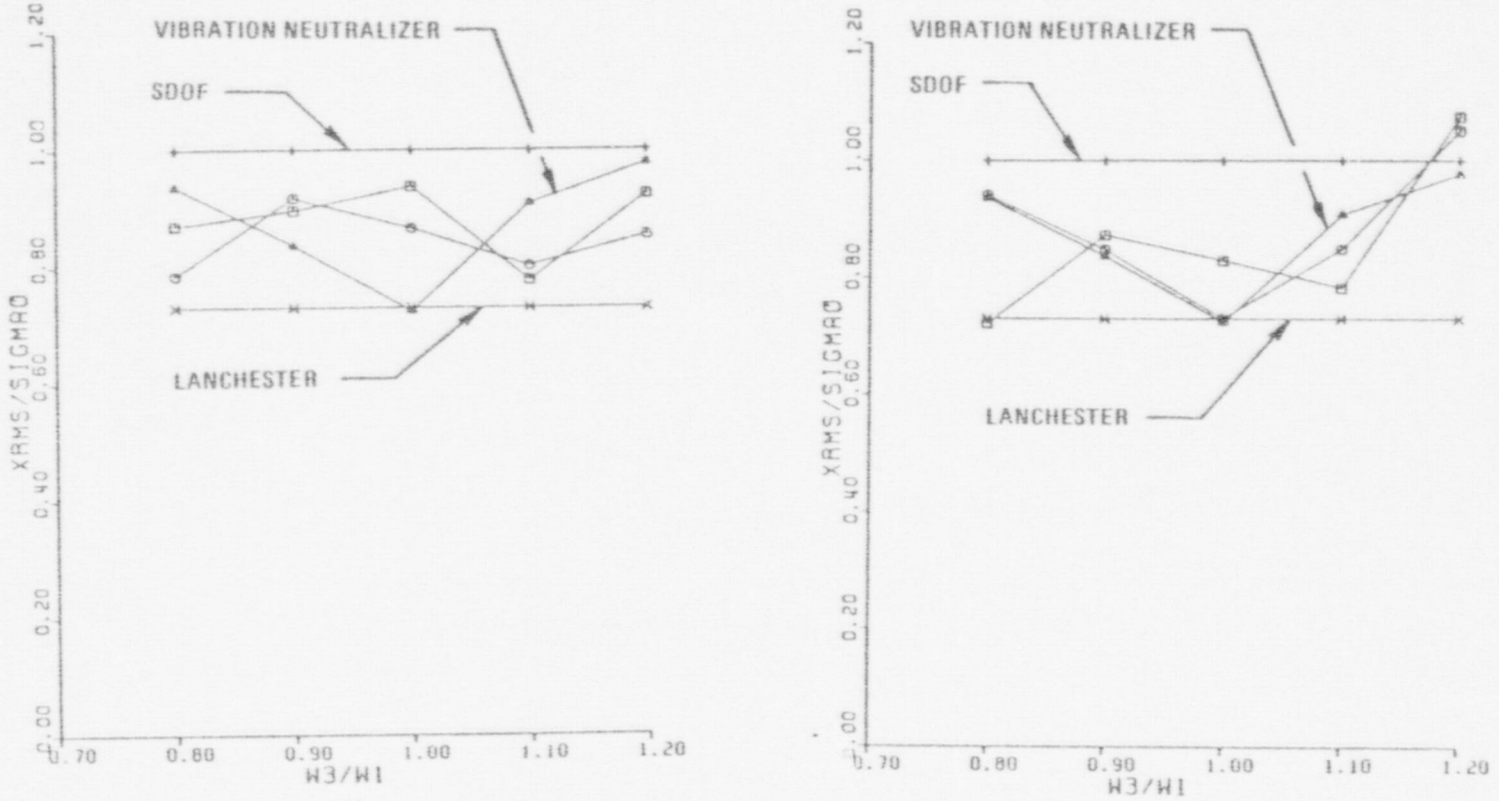

FIGURE 44 EXPERIMENTAL PARAMETER STUDY

$\zeta_1 = \zeta_3 = 0.01$, $\mu = 0.01$, $\omega_2/\omega_1 = 10.0$

(A) $D/\sigma_{x_o} = 2$; (B) $D/\sigma_{x_o} = 4$.

Symbol	ζ_2
□	0.1
○	0.4

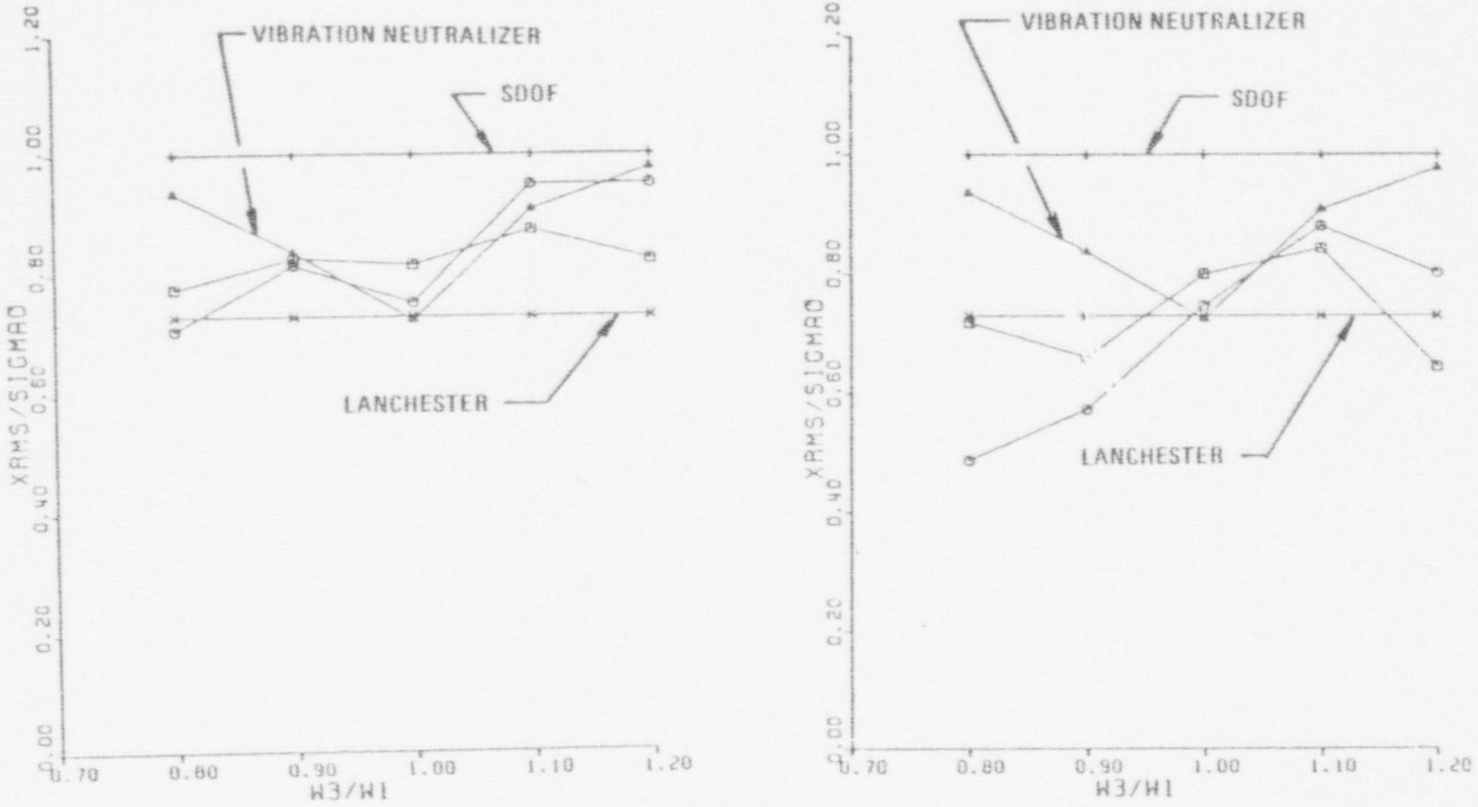

FIGURE 45 EXPERIMENTAL PARAMETER STUDY

$\zeta_1 = \zeta_3 = 0.01$, $\mu = 0.01$, $\omega_2/\omega_1 = 10.0$

(A) $D/\sigma_{x_o} = 6$; (B) $D/\sigma_{x_o} = 8$.

Symbol	ζ_2
□	0.1
○	0.4

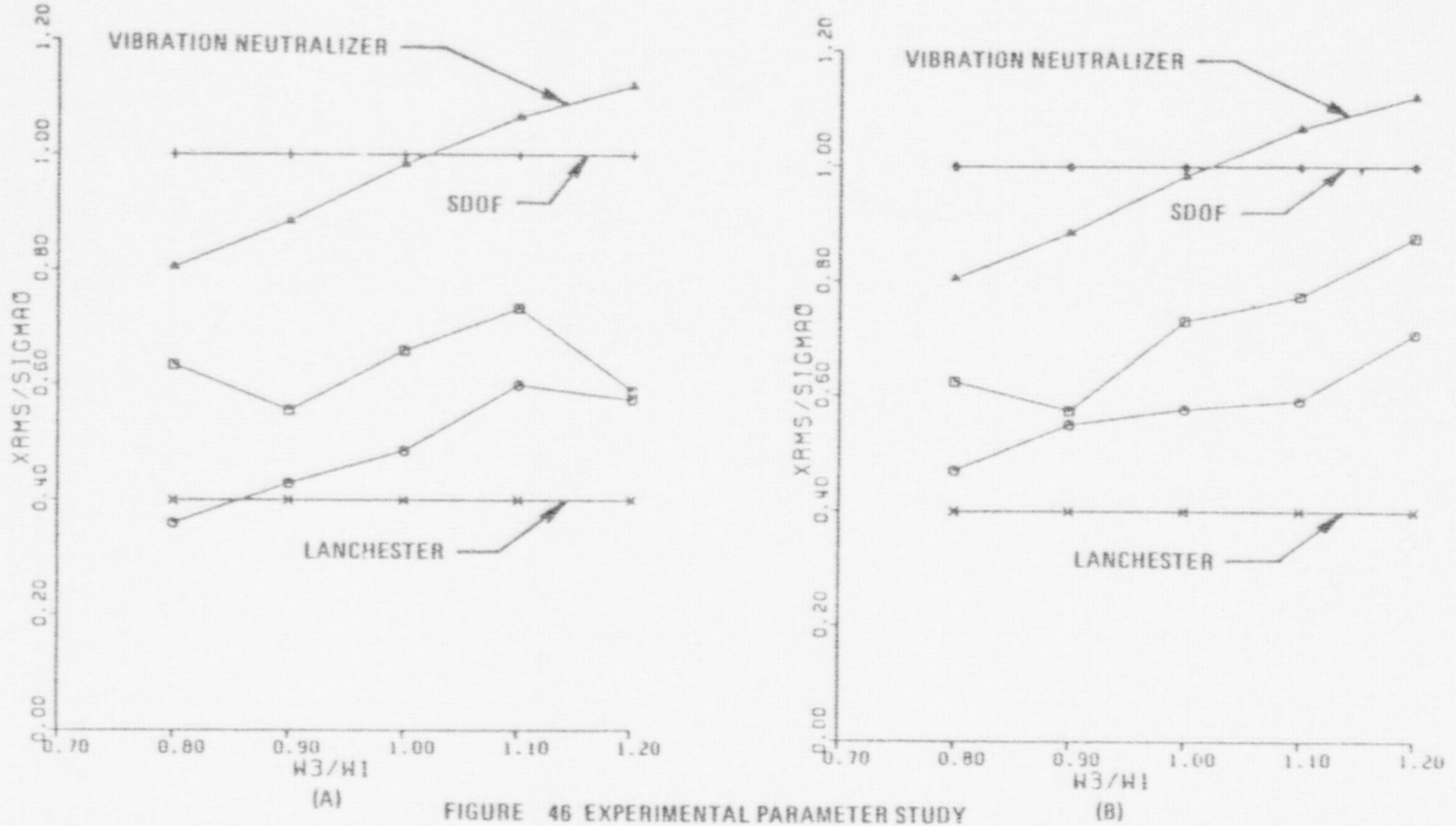

FIGURE 46 EXPERIMENTAL PARAMETER STUDY

$\zeta_1 = \zeta_3 = 0.01$, $\mu = 0.20$, $\omega_2/\omega_1 = 10.0$.

(A) $D/\sigma_{x_o} = 2$; (B) $D/\sigma_{x_o} = 4$.

Symbol	ζ_2
□	0.1
○	0.4

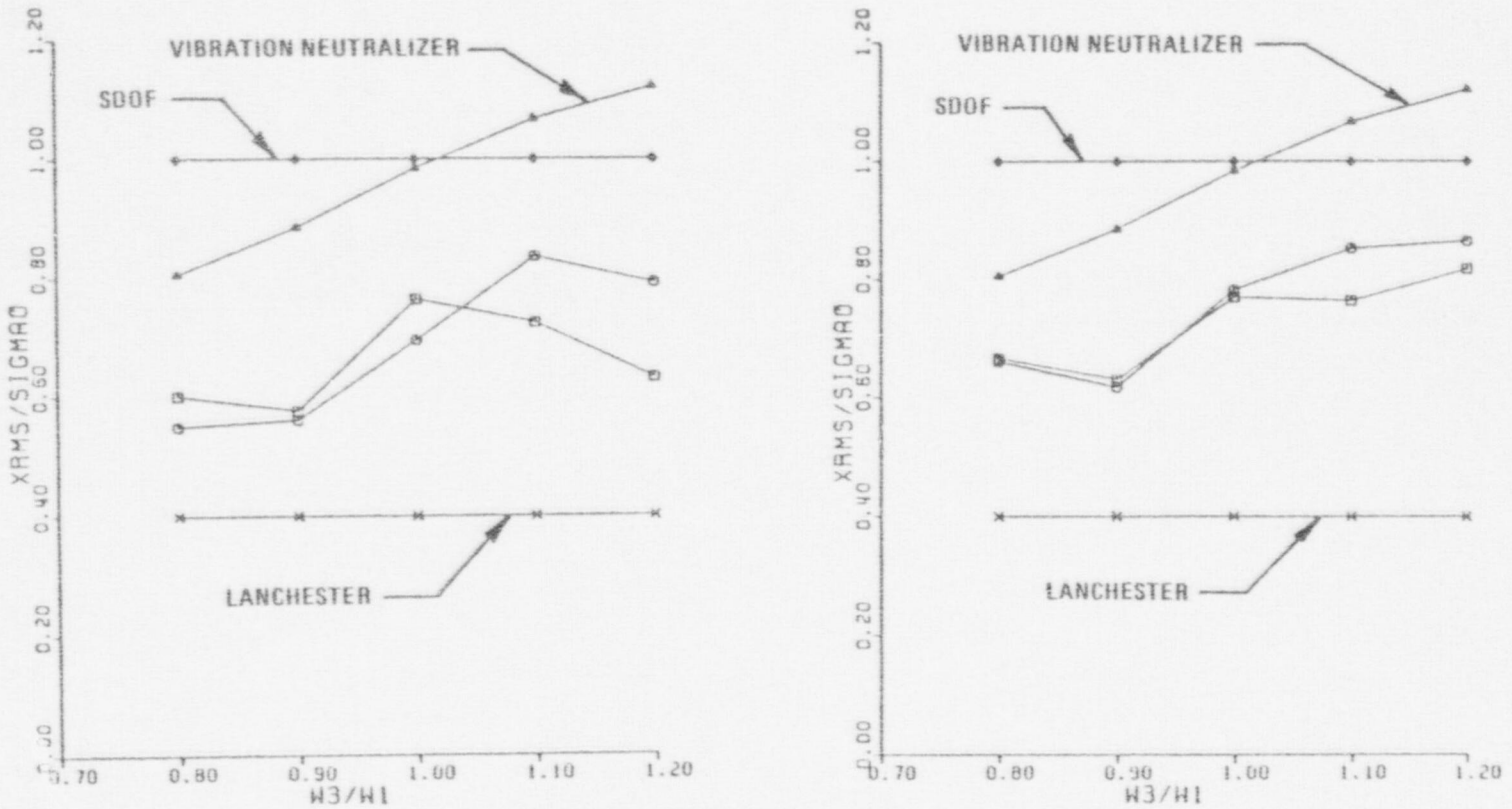

FIGURE 47 EXPERIMENTAL PARAMETER STUDY

$\zeta_1 = \zeta_3 = 0.01$, $\mu = 0.20$, $\omega_2/\omega_1 = 10.0$

(A) $D/\sigma_{x_o} = 6$; (B) $D/\sigma_{x_o} = 8$.

Symbol	ζ_2
□	0.1
○	0.4

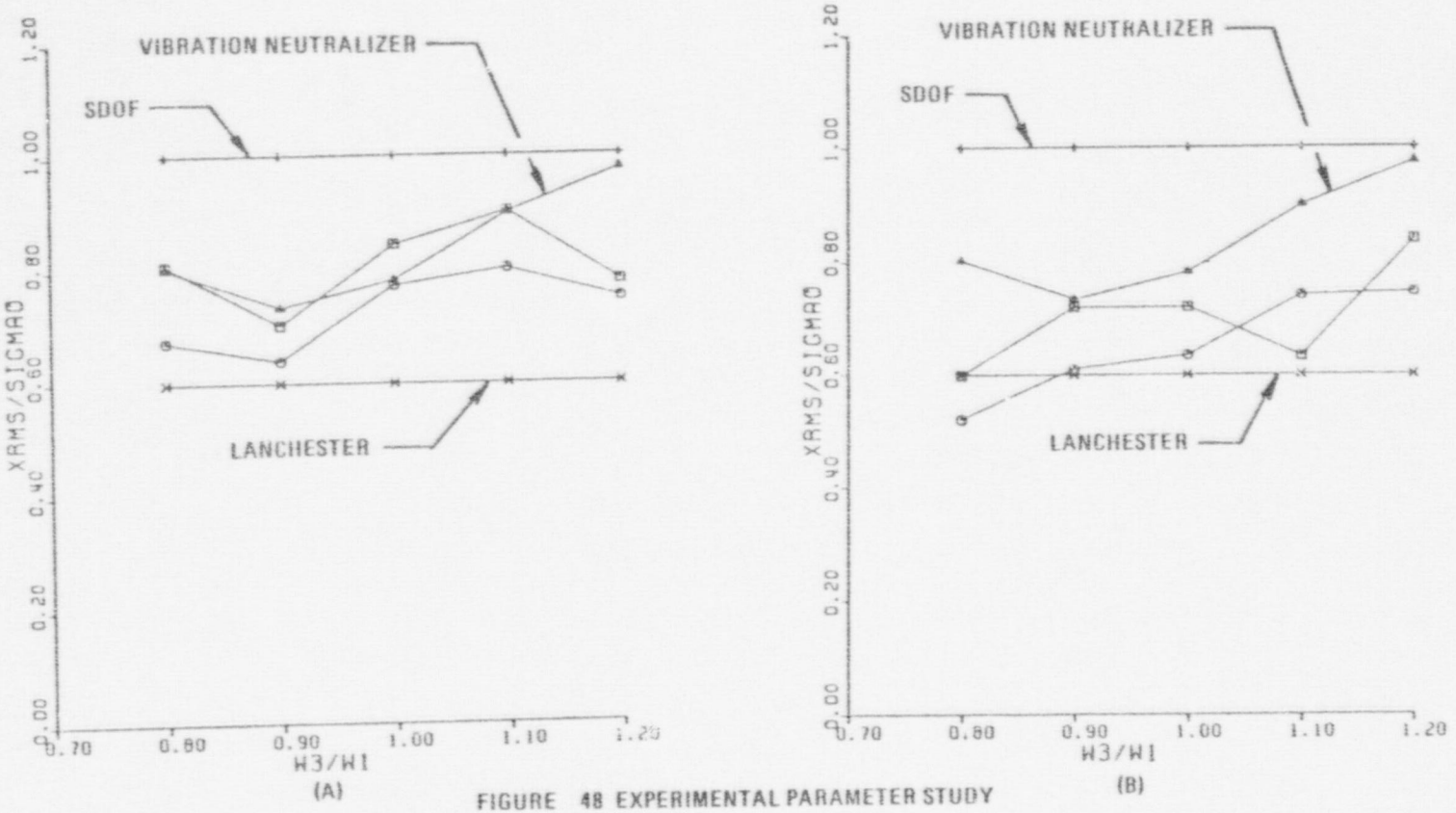

FIGURE 48 EXPERIMENTAL PARAMETER STUDY

$\zeta_1 = \zeta_3 = 0.01$, $\mu = 0.05$, $\omega_2/\omega_1 = 10.0$.

(A) $D/\sigma_{x_o} = 2$; (B) $D/\sigma_{x_o} = 4$.

Symbol	ζ_2
□	0.1
○	0.4

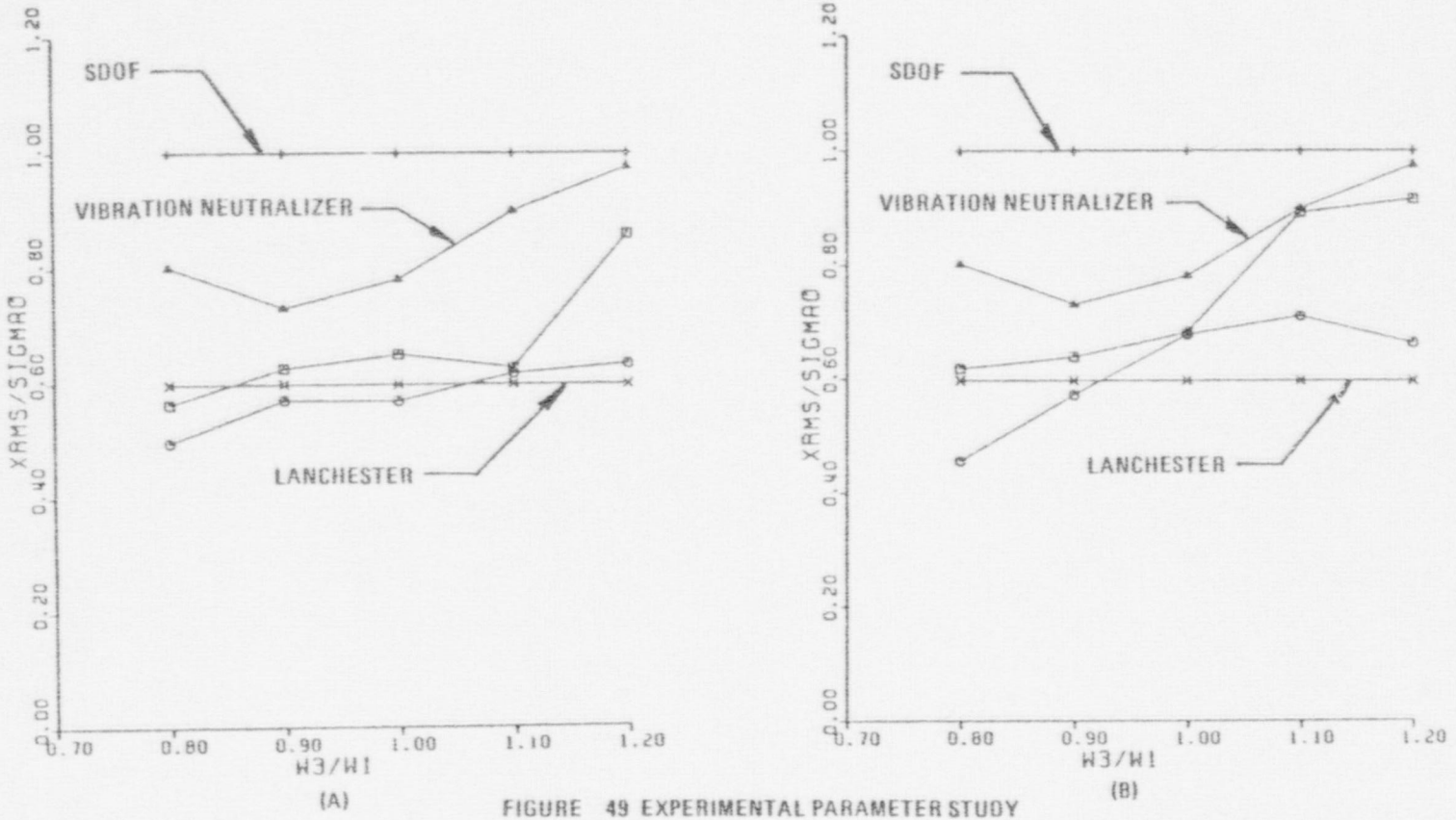

FIGURE 49 EXPERIMENTAL PARAMETER STUDY

$\zeta_1 = \zeta_3 = 0.01$, $\mu = 0.05$, $\omega_2/\omega_1 = 10.0$.

(A) $D/\sigma_{x_o} = 6$; (B) $D/\sigma_{x_o} = 8$.

Symbol	ζ_2
□	0.1
○	0.4

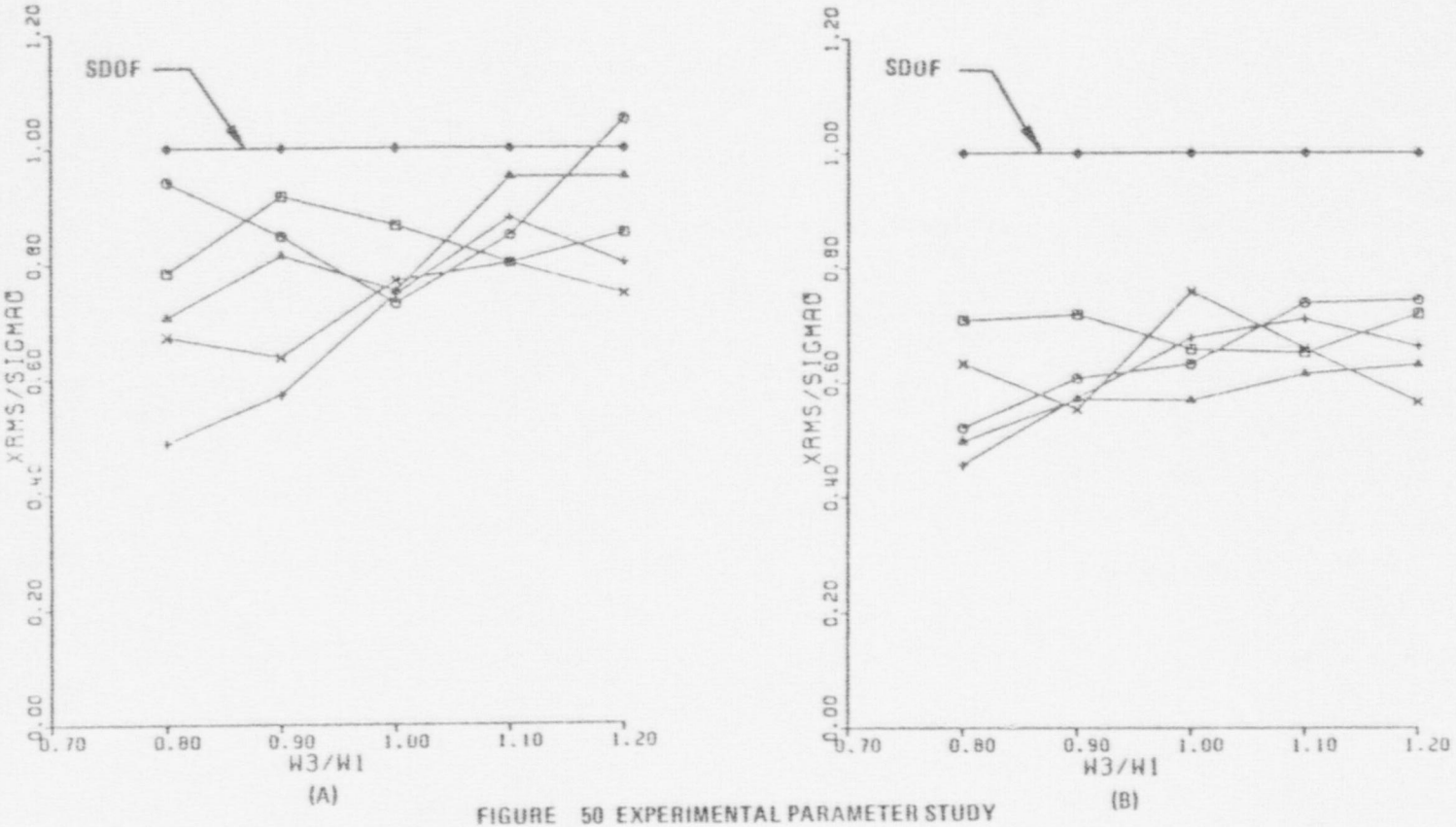

FIGURE 50 EXPERIMENTAL PARAMETER STUDY

$\zeta_1 = \zeta_3 = 0.01$, $\omega_2/\omega_1 = 10.0$, $\zeta_2 = 0.4$.

(A) $\mu = 0.01$; (B) $\mu = 0.05$.

Symbol	D/σ_{x_o}
□	2
○	4
△	6
+	8
X	10

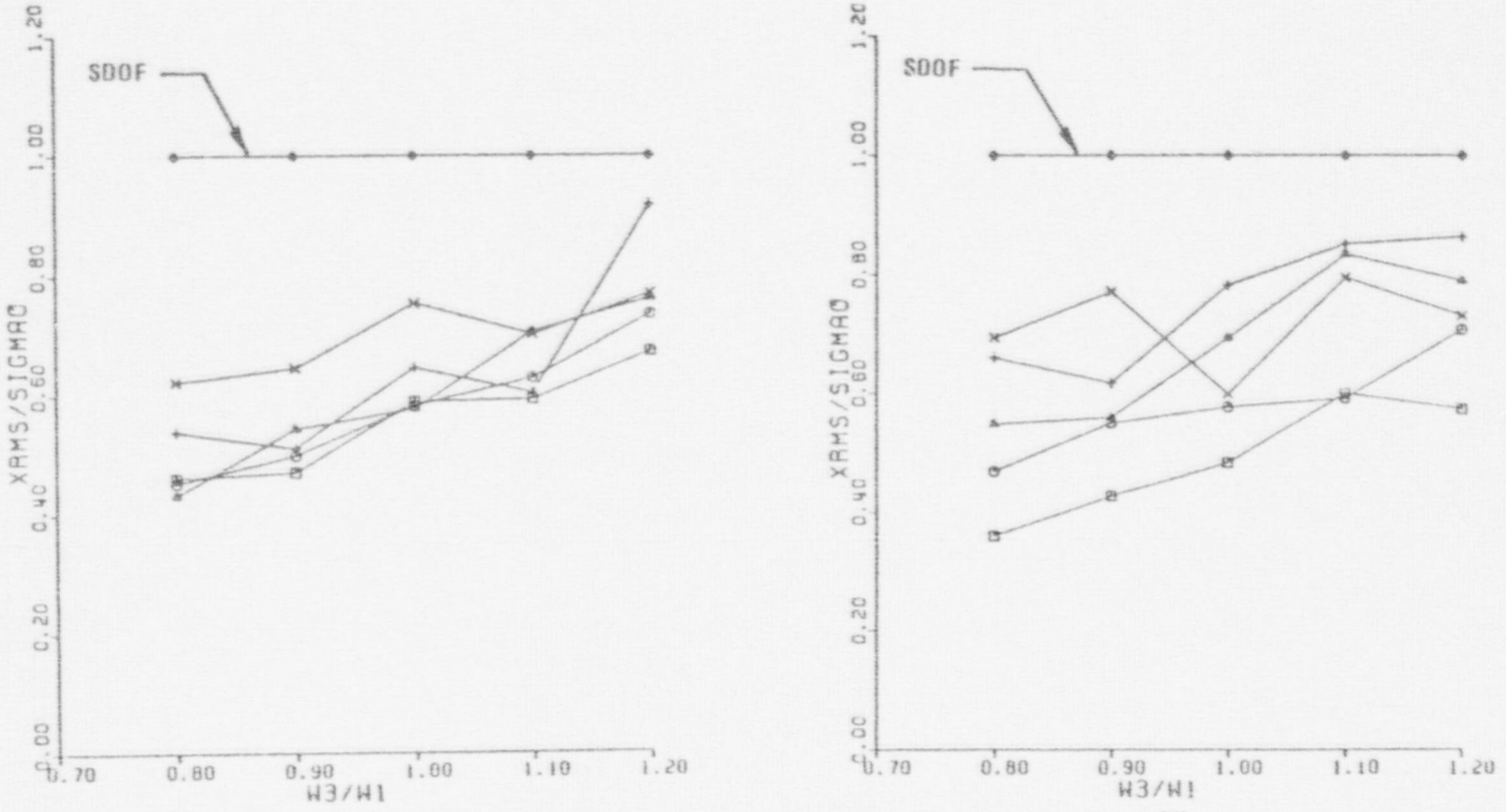

FIGURE 51 EXPERIMENTAL PARAMETER STUDY

$\zeta_1 = \zeta_3 = 0.01$, $\omega_2/\omega_1 = 10.0$, $\zeta_2 = 0.4$.

(A) $\mu = 0.10$; (B) $\mu = 0.20$.

Symbol	D/σ_{x_o}
□	2
○	4
△	6
+	8
X	10

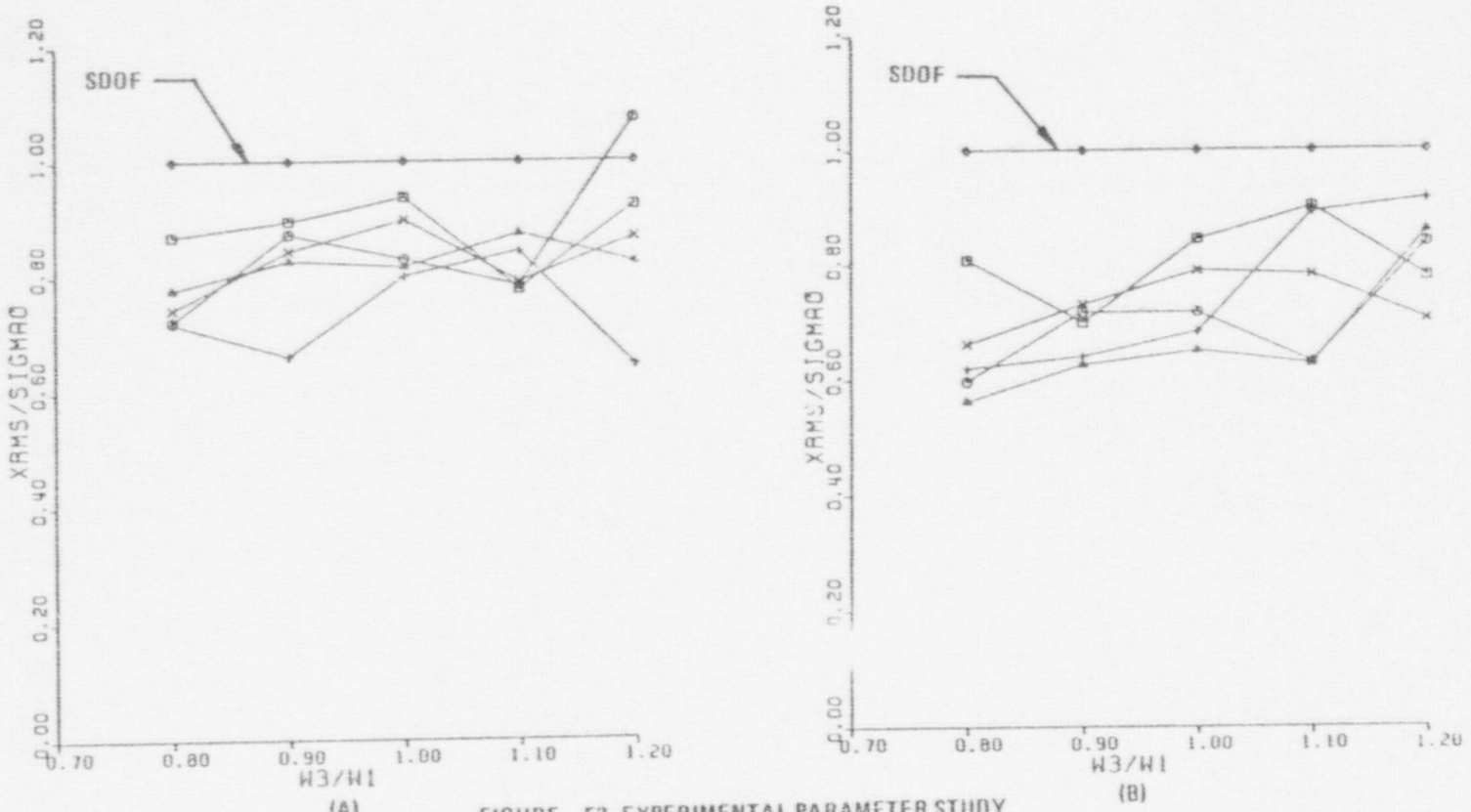

FIGURE 52 EXPERIMENTAL PARAMETER STUDY

$\zeta_1 = \zeta_3 = 0.01$, $\omega_2/\omega_1 = 10.0$, $\zeta_2 = 0.10$.

(A) $\mu = 0.01$; (B) $\mu = 0.05$.

Symbol	D/σ_{x_o}
□	2
○	4
△	6
+	8
X	10

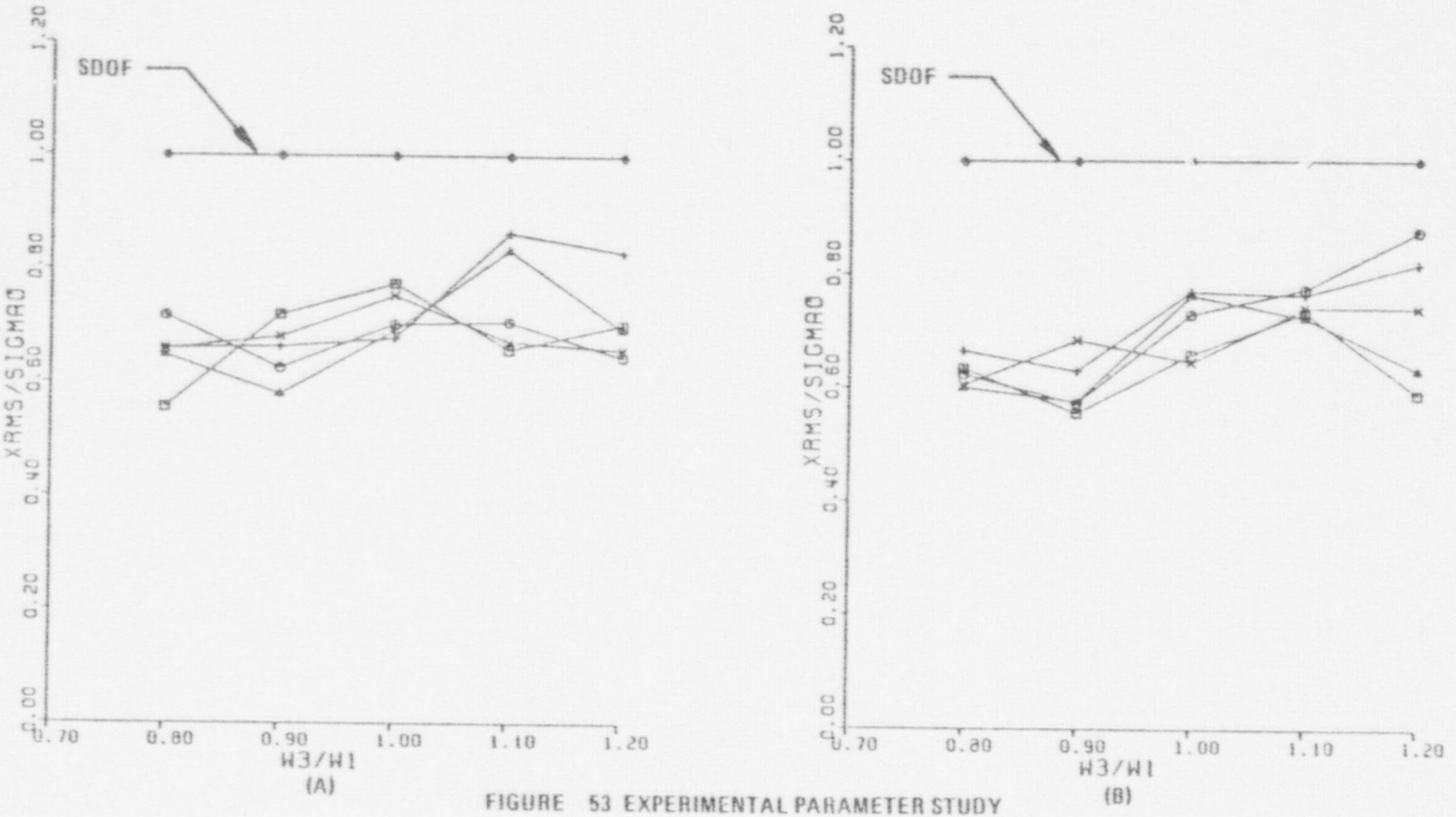

FIGURE 53 EXPERIMENTAL PARAMETER STUDY

$\zeta_1 = \zeta_3 = 0.01$, $\omega_2/\omega_1 = 10.0$, $\zeta_2 = 0.10$.

(A) $\mu = 0.10$; (B) $\mu = 0.20$.

Symbol	D/σ_{x_o}
□	2
○	4
△	6
+	8
X	10

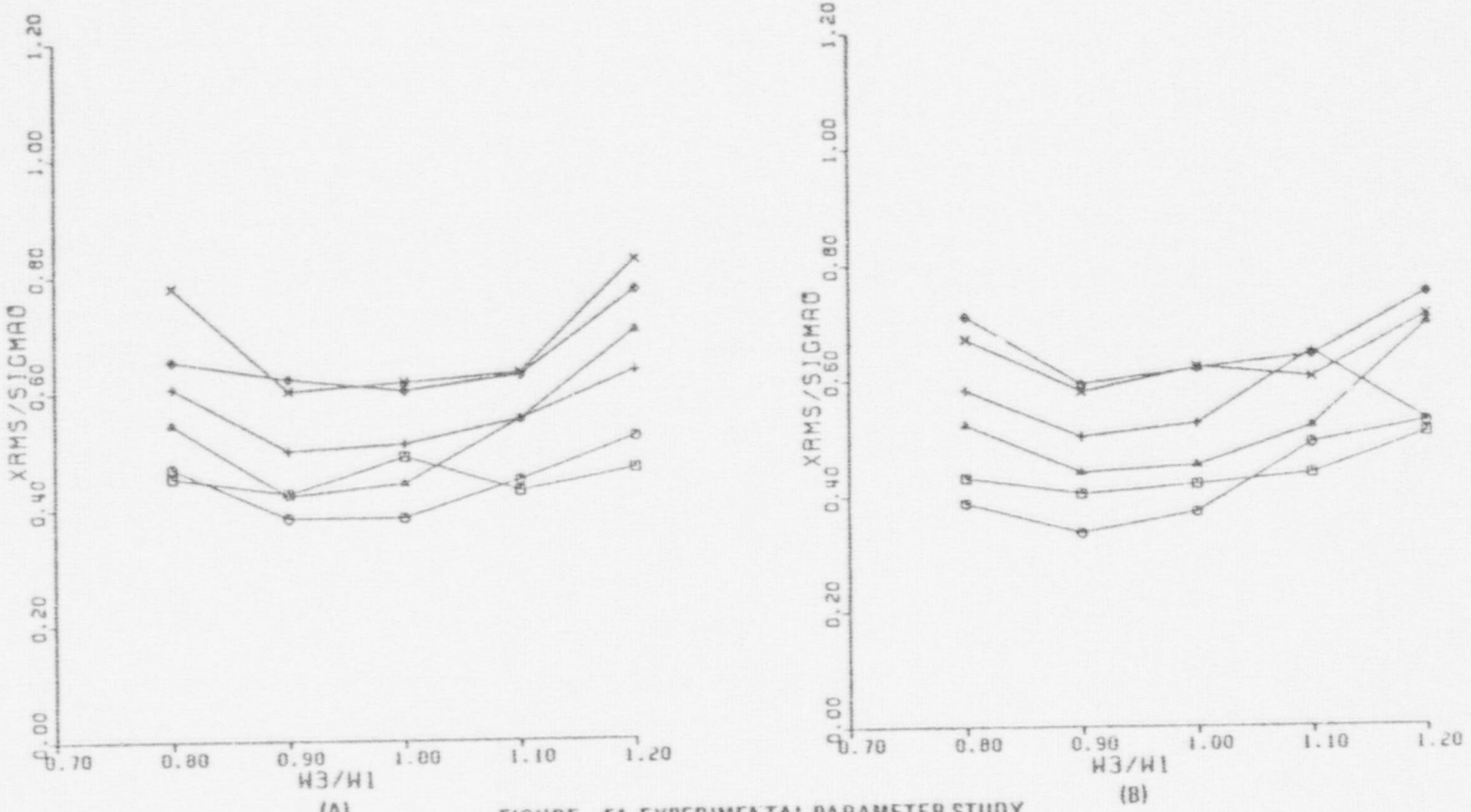

FIGURE 54 EXPERIMENTAL PARAMETER STUDY

$\zeta_1 = \zeta_3 = 0.01$, $\mu = 0.10$, $\zeta_2 = 10.0$.

(A) $\omega_2/\omega_1 = 1.0$; (B) $\omega_2/\omega_1 = 0.10$.

Symbol	D/σ_{x_o}
□	1
○	2
△	4
+	6
X	8
◇	10

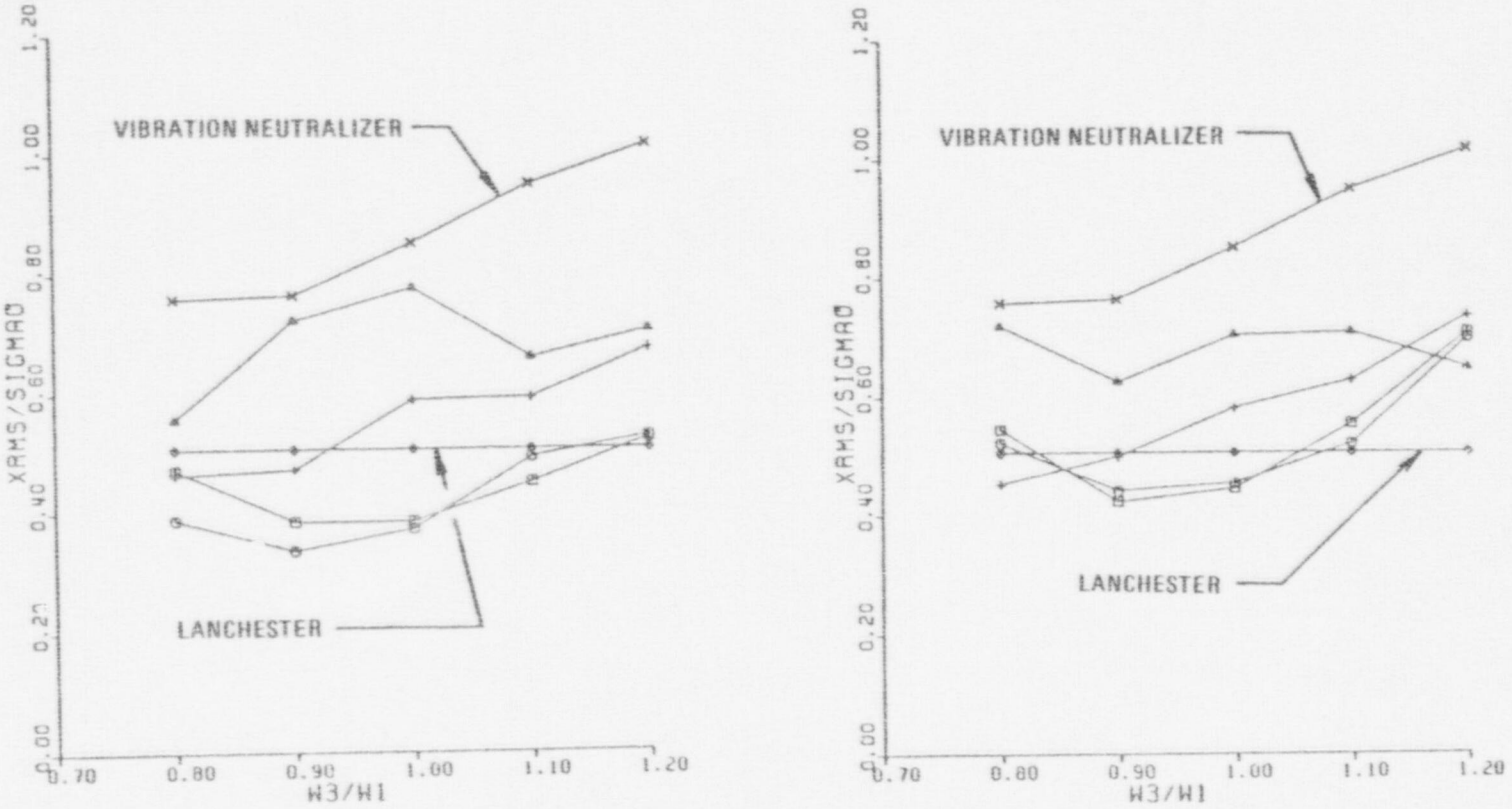

FIGURE 55 EXPERIMENTAL PARAMETER STUDY

$\zeta_1 = \zeta_3 = 0.01$, $\mu = 0.10$.

(A) $D/\sigma_{x_o} = 2$; (B) $D/\sigma_{x_o} = 4$.

Symbol	ω_2/ω_1	ζ_2
□	1.0	10.0
○	0.10	10.0
△	10.0	0.1
+	10.0	0.4

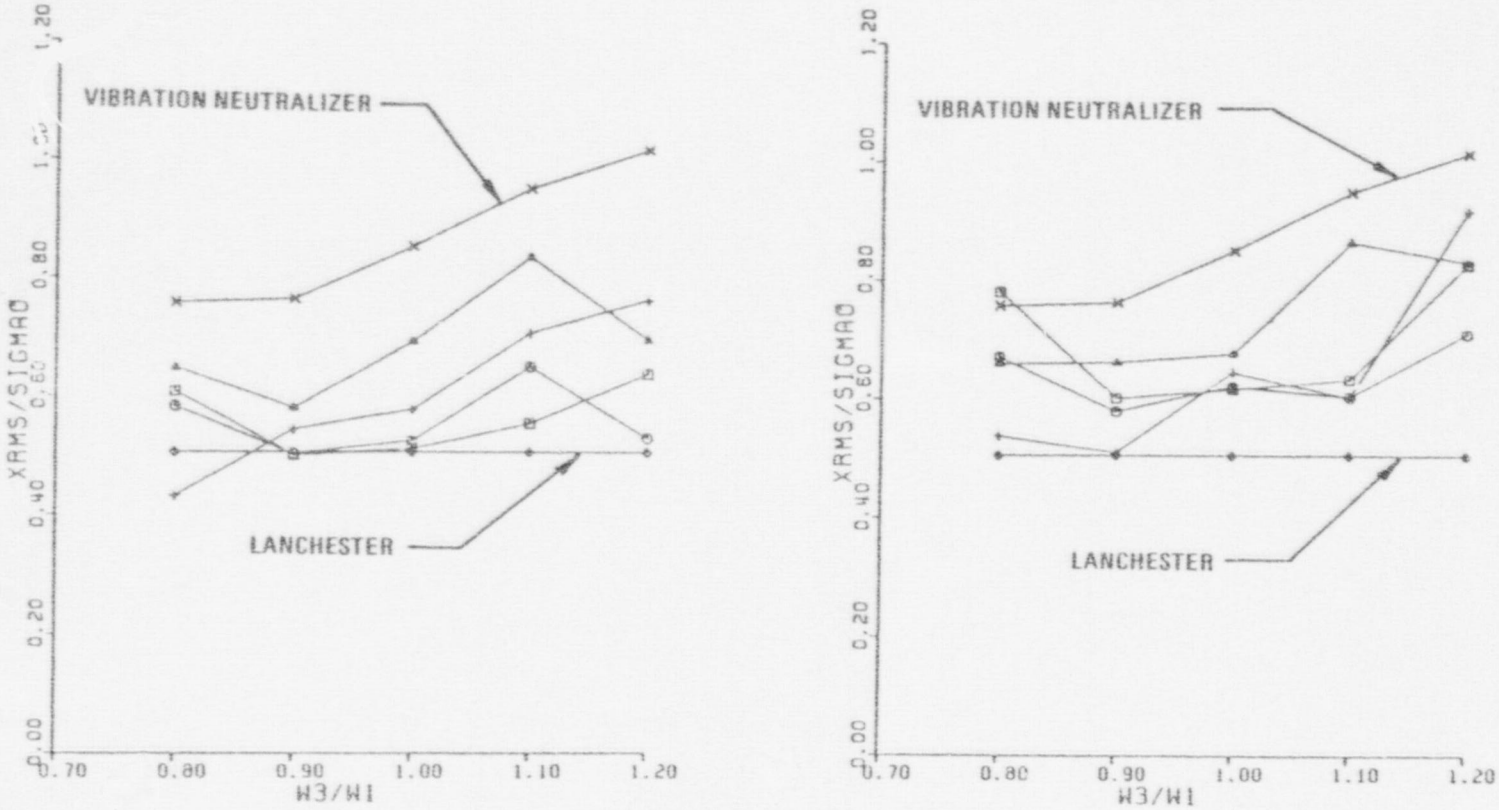

FIGURE 56 EXPERIMENTAL PARAMETER STUDY

$\zeta_1 = \zeta_3 = 0.01$, $\mu = 0.10$.

(A) $D/\sigma_{x_o} = 6$; (B) $D/\sigma_{x_o} = 8$.

Symbol	ω_2/ω_1	ζ_2
□	1.0	10.0
○	0.1	10.0
△	10.0	0.1
+	10.0	0.4

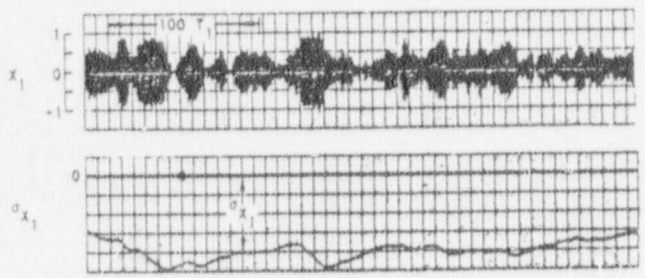

(A)

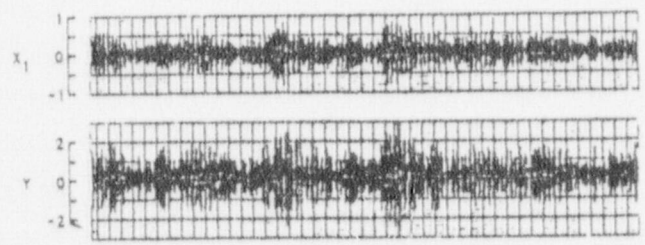

(B)

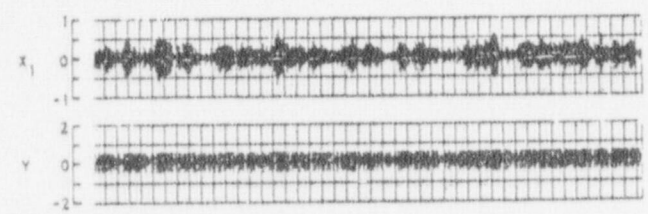

(C)

FIGURE 57 ANALOG TIME HISTORIES OF RESPONSE: $\zeta_1 = 0.01$ (A) SDOF; (B) DVN, $\mu = 0.10$, $\zeta_3 = 0.10$, $\omega 3/\omega_1 = 1$; (C) NONLINEAR DVN, $\mu = 0.10$, $\zeta_3 = 0.10$, $\omega 2/\omega_1 = 10$, $\zeta_2 = 0.4$, $\omega 3/\omega_1 = 1$, $D/\sigma_{x_o} \approx 2$

REFERENCES

1. Ormondroyd, J., and Den Hartog, J.P., "The Theory of the Dynamic Vibration Absorber," *Trans. ASME*, vol. 50, 1928, pp. 9-15.

2. Timoshenko, S., Discussion of "The Theory of Dynamic Vibration Absorber," *Trans. ASME*, vol. 50, 1928, pp. 20-21.

3. Crandall, S.H., and Mark, W.D., *Random Vibration in Mechanical Systems*, Academic Press, New York, 1963.

4. Curtis, A.J., and Boykin, T.R., "Response of Two-Degree-of-Freedom Systems to White Noise Base Excitation," *Journal of the Acoustical Society of America*, vol. 33, 1961, pp. 655-663.

5. Maezawa, S., "Steady, Forced Vibration of Unsymmetrical Piecewise-Linear Systems," *Bulletin of JSME*, vol. 4, 1961, pp. 201-212.

6. Masri, S.F., "Forced Vibration of a Class of Non-Linear Two-Degree-of-Freedom Oscillators," *International Journal of Non-Linear Mechanics*, vol. 7, 1972, pp. 663-674.

7. Klotter, K., "Non-Linear Vibrations Treated by the Averaging Methods of Ritz," *Proc. of the First National Congress of Applied Mechanics, Trans. ASME*, vol. 78, 1952, np.

8. Pipes, I.A., "Analysis of a Nonlinear Dynamic Vibration Absorber," *Journal of Applied Mechanics*, vol. 19, *Trans. ASME*, vol. 79, 1953, Series E, pp. 515-518.

9. Arnold, F.R., "Steady State Behavior of Systems Provided with Nonlinear Dynamic Vibration Absorbers," *Journal of Applied Mechanics*, vol. 22, *Trans. ASME*, vol. 77, 1955, Series E, pp. 487-492.

10. Masri, S.F., "Theory of the Dynamic Vibration Neutralizer with Motion-Limiting Stops," *Trans. ASME*, vol. 39, 1972, Series E, pp. 563-568.

11. Kaper, H.G., "The Behavior of a Mass-Spring System Provided with a Discontinuous Dynamic Vibration Absorber," *Appl. Sci. Res.*, Section A, vol. 10, 1961, np.

12. Paget, A., "The Acceleration Damper," *Engineering*, 1934, pp. 557-559.

13. Lieber, P., and Jensen, D.P., "An Acceleration Damper: Development, Design, and Some Applications," *Trans. ASME*, vol. 67, 1945, pp. 523-530.

14. Grubin, G., "On the Theory of the Acceleration Damper," *Journal of Applied Mechanics*, vol. 23, *Trans. ASME*, vol. 78, 1956, Series E, pp.373-378.

15. Egle, D.M., "An Investigation of an Impact Vibration Absorber," *Trans. ASME*, vol. 89, 1967, Series B, pp. 653-657.

16. Warburton, G.B., "On the Theory of the Acceleration Damper," *Journal of Applied Mechanics*, vol. 24, *Trans. ASME*, vol. 79, 1957, Series E, pp. 322-324.

17. Masri, S.F., and Caughey, T.K., "On the Stability of the Impact Damper," *Journal of Applied Mechanics*, vol. 33, *Trans. ASME*, vol. 88, 1966, Series E, pp. 586-592.

18. Masri, S.F., Numerical Response Characteristics of a System Provided with Impact Dampers, USC-CE101, Structural Mechanics Laboratory, University of Southern California, Los Angeles, 1970.

19. Masri, S.F., and Ibrahim, A.M., "Stochastic Excitation of a Simple System with Impact Damper," *Earthquake Engineering and Structural Dynamics*, vol. 1, 1973, pp. 337-346.

20. McGoldrick, R.T., Experiments with an Impact Vibration Damper, Report No. 816, David Taylor Model Basin, Bethesda, MD, 1952.

21. Masri, S.F., "Analytical and Experimental Studies of Impact Dampers," Ph.D. thesis, California Institute of Technology, Pasadena, 1965.

22. Sadek, M.M., "The Behavior of the Impact Damper," *Proc. Mech. Engs.*, vol. 180, 1965, No. 38, part 1, np.

23. Masri, S.F., "Motion and Stability of Two-Particle Single-Container Impact Dampers," *Trans. ASME*, vol. 34, 1967, Series E, pp. 870-875.

24. Masri, S.F., "Analytical and Experimental Studies of Multiple-Unit Impact Dampers," *Journal of the Acoustical Society of America*, vol. 45, 1969, pp. 1111-1117.

25. Masri, S.F., "General Motion of Impact Dampers," *Journal of the Acoustical Society of America*, vol. 47, 1970, pp. 229-237.

26. Masri, S.F., and Rocke, R.D., "Application of a Single-Particle Impact Damper to an Antenna Structure," *The Shock and Vibration Bulletin*, no. 39, 1969, part 4, np.

27. Mansour, W.M., and Teizeira Filho, D.R., "Impact Dampers with Coulomb Friction," *Journal of Sound and Vibration*, vol. 33, 1974, pp. 247-265.

28. Cronin, D.L., and Van, N.K., "Substitute for the Impact Damper," *Trans. ASME*, vol. 97, 1975, Series B, pp. 1295-1300.

29. Crandall, S.H., "Perturbation Techniques for Random Vibration of Non-Linear Systems," *Journal of the Acoustical Society of America*, vol. 35, 1963, pp. 1700-1705.

30. Caughey, T.K., "Equivalent Linearization Techniques," *Journal of the Acoustical Society of America*, vol. 35, 1963, pp. 1706-1711.

31. Iwan, W.D., "Application of an Equivalent Nonlinear System Approach to Dissipative Dynamical Systems," *Trans. ASME*, vol. 36, 1969, Series E, pp. 412-416.

32. Young, D.M., and Gregory, R.T., *A Survey of Numerical Mathematics*, vol. I, Addison-Wesley, New York, 1972.

33. Caughey, T.K., "The Existence and Stability of Ultraharmonics and Subharmonics in Forced Nonlinear Oscillations," *Journal of Applied Mechanics*, vol. 20, *Trans. ASME*, vol. 75, 1954, Series E, pp. 327-335.

34. Timoshenko, S., and Young, D.H., *Vibration Problems in Engineering*, D. Van Nostrand, New York, 1955.

APPENDIX A

PSD CALIBRATION OF RANDOM FORCING FUNCTION EXCITATION

The random input forcing function used for system excitation in program ID117E is generated with computer software routines GAUSS and RANDU, which are part of the IBM 360 Scientific Subroutine Package. These routines use a uniformly distributed random number generator in conjunction with the Central Limit Theorem to generate a normally distributed random variable (F) with a specified mean ($\overline{F}$) and standard deviation (σ_F). Since the time spacing between these generated random variables (DT) is also specified, it is important to be able to calibrate the PSD (i.e., power spectral density) magnitude (S_o) of the input excitation as a function of DT, $\overline{F}$, and σ_F.

The standard analytic procedures used in time series analysis require at least two data samples per cycle to identify a frequency component within real-time-based data. Hence, the highest frequency component that can be observed by sampling or generating data values at a rate of 1/DT samples per second is 1/(2DT) hertz. Therefore, the PSD of the normally distributed random excitation force will be band limited as shown in Figure A 1, with a cutoff frequency ω_2 defined as

$$\omega_2 = \frac{1}{2DT} \text{ hertz} = \frac{\pi}{DT} \text{ radians} \qquad (A.1)$$

A review of the basic definitions of statistics yields the following:

$$E[F] = \int_{-\infty}^{+\infty} F\, p(F)dF = \text{mean or expected value } (\overline{F}) \qquad (A.2)$$

$$E[F^2] = \int_{-\infty}^{+\infty} F^2 \, p(F)dF = \text{mean square value } (\overline{F^2}) \tag{A.3}$$

$$\sqrt{E[F^2]} = \text{root mean square (RMS) value} \tag{A.4}$$

$$E[(F - \overline{F})^2] = \text{variance } (\sigma_F^2) \tag{A.5}$$

Using Definitions A.2 and A.3, Definition A.5 can be written as

$$\sigma_F^2 = \int_{-\infty}^{+\infty} (F - \overline{F})^2 \, p(F)dF \tag{A.6}$$

Expanding Definition A.6, one obtains

$$\sigma_F^2 = \int_{-\infty}^{+\infty} F^2 \, p(F)dF - 2E[F] \int_{-\infty}^{+\infty} Fp(F)dF + E[F]^2 \tag{A.7}$$

$$\sigma_F^2 = \overline{F^2} - \overline{F}^2 \tag{A.8}$$

For the special case of the mean equal to zero (i.e., $\overline{F} = 0$),

$$\sigma_F^2 = E[F^2] = \overline{F^2} \tag{A.9}$$

The autocorrelation function is defined as

$$R_F(\tau) = E[F(t) \cdot F(t + \tau)] \tag{A.10}$$

When τ is equal to zero, Definition A.10 is written as

$$R_F(0) = E[F(t) \cdot F(t)] = E[F^2(t)] = \overline{F^2} \tag{A.11}$$

Thus the autocorrelation function evaluated at zero is equal to the mean square value. Using Definitions A.8 and A.11, the following relationship is obtained:

$$R_F(0) = \overline{F^2} = \sigma_F^2 + (\overline{F})^2 \tag{A.12}$$

For the special case of the mean equal to zero (i.e., $\overline{F} = 0$),

$$R_F(0) = \sigma_F^2 \tag{A.13}$$

Definition A.13 establishes the important property that a random variable with zero mean has an autocorrelation function that, when evaluated at zero, is equal to its variance.

A normally distributed, band-limited excitation forcing function with a PSD as displayed in Figure A2 will have an autocorrelation function as displayed in Figure A3; the following relationship is established if the forcing excitation has a zero mean:

$$R_F(0) = 2\, S_o(\omega_2 - \omega_1) = \sigma_F^2 \tag{A.14}$$

However, because of the nature of the excitation forcing function generated by GAUSS and RANDU, ω_1 is equal to zero. Using Definitions A.1 and A.14, one obtains

$$R_F(0) = 2\, S_o\, \omega_2 = \frac{2\pi S_o}{DT} \tag{A.15}$$

Combining Definitions A.13 and A.15, one obtains

$$\sigma_F^2 = \frac{2\pi S_o}{DT} \tag{A.16}$$

Therefore, when the mean is zero (i.e., $\bar{F} = 0$), the following relationship will calibrate the excitation PSD:

$$S_o = \frac{\sigma_F^2 \, DT}{2\pi} \tag{A.17}$$

The variable (1/BIGDT1) is an arbitrary normalization factor that is defined as the number of data points generated in the natural period of the primary system (i.e., $2\pi/\omega$). Therefore, DT can be written as

$$DT = \frac{2\pi}{\omega} \, BIGDT1 \tag{A.18}$$

Thus, Definitions A.1 and A.17 can be rewritten in normalized form as

$$S_o = \frac{\sigma_F^2 \, BIGDT1}{\omega} \tag{A.19}$$

$$\omega_2 = \frac{\omega}{2.0 \, (BIGDT1)} \tag{A.20}$$

It should be noted that although our computer-generated excitation is band limited, it can for theoretical purposes be considered "white noise" excitation, since ω_2 is much greater than any fundamental frequencies present in the system. Both of the following examples, which

represent the parameters used in all instances for the data values generated in this report, show that

$$\omega_2 = 10.0\ \omega \tag{A.21}$$

where ω is the natural frequency of the primary system. In general, the system models studied in this report have response functions that display peak values between zero and 2ω. Thus the "white noise" excitation assumption is valid.

Example No. 1

Input Parameters:

$\overline{F}$ = mean value of excitation function = 0.0

ω = 1 radian/unit time

Period = $2\pi/\omega = 2\pi$

BIGDT1 = 0.05

Calculated Parameters:

$$DT = \frac{2\pi}{\omega} \text{ BIGDT1} = 0.314$$

$$\omega_2 = \frac{\omega}{2.0 \text{ BIGDT1}} = \frac{\pi}{0.314} = 10 \text{ radians/unit time}$$

Relationship between σ_F, σ_F^2 and S_o:

σ_F Standard Deviation of Excitation	σ_F^2 Variance of Excitation	S_o PSD: One-sided	S_o PSD: Two-sided
0.158113	0.024999	0.0025	0.00125
0.316227	0.09999	0.01	0.005
0.948683	0.89999	0.09	0.045
1.581	2.499	0.25	0.125
3.16227	9.99	1.0	0.50
6.3245	39.999	4.0	2.0
15.8113	249.997	25.0	12.5
31.6227	999.995	100.0	50.0

Example No. 2

Input Parameters:

$\bar{F}$ = mean value of excitation function = 0.0

ω = 2π radians/unit time

Period = 1

BIGDT1 = 0.05

Calculated Parameters

$$DT = \frac{2\pi}{\omega} \text{ BIGDT1} = 0.05$$

$$\omega_2 = \frac{\omega}{2.0 \text{ BIGDT1}} = 62.83 \frac{\text{radians}}{\text{unit time}} = 10\ (2\pi) \frac{\text{radians}}{\text{unit time}}$$

Relationship between σ_F, σ_F^2 and S_o:

σ_F Standard Deviation of Excitation	σ_F^2 Variance of Excitation	S_o PSD: One-sided	S_o PSD: Two-sided
0.158113	0.024999	0.000397	0.000198
0.316227	0.09999	0.00159	0.000795
0.948683	0.89999	0.01432	0.007161
1.581	2.499	0.0397	0.019886
3.16227	9.99	0.1589	0.07949
6.3245	39.999	0.63646	0.31823
15.8113	249.997	3.9788	1.989
31.6227	999.995	15.915	7.957

Let the vector A as shown in Figure A4 represent the forcing function, which is a sequence of discrete independent random variables with a normal distribution, specified standard deviation, and zero mean. The time history of this forcing function (i.e., F[t]) is written as

$$F(t) = A_K \quad \text{for} \quad (K)\,DT \leq t < (K+1)\,DT \tag{A.22}$$

The autocorrelation function of this process is written as

$$E[F(t_1) \cdot F(t_2)] = E[A_K^2] \tag{A.23}$$

if t_1 and t_2 are in the same time increment (i.e., $(K)DT \leq t_1, t_2 < (K+1)DT$),

or as

$$E[F(t_1) \cdot F(t_2)] = 0 \qquad (A.24)$$

if t_1 and t_2 are not in the same time increment. This generating forcing function can be considered as an approximation to true band-limited "white noise" excitation, which has an autocorrelation function defined as

$$E[F(t_1) \cdot F(t_2)] = E[A^2]\, DT \left[\delta(t_1 - t_2)\right]^*$$

if the response of the system being studied has a characteristic time (i.e., a fundamental period equal to $2\pi/\omega$) that is large compared to DT. In this report the fundamental period of the system model was set equal to 20 DT, which was verified by experimental investigation to be sufficiently large to assure that the input forcing function did in fact approximate true band-limited "white noise" excitation.

---

* $\delta(t_1 - t_2)$ is the Dirac delta function.

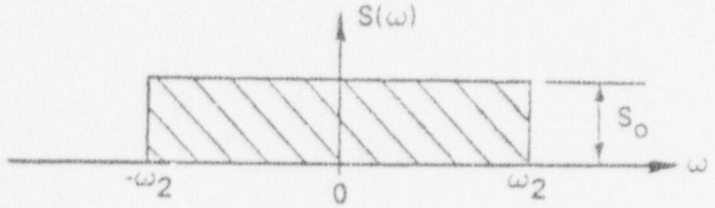

FIGURE A1

PSD OF THE FORCING EXCITATION GENERATED USING SUBROUTINES GAUSS AND RANDU

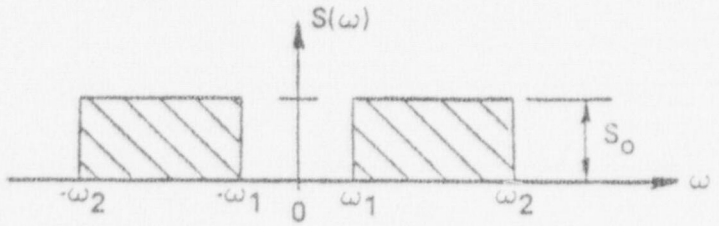

FIGURE A2

PSD OF BAND LIMITED FORCING EXCITATION

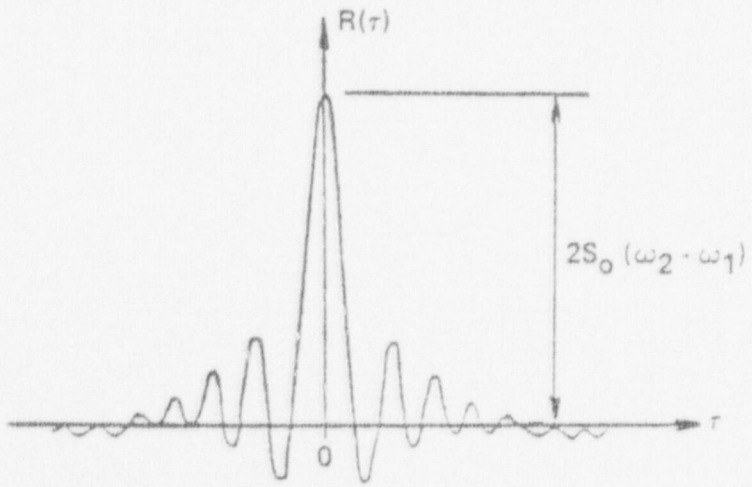

FIGURE A3

AUTOCORRELATION FUNCTION FOR BAND LIMITED FORCING EXCITATION

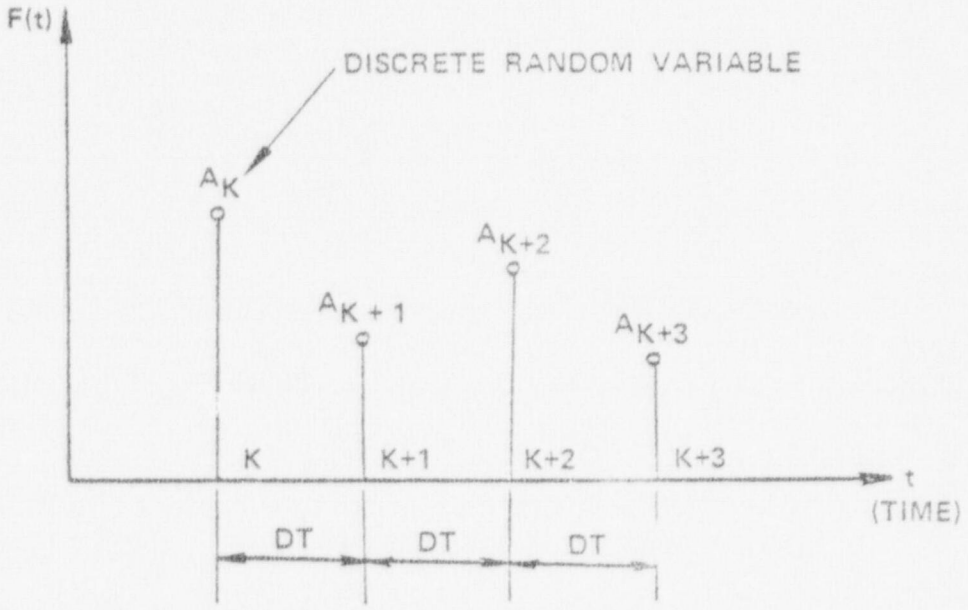

FIGURE A4
TIME HISTORY OF COMPUTER GENERATED
FORCING FUNCTION

APPENDIX B

STATISTICAL DISCUSSION OF EXPERIMENTAL RESULTS

The data values presented in this report represent an empirical "Monte Carlo" investigation, are ensemble averages of N generated time-history responses. Each of the time-history responses, which represent the numerical integration of the system model equations of motion, were obtained by using the appropriate computer program logic with an arbitrary sample of F(t) (i.e., normally distributed random forcing function with a specified mean and variance) as excitation. Initial conditions (i.e., displacement and velocity) were set equal to zero for all data samples.

Let $\langle x \rangle$ denote a simple ensemble average over an ensemble size N for a random variable x. It is statistically known that the variance of $\langle x \rangle$ is given by

$$\sigma^2_{\langle x \rangle} = \frac{\sigma^2_x}{N} \tag{B.1}$$

here σ^2_x is the variance of the random variable x. From fundamental stics the following definitions are presented:

$$E[\ ] = \text{mean value } (\overline{x}) = \int_{-\infty}^{+\infty} x\, p(x)dx \tag{B.2}$$

$$E[(x - \overline{x})^2] = \text{variance } (\sigma^2_x) = \int_{-\infty}^{+\infty} (x - \overline{x})^2\, p(x)dx \tag{B.3}$$

$$E[x^2] = \text{mean square value } (\overline{x^2}) = \int_{-\infty}^{+\infty} x^2\, p(x)dx \tag{B.4}$$

$$\int_{-\infty}^{+\infty} p(x)dx = 1 \tag{B.5}$$

$$\sigma_x^2 = \overline{x^2} - \overline{x}^2 \tag{B.6}$$

The variance of the mean square is written as

$$\sigma^2_{x^2} = E\left[\left(x^2 - E[x^2]\right)^2\right] = \int_{-\infty}^{+\infty} \left(x^2 - E[x^2]\right)^2 p(x)dx \tag{B.7}$$

From Definition B.6 with the mean (i.e., $\overline{x}$) set equal to zero one obtains the following relationship

$$E[x^2] = \overline{x^2} = \sigma_x^2 \tag{B.8}$$

Using Definition B.8, Definition B.7 can be rewritten as

$$\sigma^2_{x^2} = \int_{-\infty}^{+\infty} x^4 p(x)dx - 2\sigma_x^2 \int_{-\infty}^{+\infty} x^2 p(x)dx + \sigma_x^4 \int_{-\infty}^{+\infty} p(x)dx \tag{B.9}$$

$$\sigma^2_{x^2} = E[x^4] - \sigma_x^4 \tag{B.10}$$

Studies of $E[x^4]$ or $\sigma^2_{x^2}$ were not performed for the response data obtained in this report. However, one can obtain some useful information about the variance of $\langle x^2 \rangle$ by assuming the response x is

Gaussian even though it has been shown by Lutes* that this assumption is not always valid, especially for hysteretic or nonlinear systems. If x is a normally distributed random variable (i.e., Gaussian) with zero mean, the following relationship is useful

$$E[x^D] = \begin{cases} 1 \cdot 3 \ldots (D-1)\,\sigma_x^D & \text{for } D = \text{even} \\ 0 & \text{for } D = \text{odd} \end{cases} \tag{B.11}$$

Evaluating Definition B.11 for D equal to 4,

$$E[x^4] = 3\sigma_x^4 \tag{B.12}$$

Combining Definitions B.12 and B.10 one obtains

$$\sigma^2_{x^2} = 2\sigma_x^4 \tag{B.13}$$

Using Definition B.1 as an example, the ensemble variance of the mean square value is expressed as

$$\sigma^2_{\langle x^2 \rangle} = \frac{\sigma^2_{x^2}}{N} \tag{B.14}$$

Substituting Definition B.13 into Definition B.14 yields

$$\sigma_{\langle x^2 \rangle} = \sqrt{\frac{2\sigma_x^4}{N}} = \sigma_x^2 \left(\frac{2}{N}\right)^{1/2} \tag{B.15}$$

*Lutes, L.D., "An Approximate Technique for Treating Random Vibration of Hysteretic Systems," Report No. 4, Department of Civil Engineering, Rice University, Houston, 1969.

Definition B.15 expresses the relationship between the standard deviation of the mean square ensemble average $\langle x^2 \rangle$ of a Gaussian process with variance σ_x^2 and the number of averages N in the ensemble. This equation applies equally well to displacement or velocity. Table B.1 presents some typical numerical examples.

TABLE B.1. STATISTICAL RELATIONSHIP AS ENSEMBLE LENGTH N VARIES

N	$(2/N)^{1/2}$	$\sigma_{\langle x^2 \rangle}$
10	0.4472	$0.4472\ \sigma_x^2$
20	0.3162	$0.3162\ \sigma_x^2$
24	0.2887	$0.2887\ \sigma_x^2$
40	0.2236	$0.2236\ \sigma_x^2$
48	0.2041	$0.241\ \sigma_x^2$
60	0.1826	$0.1826\ \sigma_x^2$
80	0.1581	$0.1581\ \sigma_x^2$
160	0.1118	$0.1118\ \sigma_x^2$

For this study, N was set equal to 24. It should be noted that doubling the ensemble size, which would consequently double the computer costs, would have reduced the standard deviation of $\langle x^2 \rangle$ by

only 29%. The numerical "scatter" observed in the data values presented in this report can be associated directly with the limited number of ensemble averages generated. The primary constraint on the number of ensemble averages used in this investigation was a financial one dictated by computer costs. The number of ensemble averages chosen (i.e., N = 24) was not an unreasonably small number. However, Lutes and Shah* used as many as 80 ensemble averages in their study of the transient response of hysteretic systems.

---

*Lutes, L.D. and Shah, V.S., "Transient Random Response of Bilinear Oscillators," Report No. 17, Department of Civil Engineering, Rice University, Houston, 1970.

NRC FORM 335 (7-77) U.S. NUCLEAR REGULATORY COMMISSION

BIBLIOGRAPHIC DATA SHEET

1. REPORT NUMBER (Assigned by DDC)
NUREG/CR-0361

4. TITLE AND SUBTITLE (Add Volume No., if appropriate)
Random Vibration of a Nonlinear Two-Degree-of-Freedom Oscillator

2. (Leave blank)

3. RECIPIENT'S ACCESSION NO.

7. AUTHOR(S)
S. J. Stott and S. F. Masri

5. DATE REPORT COMPLETED
MONTH: May YEAR: 1978

9. PERFORMING ORGANIZATION NAME AND MAILING ADDRESS (Include Zip Code)
Civil Engineering Department
University of Southern California
Los Angeles, California 90007

DATE REPORT ISSUED
MONTH: August YEAR: 1978

6. (Leave blank)

8. (Leave blank)

12. SPONSORING ORGANIZATION NAME AND MAILING ADDRESS (Include Zip Code)
General Reactor Safety Research
Nuclear Regulatory Research
Nuclear Regulatory Commission
Washington, D.C. 20555

10. PROJECT/TASK/WORK UNIT NO.

11. CONTRACT NO.
NRC-04-76-262

13. TYPE OF REPORT
Topical

PERIOD COVERED (Inclusive dates)
10/1/77 - 9/30/78

15. SUPPLEMENTARY NOTES

14. (Leave blank)

16. ABSTRACT (200 words or less)

An analytical and experimental investigation is made of the dynamic response of a nonlinear two-degree-of-freedom oscillator that models some of the basic phenomena involved in the response of complex nuclear power plant systems under dynamic environments.

An approximate analytical solution is obtained for the stationary response of the system when subjected to stationary random excitation. Experimental measurements performed with an electronic analog computer and numerically simulated solutions generated by means of a digital computer verify the findings.

Results are given for the power spectral density and root-mean-squared level of the response. The effects of various system parameters on the response of the nonlinear system are determined.

17. KEY WORDS AND DOCUMENT ANALYSIS
Nonlinear Oscillations,
Single-Degree-of-Freedom,
Seismic, Hysteresis

17a. DESCRIPTORS
Structural Dynamics
Forced Vibrations
Dynamic Response

17b. IDENTIFIERS/OPEN-ENDED TERMS

18. AVAILABILITY STATEMENT
Unlimited

19. SECURITY CLASS (This report)

21. NO. OF PAGES

20. SECURITY CLASS (This page)

22. PRICE
$

NRC FORM 335 (7-77)